Naval Research Laboratory

Stennis Space Center, MS 39529-5004

NRL/MR/7320--14-9524

Validation Test Report for the NRL Ocean Surface Flux (NFLUX) Quality Control and 2D Variational Analysis System

Jackie May
Neil Van de Voorde

QinetiQ North America
Services and Solution Group
Stennis Space Center, Mississippi

Clark Rowley

Ocean Dynamics and Prediction Branch
Oceanography Division

June 11, 2014

REPORT DOCUMENTATION PAGE

Form Approved
OMB No. 0704-0188

1. REPORT DATE *(DD-MM-YYYY)*	2. REPORT TYPE	3. DATES COVERED *(From - To)*
11-06-2014	Memorandum Report	

4. TITLE AND SUBTITLE

Validation Test Report for the NRL Ocean Surface Flux (NFLUX) Quality Control and 2D Variational Analysis System

5a. CONTRACT NUMBER

5b. GRANT NUMBER

5c. PROGRAM ELEMENT NUMBER
0603207N

6. AUTHOR(S)

Jackie May,* Neil Van de Voorde,* and Clark Rowley

5d. PROJECT NUMBER

5e. TASK NUMBER

5f. WORK UNIT NUMBER
73-9066-C4-5

7. PERFORMING ORGANIZATION NAME(S) AND ADDRESS(ES)

Naval Research Laboratory
Oceanography Division
Stennis Space Center, MS 39529-5004

8. PERFORMING ORGANIZATION REPORT NUMBER

NRL/MR/7320--14-9524

9. SPONSORING / MONITORING AGENCY NAME(S) AND ADDRESS(ES)

Space & Naval Warfare Systems Command
2451 Crystal Drive
Arlington, VA 22245-5200

10. SPONSOR / MONITOR'S ACRONYM(S)

SPAWAR

11. SPONSOR / MONITOR'S REPORT NUMBER(S)

12. DISTRIBUTION / AVAILABILITY STATEMENT

Approved for public release; distribution is unlimited.

13. SUPPLEMENTARY NOTES

*QinetiQ North America, Services and Solution Group, Stennis Space Center, MS

14. ABSTRACT

The Naval Research Laboratory (NRL) Ocean Surface Flux System Version 1 (NFLUX) provides observation processing, quality control, and analysis of measurements of ocean surface state variables for application with ocean models. The three gridded analysis fields produced by the NFLUX system are 5-meter air temperature, 5-meter specific humidity, and 10-meter wind speed. The NFLUX system consists of three components: processing satellite retrievals of ocean surface state variables (NFLUX PRE), automated quality control of the observations (NFLUX QC), and 2D variational analyses of the satellite and in situ data with atmospheric models (NFLUX VAR). This document reviews and presents the current capability of the second and third components of the NFLUX system. NFLUX produces 6-hourly global and regional analysis fields, which are compared to current operational ocean forcing models (i.e., NOGAPS and COAMPS), and validated against 2 years of in situ observations.

15. SUBJECT TERMS
Satellite
Air-sea interaction
Variational analysis

16. SECURITY CLASSIFICATION OF:			17. LIMITATION OF ABSTRACT	18. NUMBER OF PAGES	19a. NAME OF RESPONSIBLE PERSON
a. REPORT	b. ABSTRACT	c. THIS PAGE			Clark Rowley
Unclassified Unlimited	Unclassified Unlimited	Unclassified Unlimited	Unclassified Unlimited	111	19b. TELEPHONE NUMBER *(include area code)* (228) 688-5809

Standard Form 298 (Rev. 8-98)
Prescribed by ANSI Std. Z39.18

TABLE OF CONTENTS

FIGURES

TABLES

EQUATIONS

EXECUTIVE SUMMARY

The Naval Research Laboratory (NRL) Ocean Surface Flux System Version 1 (NFLUX) provides observation processing, quality control, and analysis of measurements of ocean surface state variables for application with ocean models. The NFLUX system consists of three components: processing satellite retrievals of ocean surface state variables (NFLUX PRE), automated quality control of the observations (NFLUX QC), and 2D variational analyses of the satellite and *in situ* data with atmospheric models (NFLUX VAR). This document will review and present the current capability of the second and third components of the NFLUX system, which leverage the Navy Coupled Ocean Data Assimilation (NCODA) system. The first component of the NFLUX system is described in a separate report.

The three gridded analysis fields produced by the NFLUX system are 5-meter air temperature, 5-meter specific humidity, and 10-meter wind speed. NFLUX produces 6-hourly global and regional analysis fields, which are compared to current operational ocean forcing models (i.e. NOGAPS and COAMPS), and validated against 2 years of *in situ* observations.

The assimilated data include: Advanced Microwave Sounding Unit (AMSU) and Special Sensor Microwave Imager/Sounder (SSMIS) satellite data records (SDR), Windsat environmental data records (EDR), and *in situ* data. AMSU data are available from the National Oceanic and Atmospheric Administration (NOAA) and European Organization for the Exploitation of Meteorological Satellites (EUMETSAT) platforms. SSMIS data are available from the Department of Defense (DoD) platforms. Windsat data are from the Coriolis platform.

NFLUX and NOGAPS/COAMPS air temperature comparisons were found to be very similar. Each of the models showed a low mean bias, high correlation, and high overall skill compared to *in situ* observations. Each model shows an extended area of relatively constant temperatures within the Western Pacific warm pool. This feature is also seen when model sea surface temperatures are compared to *in situ* observations. Further work is needed to resolve this issue.

NOGAPS/COAMPS specific humidity shows a capping effect above approximately 28 g/kg. NFLUX applies a correction to high specific humidity values to account for the capping; however, the correction also causes more scatter/noise. In the tropics, NFLUX shows a strong moist bias, while NOGAPS/COAMPS show a strong dry bias. Compared to *in situ* observations, NFLUX shows a lower mean bias than NOGAPS/COAMPS. However, NFLUX also shows a lower correlation, due to the greater scatter, which results in a lower overall skill.

The global wind speed field is much noisier than either air temperature or specific humidity, causing wind speed correlations and overall skill to be reduced. NFLUX wind speeds were generally stronger than NOGAPS/COAMPS wind speeds. Each of the models showed high wind speed bias at less than approximately 5 m/s. Compared to *in situ* observations, NFLUX showed a smaller mean bias, higher correlation, and higher overall skill than NOGAPS/COAMPS.

1.0 INTRODUCTION

The Naval Research Laboratory (NRL) Ocean Surface Flux System Version 1 (NFLUX) processes, quality controls, and assimilates remotely-sensed and *in situ* observations to generate gridded analysis fields of ocean surface state variables used in estimating atmosphere-ocean fluxes of heat and momentum. The NFLUX system consists of three primary components. The first component retrieves measurements of near-surface atmospheric state parameters using observed brightness temperatures from passive microwave sensors including the Special Sensor Microwave Imager/Sounder (SSMIS) onboard Department of Defense (DoD) Meteorological Satellite Program (DMSP) platforms and the Advanced Microwave Sounding Unit (AMSU) onboard National Oceanic and Atmospheric Administration (NOAA) and European Organization for the Exploitation of Meteorological Satellites (EUMETSAT) platforms. Measurements of surface scalar wind speed from the Windsat sensor, as well as *in situ* observations from NOAA buoys and Voluntary Observing Ships (VOS), are also processed. The second component applies an automated quality control (QC) to all *in situ* and satellite observations. The third component performs 2D variational analyses of *in situ* and satellite observations with atmospheric model forecasts to produce gridded global and regional estimates of surface atmospheric state parameters over the ocean.

The quality control and variational analysis components of NFLUX are built on the Navy Coastal Ocean Data Assimilation (NCODA) system (Cummings, 2005), and use NCODA software to provide many underlying utility components. The NFLUX version 1 system produces global gridded fields of surface air temperature, surface specific humidity, and 10-meter scalar wind speed.

This validation report documents the performance of the NFLUX quality control and 2D analysis components in three regional studies in comparison with *in situ* observations and current operational ocean forcing products from Navy meteorological models (i.e., NOGAPS and COAMPS).

2.0 VALIDATION TEST DESIGN

2.1 Validation measures

The statistical metrics used in this report are mean error (*ME*), standard deviation (*SD*), root mean square error (RMSE), and correlation coefficient (R^2). They are expressed as follows:

$$ME = \bar{Y} - \bar{X}, \tag{1}$$

$$SD = \left[\frac{1}{n}\sum_{i=1}^{n}\left((Y_i - \bar{Y}) - (X_i - \bar{X})\right)^2\right]^{1/2}, \tag{2}$$

$$RMSE = \left[\frac{1}{n}\sum_{i=1}^{n}(Y_i - X_i)^2\right]^{1/2}, \tag{3}$$

Manuscript approved May 13, 2014.

$$R^2 = \left[\frac{1}{n}\sum_{i=1}^{n}(X_i - \bar{X})(Y_i - \bar{Y})/(\sigma_X \sigma_Y)\right]^2, \quad \textbf{(4)}$$

where X_i are the *in situ* observations, Y_i are the NFLUX analysis or NOGAPS / COAMPS forecast field values, σ_x and σ_y are the corresponding standard deviations, and the overbar represents a simple average. *ME* measures the overall mean bias, *SD* is the standard deviation of the difference between the *in situ* and model data, RMSE measures the absolute error between the *in situ* and model data, and R^2 is a measure of the linear association between the model and the observation. The *ME* and *SD* are also tested for statistical significance at the 95% confidence interval, using a two-tailed t-test for *ME* and a chi-squared test for *SD*.

2.2 Verifying observations

Validation is performed on the 00Z and 12Z analysis or forecast fields. *In situ* observations assigned an error estimate of .90 or less by the NFLUX QC, and observed within three hours of the analysis time, are used to create the matchup validation data set. If multiple *in situ* observations exist at the same latitude and longitude or have the same call sign, only the closest in time to the analysis time is used.

Performance measures are calculated separately for matchup datasets of (nominally) assimilated and unassimilated *in situ* observations. In the assimilated data comparisons, we presumed that the *in situ* observations were available for assimilation in the analysis for that forecast (for both NFLUX and the model forecast fields). The assimilated *in situ* data comparisons are made for NFLUX analysis fields, model analysis fields, and model 12 h forecast fields. For example, NFLUX analysis and model analysis fields from 12Z 1 January and 12 h model forecast fields from 00Z 1 January are verified against *in situ* observations from 12Z 1 January.

The unassimilated *in situ* data comparisons are performed by persisting NFLUX and forecast model fields forward 12 h, and validating against verifying *in situ* observations that we presume were not assimilated in that cycle based on the observation time. For example, NFLUX analysis and model analysis fields from 12Z 1 January are verified against *in situ* observations from 00Z 2 January. We considered using 24 h persistence instead of 12 h to match the diurnal cycle; however, we found the skill was greatly reduced due to the short atmospheric time scales.

These comparisons are relevant to an operational implementation of NFLUX used to post-processes meteorological model forecast output for ocean model initialization. A comparison of persisted NFLUX analyses against valid atmospheric model forecast fields using unassimilated observations was not performed, as it would not be relevant to the skill of an operational NFLUX system. The NFLUX system is not intended to provide forecast ocean surface state variables.

The matchups are further divided to distinguish performance on coastal areas versus the open ocean: the full global set includes all matchups in the data set, the coastal subset includes matchups within 111 km of land, and the open ocean subset includes matchups greater than 111km of land. The open ocean subsets are further divided by season: December-January-

February (DJF); March-April-May (MAM); June-July-August (JJA); and September-October-November (SON). The open ocean subset for the global test case is also examined by latitude band: 90°S to 15°S, 15°S to 0°N, 0°N to 15°N, 15°N to 30°N, 30°N to 45°N, 45°N to 90°N.

2.3 Analysis domains

We examine validation datasets for three test cases: global, western Pacific, and eastern Pacific, from 1 January 2010 through 31 December 2011 for each case. The NFLUX grid characteristics of each domain are given in Table 1, while a map outlining the boundaries of each region is shown in Figure 1. The global test case allows for large scale biases to be investigated. The western Pacific test case covers multiple areas of Navy interest, and includes the significant air-sea interaction associated with the Kuroshio front in the East China Sea (e.g., Xu et al., 2011). The eastern Pacific test case represents a basin area with frequent winter storms (e.g. Graham and Diaz, 2001) and persistent coastal stratus clouds (e.g., Klein and Hartmann, 1993).

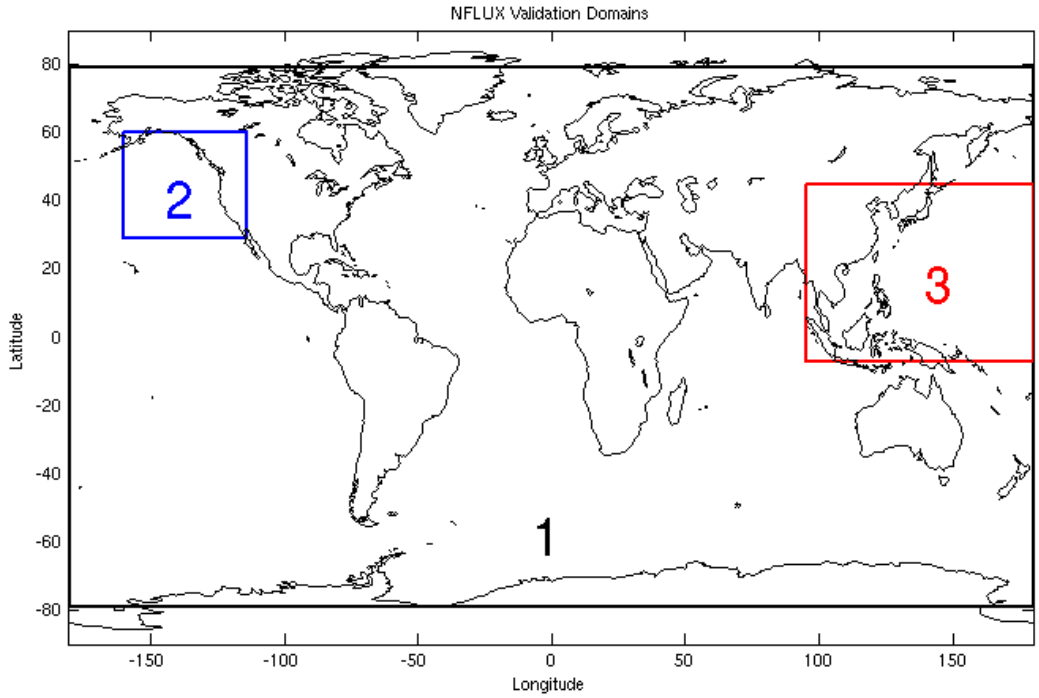

Figure 1: Validation test case domains. Three regions were chosen to represent different atmospheric features.

Table 1: Validation test case grids. The test case grid domains match those provided by NOGAPS/COAMPS.

Test Case	Area	Latitude Range	Longitude Range	Grid Resolution	Grid Points
1	Global	79.15°S to 79.15°N	180°W to 180°E	24 km	1669 x 1251
2	East Pacific	29°N to 60°N	160°W to 114°W	0.2 degrees	231 x 156
3	West Pacific	7°S to 45°N	95°E to 180°E	0.2 degrees	426 x 261

2.4 Analysis products

2.4.1 NOGAPS

The Navy Operational Global Atmospheric Prediction System (NOGAPS) is a complete atmospheric forecast and data assimilation system used to produce global predictions of atmospheric and oceanic parameters (Hogan and Rosmond, 1991). The focus is on relatively short time scales of numerical weather prediction, as opposed to climate; therefore, a one-way coupling strategy is implemented. The assimilation of new data (update cycle) occurs every 6 hours, with forecast fields available every 3 hours. NOGAPS uses the NRL Atmospheric Variational Data Assimilation (NAVDAS) – Accelerated Representer (AR) system, an operational four-dimensional weak-constraint data assimilation system (Xu et al., 2005; Rosmond and Xu, 2006). The SST analysis used within NOGAPS is produced by NCODA and is updated twice a day using a 24 hour data window, which eliminates any diurnal effects. The SSTs are kept constant throughout the forecast period. The global test case uses the NOGAPS atmospheric model forecast fields archived in the NRL Code 7300 archive. The NOGAPS fields are application-grid data that have been interpolated to a uniform 0.5° resolution. We use the NOGAPS 2 m air temperature, 2 m specific humidity (estimated from the model 2 m dew point depression and the air temperature), and 10 m wind speed. At the time of this study, NOGAPS was the primary source of forcing for U.S. Navy global ocean models. As of 13 March 2013, NOGAPS was replaced by the Navy Global Environmental Model (NAVGEM).

2.4.2 COAMPS

The Coupled Ocean Atmosphere Prediction System (COAMPS) is used to make regional predictions of atmospheric and oceanic parameters (Hodur, 1997). Like NOGAPS, COAMPS consists of complete data assimilation and forecast model components. The U.S. Navy uses COAMPS for numerical weather predictions in various regions around the world, and forcing for regional and coastal ocean models. The update cycle is every 6 hours, with forecast fields available every 3 hours. The NAVDAS data assimilation system is used to produce the COAMPS analyses. The SST analysis used within COAMPS is produced using the same method as described for NOGAPS. The regional test cases use the COAMPS atmospheric model forecast fields archived in the NRL Code 7300 archive. The COAMPS fields used are application-grid data interpolated to a uniform 0.2º resolution. We use the COAMPS 2 m air temperature, 2 m specific humidity (estimated from the model 2 m dew point depression and the air temperature), and 10 m wind speed.

2.4.3 NFLUX

The NFLUX version 1 system produces global gridded fields of air temperature, specific humidity, and scalar wind speed over the ocean surface. The NFLUX system was cycled with a six-hourly update cycle from 1 January 2010 through 31 December 2011 for each test case.

2.4.3.1 Quality Control

An automatic quality control (QC), or error estimate, is applied to all of the satellite and *in situ* observations. The QC system is built on NCODA (Cummings, 2005). The QC decision making uses both monthly climates as well as the previous NFLUX analysis field. The monthly climate fields were constructed using SeaFlux data (Curry et al., 2004). The SeaFlux project was designed to produce high quality (every 3 hours) satellite-based ocean surface turbulent flux datasets that could be used in climate studies. Input parameters (including air temperature, specific humidity, and wind speed) used to calculate the turbulent fluxes were stored, along with the fluxes, and are freely available from the SeaFlux website: www.seaflux.org. The global SeaFlux products from January 1998 through December 2007 were used to create the parameter specific monthly climate fields used in the NFLUX system.

2.4.3.2 Analysis variables

NFLUX produces analyses of nominal height 5 m (air temperature and specific humidity) and 10 m (wind speed). The satellite retrievals are based on a combination of buoy and height-adjusted ship measurements. Buoy air temperature and specific humidity observation heights are nominally at 5m. Ship measurement heights vary from 10 m to 40 m (Kent et al., 2007). When possible, we height-adjust ship measurements to 5 m air temperature and specific humidity and 10 m wind speed using COARE 3.0 (Fairall et al., 2003) to more closely correspond to typical buoy instrument heights, as buoys make up the bulk of the *in situ* measurements used in deriving the retrievals. The *in situ* and satellite temperature and humidity measurements are not further height-adjusted to 2 m to match the height associated with NOGAPS and COAMPS.

NOGAPS and COAMPS provide air temperature and wind speed fields as direct model outputs; however, the specific humidity (Qa) fields must be calculated. Specific humidity is calculated following WMO (2006) using input air temperature (*Ta*), dew point depression (*dptdp*), and pressure fields (*pres*). Equations (5)-(7) describe the specific humidity calculation, where *dpt* is the dew point and *vp* is the vapor pressure.

$$dpt = Ta - dptdp \tag{5}$$

$$vp = 6.1121 * e^{\frac{17.6\ 2dpt}{24\ 312+dpt}} \tag{6}$$

$$Qa = \frac{0.622 * vp}{pres - 0.378 * vp} \tag{7}$$

2.4.3.3 Observation handling

Both satellite and *in situ* observations were required to have a QC value of .90 or less and an observation time within three hours of the NFLUX analysis run time in order to be assimilated. The available *in situ* and satellite observations are used to form super observations at 1.5 (1.2) times the global (regional) analysis grid mesh interval. We investigated greater adjustments to

the super observations; however, this resulted in a degraded analysis. We also investigated adjustments to a secondary over-sampling option, but the impact on the results was minimal, and the super observation technique above was maintained.

2.4.3.4 Prediction fields

The prediction or background field for each NFLUX analysis blends a model forecast (NOGAPS or COAMPS) with the previous NFLUX analysis increment field. The increment field is a gridded correction field, applied to the prediction field to produce the analysis field. We tested several additional techniques not presented here for defining appropriate background fields for the NFLUX analyses, including using persisted NOGAPS or COAMPS analysis fields, using only the previous NFLUX analysis field, and using multiple previous analysis fields. We determined that the blending of the NOGAPS (COAMPS) forecast with previous NFLUX analysis fields gave the best performance. Using the blending approach, we found that adding multiple previous NFLUX analyses fields produced similar results, so we include only the one previous NFLUX analysis correction. Using the NOGAPS (COAMPS) analysis fields rather than the forecast fields gave a slight improvement, but the validation testing here is performed as if in a real-time system in which the next NOGAPS (COAMPS) analysis may not yet be available.

2.4.3.5 Correlation Length scales

Each of the surface forcing parameters has its own spatial correlation scale, or prediction error covariance structure. The NCODA ocean analysis by default uses the climatological ocean first baroclinic mode, Rossby radius of deformation, as a basis for the correlation length scales that define the covariance structure. The NFLUX analysis similarly uses a set of climatological length scales to define the horizontal covariances.

To estimate error covariance length scales, we used a time series of 0.5° NOGAPS 12 h forecasts and verifying analyses for each parameter, every 2 days at 00 Z for 6 years (2005-2010). We chose this set up to sufficiently sample a wide variety of atmospheric conditions. At each verifying time, an error field was calculated as the difference between the 12 h forecast field and the verifying analysis field. At every point on a uniform 1° grid, neighboring error values from the difference field were accumulated in 50 km bins, from 50 km to 500 km, and the bin covariances were fit with a Gaussian function. The characteristic scale of the Gaussian function was defined as the length scale at that grid point. The time series of correlation length fields were then averaged, and a two-way smoothing filter was applied to produce the final error correlation length scales that are used in the NFLUX system (Figure 2). The length scales are used as the basis for the analytical-form horizontal covariance structure in each of the test cases. The second-order autoregressive (SOAR) form was used as the analytical covariance structure.

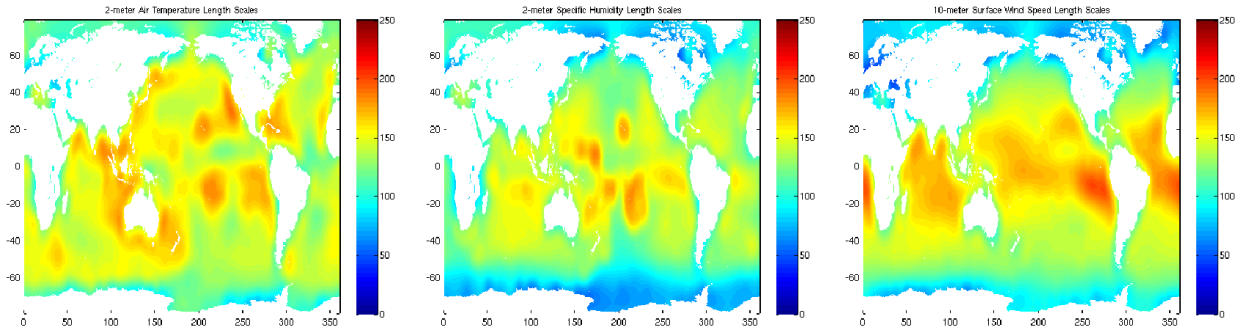

Figure 2: NFLUX horizontal length scales. Each surface parameter has a unique length scale. Air temperature is shown on the left, specific humidity is shown in the middle, and wind speed is shown on the right.

3.0 TEST CASE 1: GLOBAL

The global domain spans from 0-360°E and 79.15°S-79.15°N with a horizontal resolution of 24 km. The Mercator grid has 1669 x 1251 grid points. The NOGAPS 12 h forecast field is blended with the previous NFLUX correction field to generate the background field for the NFLUX analysis. NFLUX analysis performance is compared against NOGAPS analysis fields and NOGAPS 12 h forecast fields. Validation statistics are calculated for assimilated and unassimilated *in situ* matchup data.

3.1 Air Temperature Results

Figure 3 shows mean air temperature error using unassimilated *in situ* observations of the NFLUX analyses (top) and the NOGAPS analyses (bottom) over the full 2 year data set. Both NFLUX and NOGAPS show non-zero mean biases compared to the *in situ* observations, with large areas of noticeable cold or warm bias. The overall spatial pattern of the biases is similar in NFLUX and NOGAPS, with warm biases in the western Pacific and north Atlantic, and cool biases in the central Pacific. NFLUX is too warm in the eastern Pacific and the west coast of South Africa, and too cool in the eastern Mediterranean, while NOGAPS is too cool in the western North Pacific and the eastern tropical Atlantic.

Figure 4 shows the 2 year gridded global mean air temperature difference between NFLUX and NOGAPS (left), with the zonal average of the difference (right). The zonal average represents the average at constant latitude. Generally, NFLUX has warmer temperatures than NOGAPS. This is most noticeable along the Gulf Stream, Kuroshio Current, and in the tropics. This agrees well with warm bias areas identified in NFLUX and a wide cold bias in NOGAPS from Figure 3. In the Southern Ocean, NFLUX has cooler air temperatures than either of the NOGAPS products. There are few to none *in situ* matchups to validate this region (see Figure 3), so it is only noted here as an area of differences.

While Figure 3 and Figure 4 qualitatively show long term differences between NFLUX and NOGAPS, we can further investigate these differences quantitatively using assimilated and unassimilated *in situ* matchups. The left (right) side of Table 2 compares NFLUX to NOGAPS air temperature using assimilated (unassimilated) *in situ* observations. The means and standard deviations were tested at the 95% confidence level and each was found to be significantly different compared to NFLUX.

As seen in Table 2 for the open-ocean, both NFLUX and NOGAPS compare better to the assimilated data rather than the unassimilated. NOGAPS shows slightly better test statistics using assimilated observations, while NFLUX shows improvement over NOGAPS using unassimilated observations.

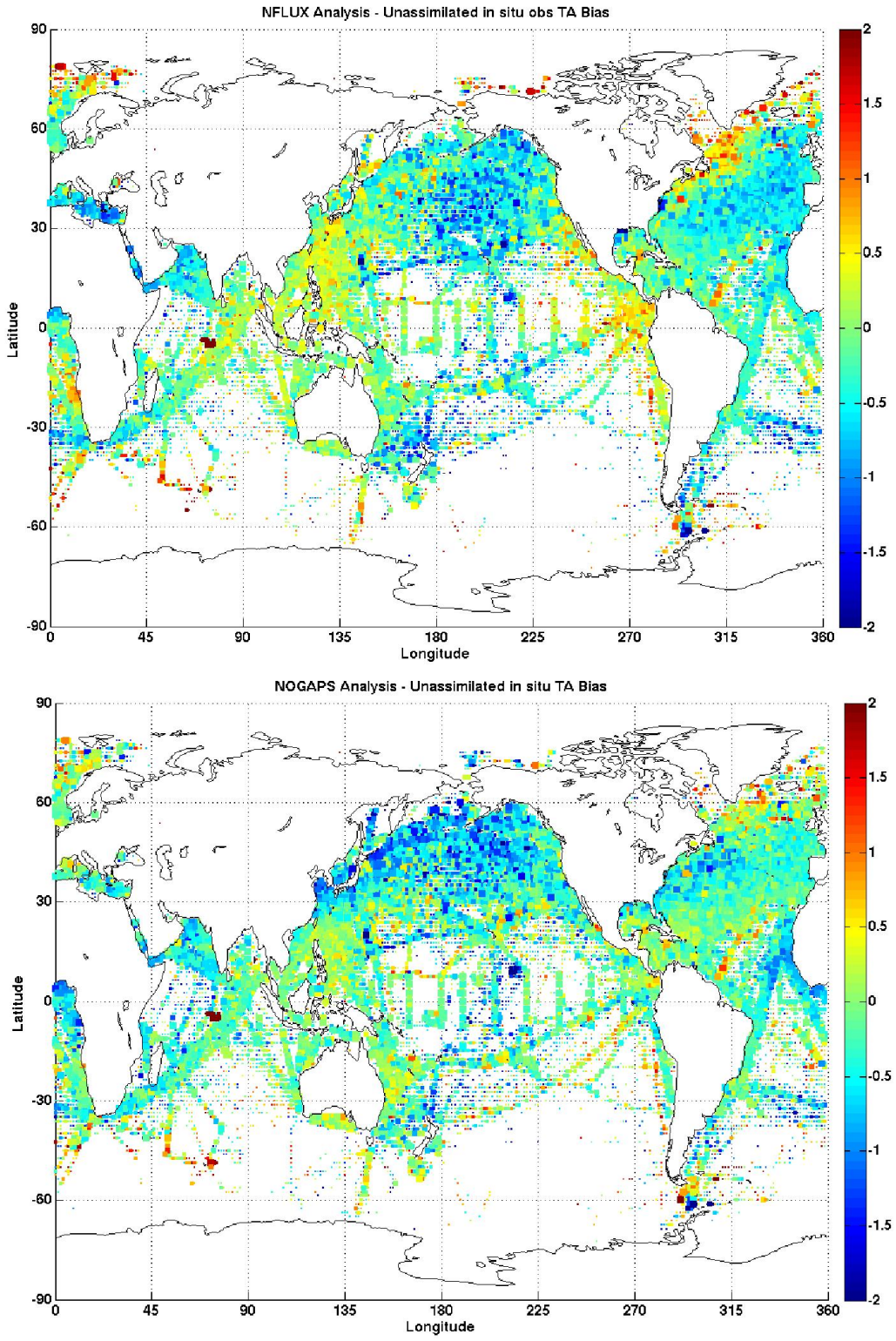

Figure 3: Global 2-year average air temperature bias (°C). The NFLUX (NOGAPS) bias compared to unassimilated observations is shown in the top (bottom) panel. Colored square sizes represent the number of observations in each grid box, ranging from 5 to 50 observations.

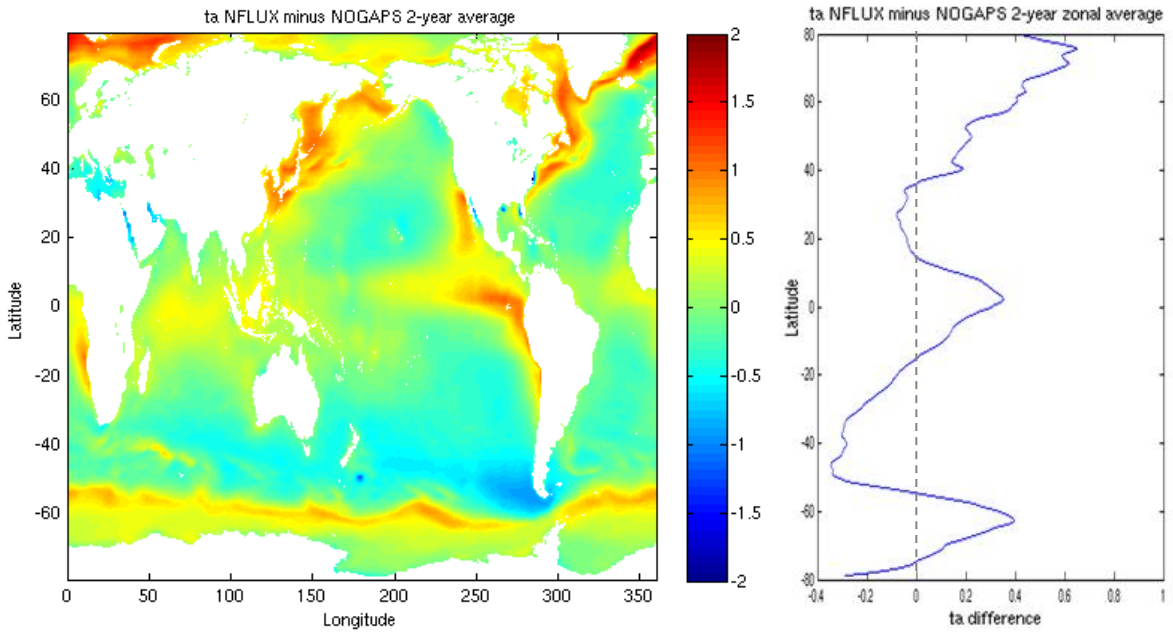

Figure 4: Global 2-year average NFLUX minus NOGAPS air temperature difference (°C). The left panel shows the global gridded difference. The right panel shows the zonally averaged difference.

Table 2: Air temperature errors over the global ocean. Errors are shown relative to both assimilated (left columns) and unassimilated (right columns) *in situ* observations for all comparisons (global), near land (coastal), and open ocean (ocean). The best test statistic in each column is highlighted in blue. Means and standard deviations that are not significantly different compared to NFLUX at the 95% confidence interval are denoted with an asterisk (*).

	ME	SD	RMSE	R^2		ME	SD	RMSE	R^2
Global		N = 778480							
NFLUX Analysis	-0.1560	1.6099	1.6175	0.9634	NFLUX 12h persist	-0.1681	1.9984	2.0055	0.9440
NOGAPS Analysis	-0.1272	1.5519	1.5571	0.9663	NOGAPS 12h persist	-0.1391	2.0691	2.0738	0.9407
NOGAPS 12h fcst	-0.0310	1.5723	1.5726	0.9652					
Coastal		N = 343842							
NFLUX Analysis	-0.2043	2.0805	2.0905	0.9294	NFLUX 12h persist	-0.2259	2.6465	2.6562	0.8873
NOGAPS Analysis	-0.0646	1.9859	1.9870	0.9384	NOGAPS 12h persist	-0.0829	2.7415	2.7427	0.8843
NOGAPS 12h fcst	0.0272	2.0201	2.0203	0.9354					
Ocean		N = 434638							
NFLUX Analysis	-0.1179	1.1021	1.1084	0.9820	NFLUX 12h persist	-0.1225	1.2678	1.2737	0.9762
NOGAPS Analysis	-0.1768	1.0901	1.1044	0.9824	NOGAPS 12h persist	-0.1835	1.3107	1.3235	0.9746
NOGAPS 12h fcst	-0.0770	1.0929	1.0956	0.9823					

Scatterplots of the assimilated (unassimilated) open ocean matchups are shown in Figure 5 (Figure 6), along with corresponding histograms comparing the probability of the mean bias. The color scale shown in the scatterplots represents the density of observations. Warm colors represent the highest density of observations, while cool colors represent few observations.

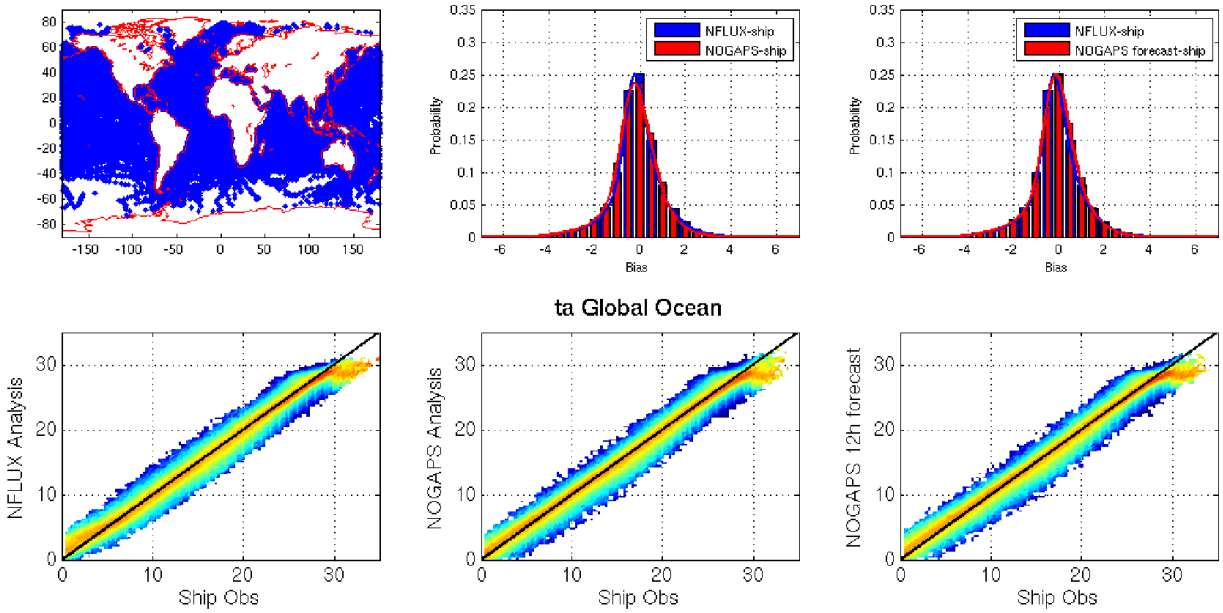

Figure 5: Air temperature over global open ocean using assimilated *in situ* data. The distribution of the matched up observations is shown in the top left panel. The top middle (right) panel shows a histogram of the probability of the mean bias of NFLUX analysis, shown in blue, and NOGAPS analysis (NOGAPS 12-hour forecast), shown in red. The bottom panels show scatterplots of the *in situ* observations versus NFLUX analysis (left), NOGAPS analysis (middle), and NOGAPS 12-hour forecast (right).

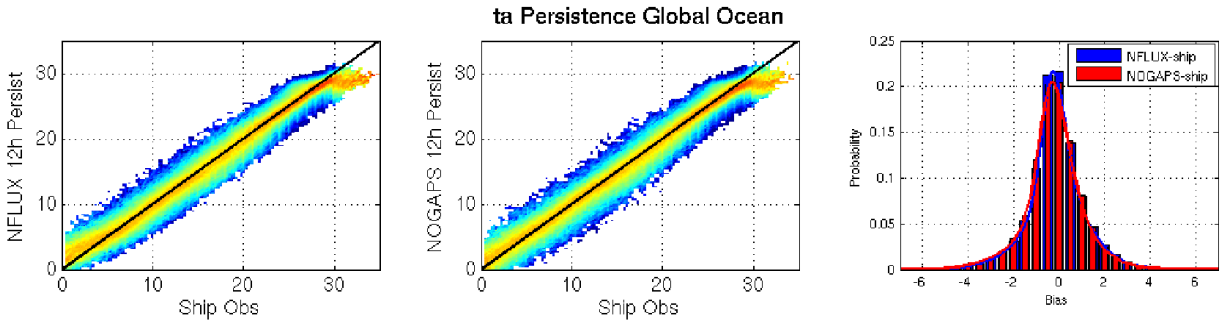

Figure 6: Air temperature over global open ocean using unassimilated *in situ* data. The right panel shows a histogram of the probability of the mean bias of NFLUX analysis (blue) and NOGAPS analysis (red). Scatterplots of the *in situ* observations versus NFLUX analysis (left) and NOGAPS analysis (middle) are also shown.

As seen in the scatterplots, each of the model products is unable to accurately represent very high temperatures resulting in a cold bias. However, NFLUX seems to have a slightly extended one-to-one relationship compared to NOGAPS. Less than approximately 30°C for NFLUX and 28°C for NOGAPS, a close one-to-one relationship can be seen in each of the model products. At very low temperatures, less than approximately 5°C, a slight warm bias is seen in NFLUX that is not present in NOGAPS.

3.1.1 Latitude Bands

The open ocean test statistics for each of the six latitude bands are presented in Table 3, with the corresponding scatterplots of the model versus assimilated (unassimilated) observations shown in Figure 7 (Figure 8). For assimilated matchups (left side of Table 3 and Figure 7), NFLUX performs better than NOGAPS in the tropical regions, from 15°S to 15°N. Outside of the tropics NOGAPS performs slightly better than NFLUX. It is interesting to note that in the 90°S to 15°S band, the standard deviations of NFLUX and the NOGAPS 12-hour forecast are not statistically different; the correlations are also very similar. For unassimilated matchups (right side of Table 3 and Figure 8), NFLUX shows overall improvement over NOGAPS in all latitude bands except 15°N to 30°N, and the mean bias in the polar bands. The 15°N to 30°N latitude band will be discussed further in the western Pacific region (section 5.1).

As discussed in the total open ocean, the scatterplots show the cold bias at high temperatures in the 90°S to 30°N latitude bands. The higher latitude bands do not have warm enough temperatures to show the bias. The warm bias seen with NFLUX at low temperatures is seen in the 30°N to 90°N latitude bands; however, it is not seen the 90°S to 15°S latitude band.

Table 3: Air temperature errors over the global open ocean by latitude band. Errors are shown relative to both assimilated (left columns) and unassimilated (right columns) *in situ* observations. The best test statistic in each column is highlighted in blue. Means and standard deviations that are not significantly different compared to NFLUX at the 95% confidence interval are denoted with an asterisk (*).

	ME	SD	RMSE	R^2		ME	SD	RMSE	R^2
Latitude 45 to 90		N = 106514							
NFLUX Analysis	-0.1593	1.2019	1.2124	0.9180	NFLUX 12h persist	-0.1714	1.3847	1.3953	0.8907
NOGAPS Analysis	-0.0939	1.1793	1.1831	0.9208	NOGAPS 12h persist	-0.1149	1.4775	1.4819	0.8766
NOGAPS 12h fcst	0.0527	1.2173	1.2184	0.9156					
Latitude 30 to 45		N = 64739							
NFLUX Analysis	-0.1770	1.4237	1.4346	0.9452	NFLUX 12h persist	-0.1913	1.7249	1.7355	0.9186
NOGAPS Analysis	-0.3011	1.3498	1.3830	0.9504	NOGAPS 12h persist	-0.3174	1.7884	1.8163	0.9140
NOGAPS 12h fcst	-0.2180	1.3443	1.3619	0.9506					
Latitude 15 to 30		N = 72999							
NFLUX Analysis	-0.1204	1.1382	1.1445	0.9057	NFLUX 12h persist	-0.1184	1.3184	1.3237	0.8721
NOGAPS Analysis	-0.0920	1.0867	1.0906	0.9136	NOGAPS 12h persist	-0.0903	1.3047	1.3078	0.8766
NOGAPS 12h fcst	-0.0808	1.0778	1.0808	0.9143					
Latitude 0 to 15		N = 95469							
NFLUX Analysis	0.0124	0.8497	0.8497	0.7445	NFLUX 12h persist	0.0144	0.9240	0.9241	0.6968
NOGAPS Analysis	-0.1881	0.9127	0.9319	0.7051	NOGAPS 12h persist	-0.1854	0.9456	0.9636	0.6844
NOGAPS 12h fcst	-0.0583	0.9018	0.9037	0.7112					
Latitude -15 to 0		N = 69195							
NFLUX Analysis	-0.1006	0.7449	0.7516	0.8742	NFLUX 12h persist	-0.1006	0.8002	0.8065	0.8543
NOGAPS Analysis	-0.2329	0.7956	0.8290	0.8561	NOGAPS 12h persist	-0.2334	0.8290	0.8612	0.8434
NOGAPS 12h fcst	-0.1241	0.7735	0.7834	0.8639					
Latitude -90 to -15		N = 25722							
NFLUX Analysis	-0.3201	1.2135	1.2550	0.9617	NFLUX 12h persist	-0.3249	1.3321	1.3711	0.9538
NOGAPS Analysis	-0.2546	*1.2192	1.2454	0.9614	NOGAPS 12h persist	-0.2548	1.3562	1.3799	0.9521
NOGAPS 12h fcst	-0.1909	*1.1977	1.2128	0.9627					

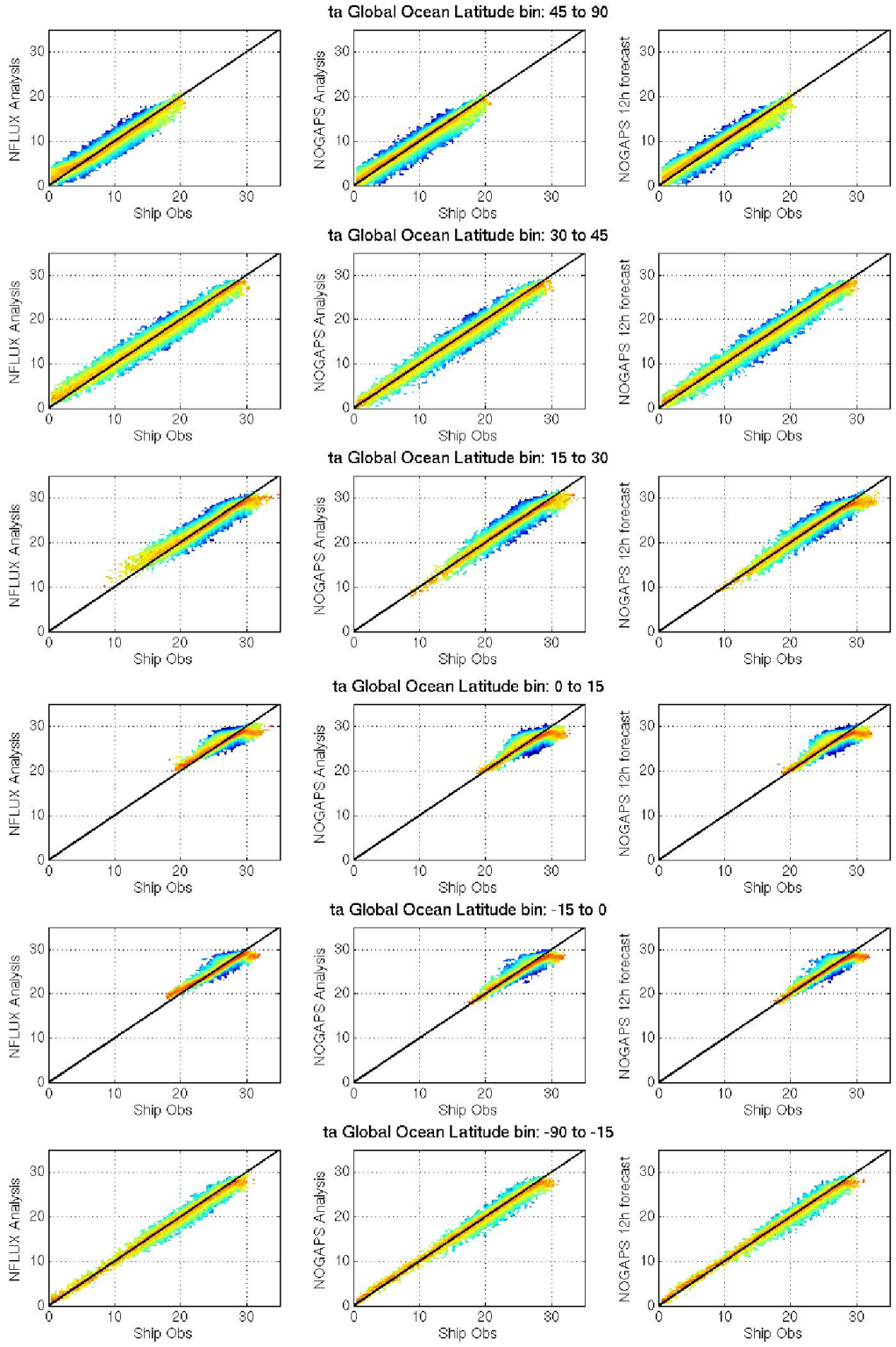

Figure 7: Air temperature over global open ocean by latitude using assimilated *in situ* data. Scatterplots of the *in situ* observations versus NFLUX analysis (left), NOGAPS analysis (middle), and NOGAPS 12-hour forecast (right) are shown.

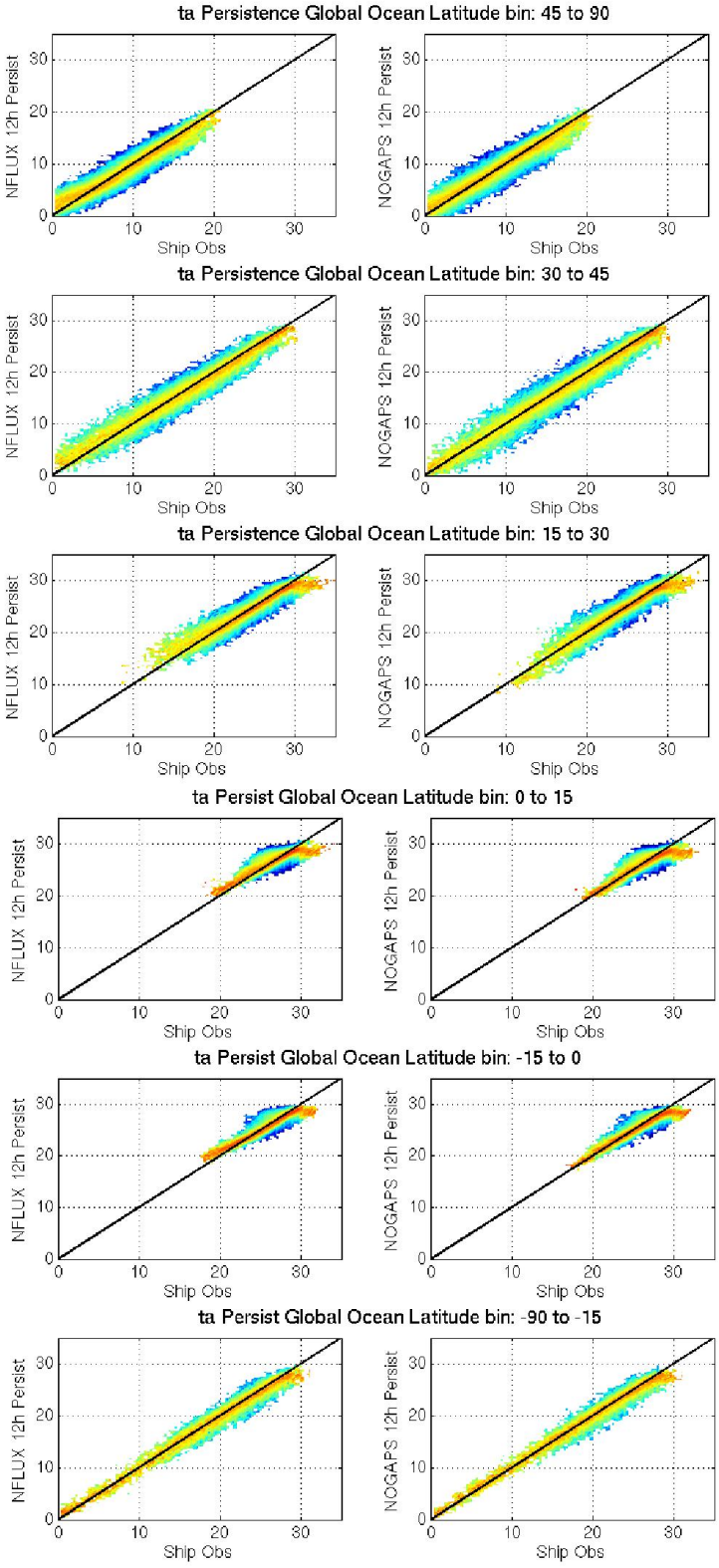

Figure 8: Air temperature over global open ocean by latitude using unassimilated *in situ* data. Scatterplots of the *in situ* observations versus NFLUX analysis (left) and NOGAPS analysis (right) are shown.

3.1.2 Seasonal

The seasonal test statistics are presented in Table 4, while corresponding scatterplots of the model versus assimilated (unassimilated) observations are shown in Figure 9 (Figure 10). For assimilated matchups (left side of Table 4 and Figure 9), NFLUX and NOGAPS mean bias and standard deviations are significantly different at the 95% confidence interval for all but the MAM season. NOGAPS does have smaller errors in all but the JJA season. For unassimilated matchups (right side of Table 4 and Figure 10), NFLUX shows improvement over NOGAPS in all seasons for all test statistics, with no significant difference in the mean bias in the MAM season. Both the cold bias at high temperatures and the warm bias at low temperatures can be seen in the scatterplots for each season.

Table 4: Air temperature errors over the global open ocean by season. Errors are shown relative to both assimilated (left columns) and unassimilated (right columns) *in situ* observations. The best test statistic in each column is highlighted in blue. Means and standard deviations that are not significantly different compared to NFLUX at the 95% confidence interval are denoted with an asterisk (*).

	ME	SD	RMSE	R^2		ME	SD	RMSE	R^2
DJF		N = 114819							
NFLUX Analysis	-0.0556	1.1610	1.1623	0.9839	NFLUX 12h persist	-0.0616	1.3857	1.3870	0.9769
NOGAPS Analysis	-0.1337	1.1292	1.1371	0.9847	NOGAPS 12h persist	-0.1410	1.4441	1.4510	0.9749
NOGAPS 12h fcst	0.0046	1.1341	1.1341	0.9846					
MAM		N = 99675							
NFLUX Analysis	-0.2519	1.0958	1.1244	0.9850	NFLUX 12h persist	-0.2718	1.2519	1.2810	0.9805
NOGAPS Analysis	*-0.2436	*1.0872	1.1141	0.9851	NOGAPS 12h persist	*-0.2636	1.2884	1.3151	0.9791
NOGAPS 12h fcst	-0.1415	1.0861	1.0952	0.9851					
JJA		N = 105815							
NFLUX Analysis	-0.1063	1.0807	1.0859	0.9757	NFLUX 12h persist	-0.1169	1.1727	1.1785	0.9714
NOGAPS Analysis	-0.2263	1.0985	1.1216	0.9751	NOGAPS 12h persist	-0.2413	1.2162	1.2399	0.9696
NOGAPS 12h fcst	-0.1743	1.1029	1.1166	0.9748					
SON		N = 114329							
NFLUX Analysis	-0.0742	1.0558	1.0584	0.9793	NFLUX 12h persist	-0.0586	1.2313	1.2327	0.9719
NOGAPS Analysis	-0.1160	1.0384	1.0448	0.9800	NOGAPS 12h persist	-0.1029	1.2661	1.2703	0.9703
NOGAPS 12h fcst	-0.0126	1.0353	1.0354	0.9802					

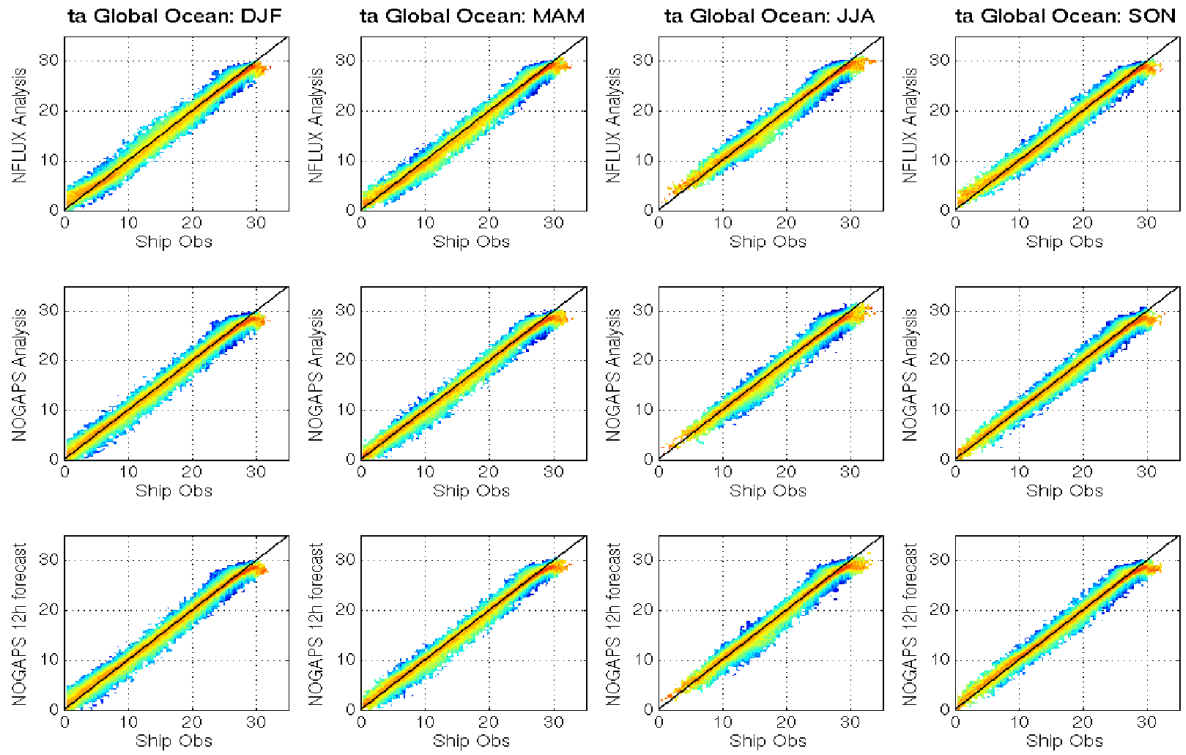

Figure 9: Air temperature over global open ocean by season using assimilated *in situ* data. Scatterplots of the *in situ* observations versus NFLUX analysis (top), NOGAPS analysis (middle), and NOGAPS 12-hour forecast (bottom) are shown.

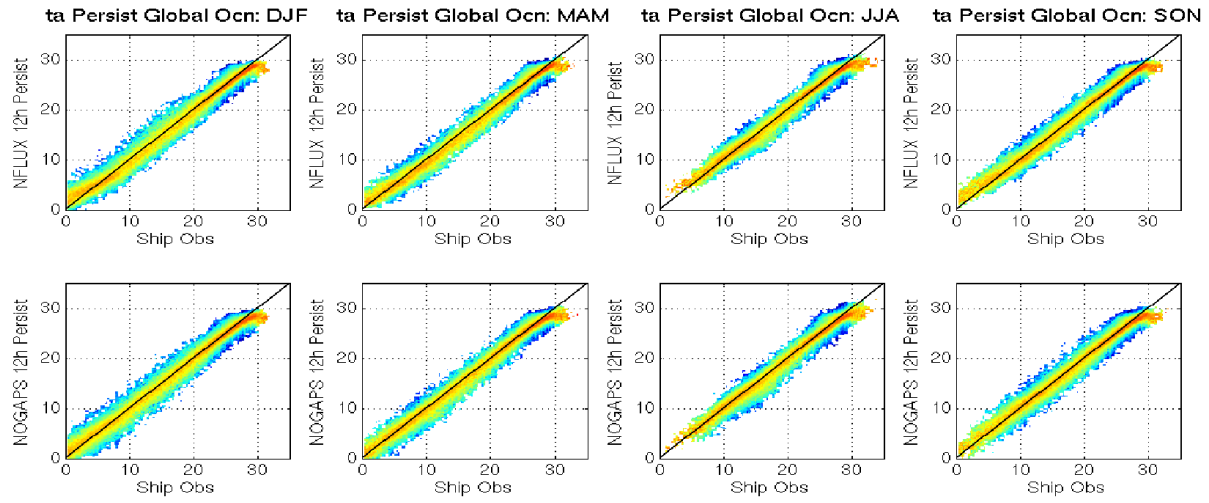

Figure 10: Air temperature over global open ocean by season using unassimilated *in situ* data. Scatterplots of the *in situ* observations versus NFLUX analysis (top) and NOGAPS analysis (bottom) are shown.

3.2 Specific Humidity Results

Figure 11 shows mean specific humidity error using unassimilated *in situ* observations of the NFLUX analyses (top) and the NOGAPS analyses (bottom) over the full 2 year data set. NFLUX shows an overall moist bias, with the largest differences in the tropics. NOGAPS shows an overall dry bias, with the largest differences in the western Atlantic and western Pacific.

Figure 12 shows the 2 year annual specific humidity difference between NFLUX and NOGAPS (left), along with the zonal average (right). With the general warm bias in NFLUX and the cold bias in NOGAPS, it is not surprising to see the large differences between the two systems, especially within the tropics. This also agrees well with NFLUX air temperature generally being warmer than NOGAPS. Conversely, NFLUX showed cooler temperature than NOGAPS in the Southern Ocean. In this area, NFLUX also shows drier conditions than NOGAPS, although there are no *in situ* observations available for validation.

NFLUX versus NOGAPS specific humidity estimates are compared using assimilated and unassimilated *in situ* matchups (Table 5). The means and standard deviations are all significantly different. In the open ocean, NFLUX has a much smaller mean bias compared to NOGAPS using both assimilated and unassimilated matchups. However, NOGAPS has a smaller standard deviation which leads to a higher correlation compared to NFLUX.

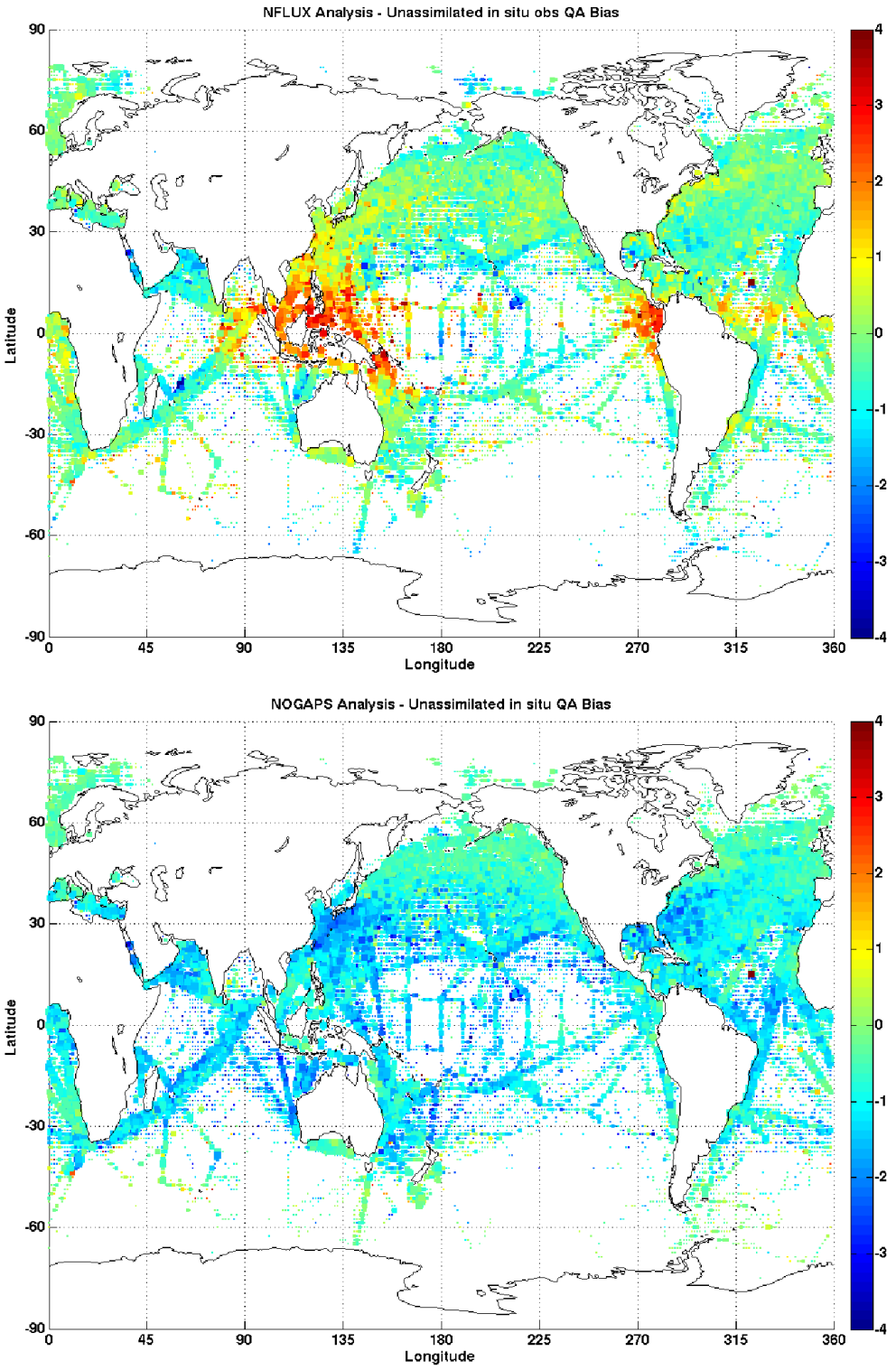

Figure 11: Global 2-year average specific humidity bias (g/kg). The NFLUX (NOGAPS) bias compared to unassimilated observations is shown in the top (bottom) panel. Colored square sizes represent the number of observations in each grid box, ranging from 5 to 50 observations.

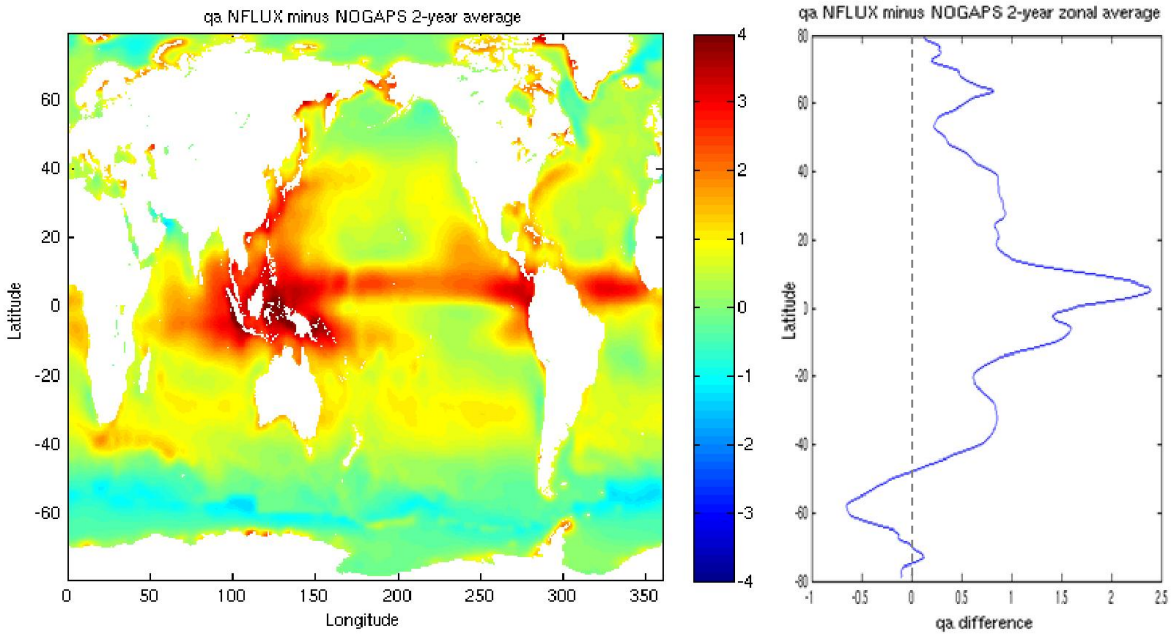

Figure 12: Global 2-year average NFLUX minus NOGAPS specific humidity difference (g/kg). The left panel shows the global gridded difference. The right panel shows the zonally averaged difference.

Table 5: Specific humidity errors over the global ocean. Errors are shown relative to both assimilated (left columns) and unassimilated (right columns) *in situ* observations for all comparisons (global), near land (coastal), and open ocean (ocean). The best test statistic in each column is highlighted in blue. Means and standard deviations that are not significantly different compared to NFLUX at the 95% confidence interval are denoted with an asterisk (*).

	ME	SD	RMSE	R^2		ME	SD	RMSE	R^2
Global		N = 429701							
NFLUX Analysis	0.2363	1.9380	1.9523	0.8849	NFLUX 12h persist	0.2344	2.1288	2.1416	0.8623
NOGAPS Analysis	-0.5267	1.8208	1.8955	0.8969	NOGAPS 12h persist	-0.5433	2.0700	2.1401	0.8660
NOGAPS 12h fcst	-0.7130	1.9554	2.0813	0.8812					
Coastal		N = 189510							
NFLUX Analysis	0.4299	2.0838	2.1277	0.8628	NFLUX 12h persist	0.4249	2.2912	2.3303	0.8350
NOGAPS Analysis	-0.3838	2.1863	2.2197	0.8489	NOGAPS 12h persist	-0.3920	2.4024	2.4342	0.8168
NOGAPS 12h fcst	-0.5341	2.3057	2.3667	0.8318					
Ocean		N = 240191							
NFLUX Analysis	0.0836	1.8001	1.8020	0.9021	NFLUX 12h persist	0.0841	1.9783	1.9801	0.8828
NOGAPS Analysis	-0.6395	1.4599	1.5938	0.9324	NOGAPS 12h persist	-0.6627	1.7549	1.8759	0.9015
NOGAPS 12h fcst	-0.8541	1.6127	1.8249	0.9176					

Scatterplots of NFLUX and NOGAPS specific humidity versus assimilated (unassimilated) *in situ* observations, as well as histograms of the probability of the mean bias, are shown in Figure 13 (Figure 14). Both the assimilated and unassimilated matchups are very similar. From approximately 4 g/kg to 18 g/kg NFLUX shows a fairly close one-to-one relationship with the *in situ* observations. In this range, NOGAPS also shows a closer linear relationship; however, the one-to-one fit is shifted to reveal an overall dry bias. Less than approximately 4 g/kg, a slight moist bias can be seen in each of the products.

At high specific humidity values, greater than approximately 18 g/kg, NFLUX and NOGAPS show very different patterns. NOGAPS displays a capping effect, similar to that seen with air temperature. The majority of NOGAPS observations remain lower than 20 g/kg while the *in situ* observations reach 25 g/kg, which causes a dry bias. NFLUX does not show the same capping effect that is seen with NOGAPS. Instead, NFLUX displays a more one-to-one relationship at high specific humidity values; however, the spread for NFLUX observations becomes larger as the specific humidity increases. This causes a larger standard deviation, which reduces the correlation, as seen in Table 5.

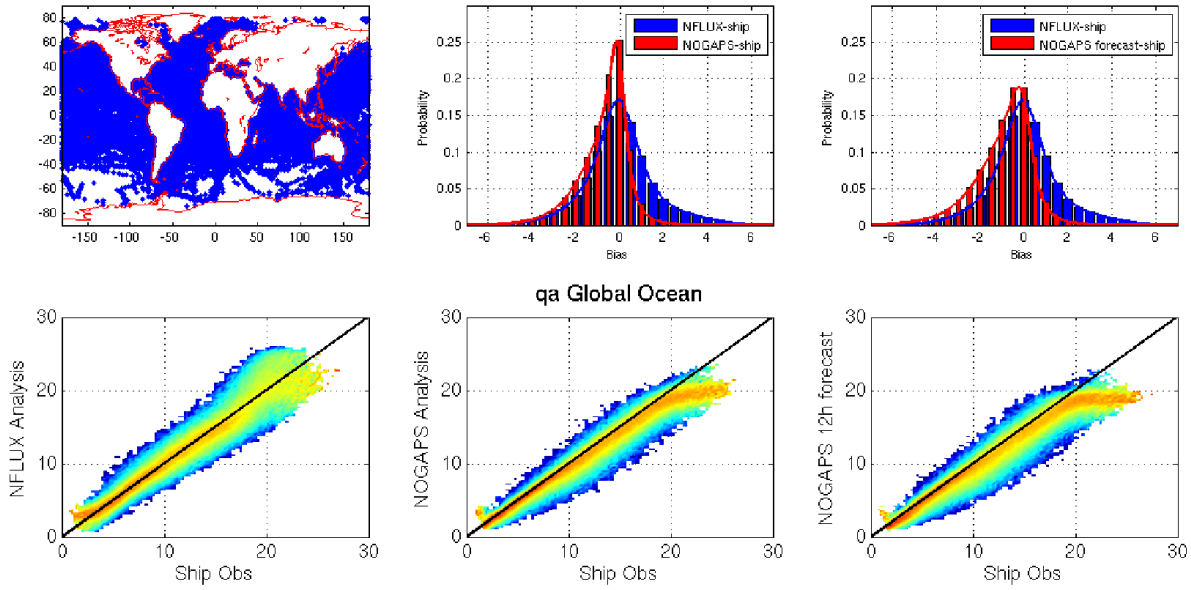

Figure 13: Specific humidity over global open ocean using assimilated *in situ* data. The distribution of the matched up observations is shown in the top left panel. The top middle (right) panel shows a histogram of the probability of the mean bias of NFLUX analysis, shown in blue, and NOGAPS analysis (NOGAPS 12-hour forecast), shown in red. The bottom panels show scatterplots of the *in situ* observations versus NFLUX analysis (left), NOGAPS analysis (middle), and NOGAPS 12-hour forecast (right).

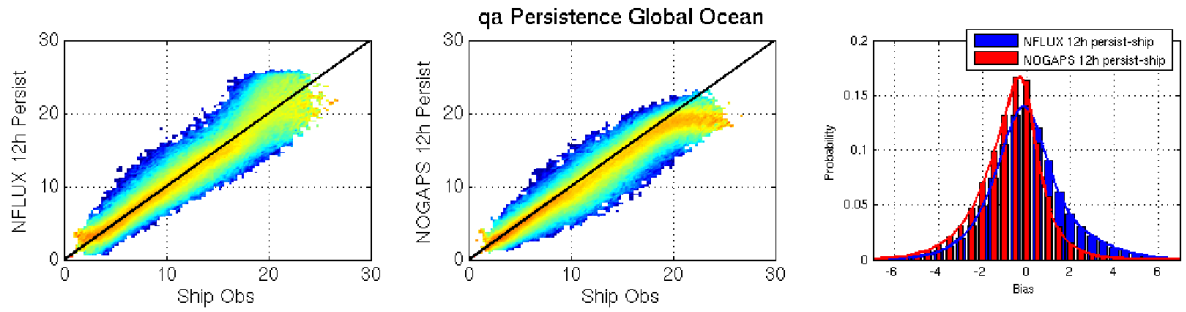

Figure 14: Specific humidity over global open ocean using unassimilated *in situ* data. The right panel shows a histogram of the probability of the mean bias of NFLUX analysis (blue) and NOGAPS analysis (red). Scatterplots of the *in situ* observations versus NFLUX analysis (left) and NOGAPS analysis (middle) are also shown.

3.2.1 Latitude Bands

Specific humidity open ocean matchups by latitude band are presented in Table 6, while the corresponding scatterplots using assimilated (unassimilated) observations are shown in Figure 15 (Figure 16). For both assimilated and unassimilated matchups, NFLUX has a lower mean bias than NOGAPS in all latitude bands except the 0°N to 15°N band. The NOGAPS analysis generally performs better in the remaining test statistics. The scatterplots show the large spread at high specific humidity values in most of the bands which increases the standard deviation and lowers the correlation for NFLUX. It is interesting to note that both NFLUX and NOGAPS have higher errors in the 0°N to 15°N band compared to the other bands; however, further investigation is required to know the reasons for the large errors.

Table 6: Specific humidity errors over the global open ocean by latitude band. Errors are shown relative to both assimilated (left columns) and unassimilated (right columns) *in situ* observations. The best test statistic in each column is highlighted in blue. Means and standard deviations that are not significantly different compared to NFLUX at the 95% confidence interval are denoted with an asterisk (*).

	ME	SD	RMSE	R^2		ME	SD	RMSE	R^2
Latitude 45 to 90		N = 83190							
NFLUX Analysis	0.0179	0.8733	0.8735	0.8502	NFLUX 12h persist	0.0069	1.1096	1.1096	0.7629
NOGAPS Analysis	-0.2156	0.5965	0.6342	0.9206	NOGAPS 12h persist	-0.2299	0.9791	1.0057	0.7940
NOGAPS 12h fcst	-0.3067	0.7318	0.7935	0.8876					
Latitude 30 to 45		N = 44823							
NFLUX Analysis	-0.0902	1.4657	1.4685	0.8551	NFLUX 12h persist	-0.0945	1.7844	1.7869	0.7898
NOGAPS Analysis	-0.8509	1.2605	1.5208	0.8939	NOGAPS 12h persist	-0.8897	1.7435	1.9573	0.8031
NOGAPS 12h fcst	-1.0753	1.4394	1.7967	0.8651					
Latitude 15 to 30		N = 52019							
NFLUX Analysis	0.1323	2.0152	2.0195	0.7462	NFLUX 12h persist	0.1393	2.2067	2.2111	0.7011
NOGAPS Analysis	-0.8404	1.4717	1.6947	0.8561	NOGAPS 12h persist	-0.8553	1.8350	2.0245	0.7818
NOGAPS 12h fcst	-1.1262	1.6395	1.9891	0.8213					
Latitude 0 to 15		N = 26083							
NFLUX Analysis	0.9710	3.2555	3.3972	0.2757	NFLUX 12h persist	1.0004	3.3328	3.4796	0.2554
NOGAPS Analysis	-0.5892	2.8875	2.9469	0.3699	NOGAPS 12h persist	-0.6016	3.0052	3.0648	0.3075
NOGAPS 12h fcst	-0.9901	2.9898	3.1494	0.3197					
Latitude -15 to 0		N = 11564							
NFLUX Analysis	-0.0324	2.1353	2.1354	0.5448	NFLUX 12h persist	-0.0037	2.2547	2.2546	0.5074
NOGAPS Analysis	-1.3407	1.3110	1.8752	0.7518	NOGAPS 12h persist	-1.3807	1.5600	2.0832	0.6490
NOGAPS 12h fcst	-1.6351	1.5164	2.2300	0.6672					
Latitude -90 to -15		N = 22512							
NFLUX Analysis	-0.4088	1.4930	1.5479	0.8793	NFLUX 12h persist	-0.4193	1.6772	1.7288	0.8489
NOGAPS Analysis	-1.0187	1.2114	1.5828	0.9196	NOGAPS 12h persist	-1.0669	1.5676	1.8962	0.8642
NOGAPS 12h fcst	-1.2488	1.4248	1.8946	0.8880					

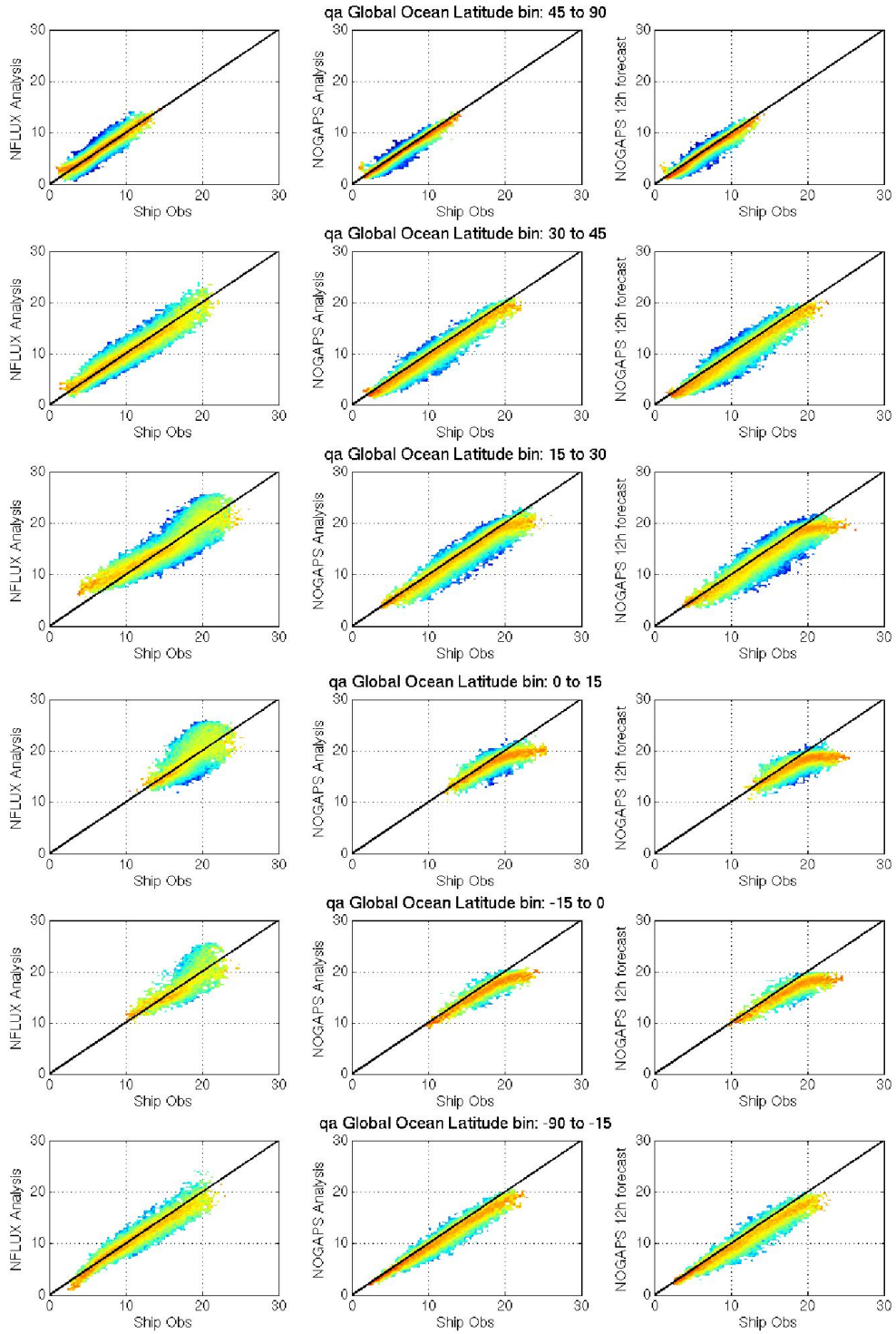

Figure 15: Specific humidity over global open ocean by latitude using assimilated *in situ* data. Scatterplots of the *in situ* observations versus NFLUX analysis (left), NOGAPS analysis (middle), and NOGAPS 12-hour forecast (right) are shown.

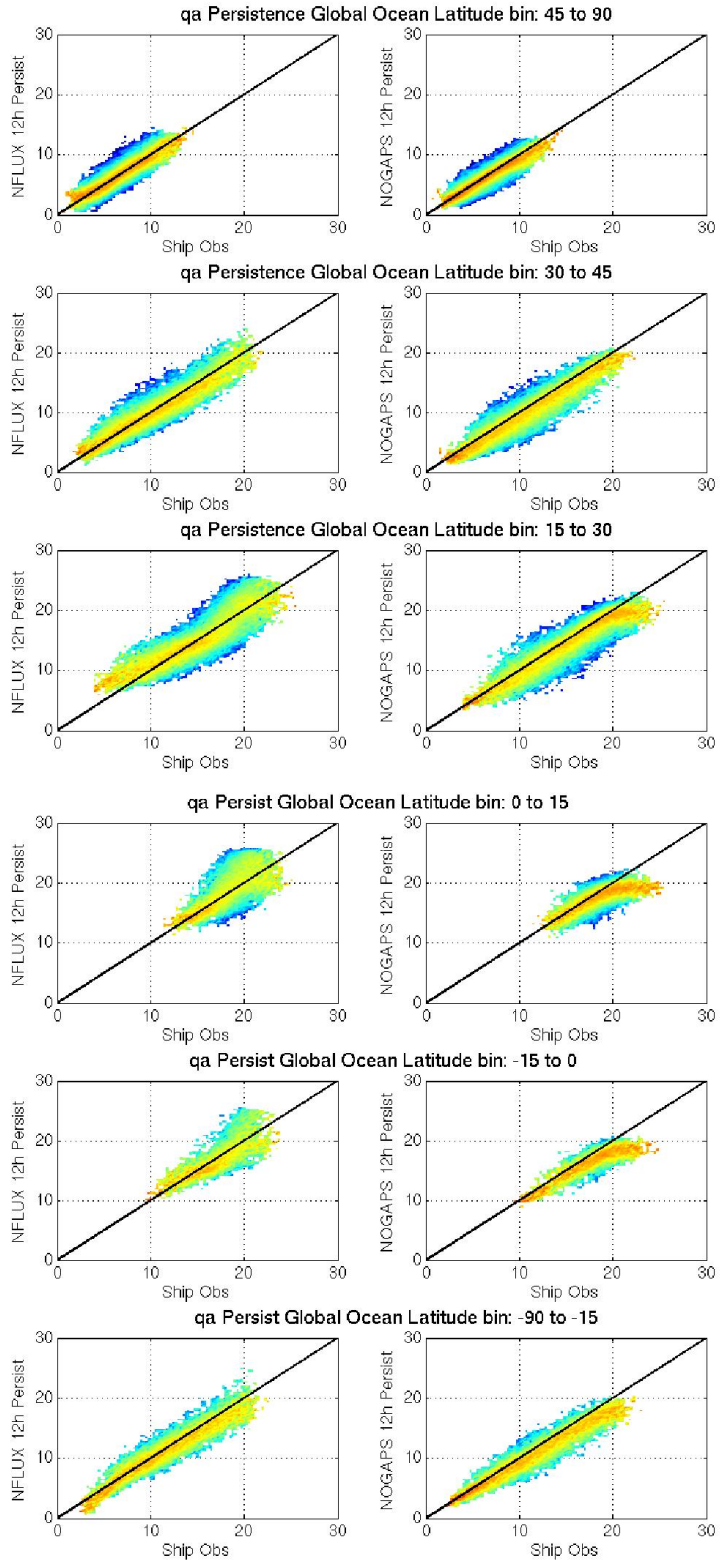

Figure 16: Specific humidity over global open ocean by latitude using unassimilated *in situ* data. Scatterplots of the *in situ* observations versus NFLUX analysis (left) and NOGAPS analysis (right) are shown.

3.2.2 Seasonal

The open ocean specific humidity seasonal errors are shown in Table 7, with scatterplots using assimilated (unassimilated) observations shown in Figure 17 (Figure 18). The results are similar to those already presented. Using both assimilated and unassimilated observations, NFLUX shows a smaller mean bias compared to NOGAPS products. NOGAPS has smaller errors in the remaining test statistics. Although NOGAPS shows a capping effect at high specific humidity values, it also has less spread in the observations which results in a smaller standard deviation and higher correlation.

Table 7: Specific humidity errors over the global open ocean by season. Errors are shown relative to both assimilated (left columns) and unassimilated (right columns) *in situ* observations. The best test statistic in each column is highlighted in blue. Means and standard deviations that are not significantly different compared to NFLUX at the 95% confidence interval are denoted with an asterisk (*).

	ME	SD	RMSE	R^2		ME	SD	RMSE	R^2
DJF		N = 66699							
NFLUX Analysis	-0.0845	1.6961	1.6982	0.9097	NFLUX 12h persist	-0.0881	1.8931	1.8952	0.8884
NOGAPS Analysis	-0.7581	1.4446	1.6315	0.9341	NOGAPS 12h persist	-0.7887	1.7682	1.9361	0.9001
NOGAPS 12h fcst	-1.0065	1.5811	1.8743	0.9209					
MAM		N = 52777							
NFLUX Analysis	-0.2045	1.7079	1.7201	0.9097	NFLUX 12h persist	-0.2225	1.8795	1.8926	0.8915
NOGAPS Analysis	-0.5734	1.4371	1.5472	0.9355	NOGAPS 12h persist	-0.6062	1.7086	1.8129	0.9076
NOGAPS 12h fcst	-0.7760	1.5806	1.7608	0.9228					
JJA		N = 56326							
NFLUX Analysis	0.3949	1.8451	1.8869	0.8898	NFLUX 12h persist	0.3971	1.9805	2.0199	0.8742
NOGAPS Analysis	-0.4776	1.4325	1.5100	0.9280	NOGAPS 12h persist	-0.5010	1.6789	1.7521	0.9004
NOGAPS 12h fcst	-0.6567	1.5804	1.7114	0.9133					
SON		N = 64389							
NFLUX Analysis	0.2215	1.8808	1.8938	0.8882	NFLUX 12h persist	0.2399	2.0839	2.0977	0.8640
NOGAPS Analysis	-0.7124	1.5013	1.6618	0.9239	NOGAPS 12h persist	-0.7199	1.8292	1.9658	0.8861
NOGAPS 12h fcst	-0.9329	1.6764	1.9185	0.9049					

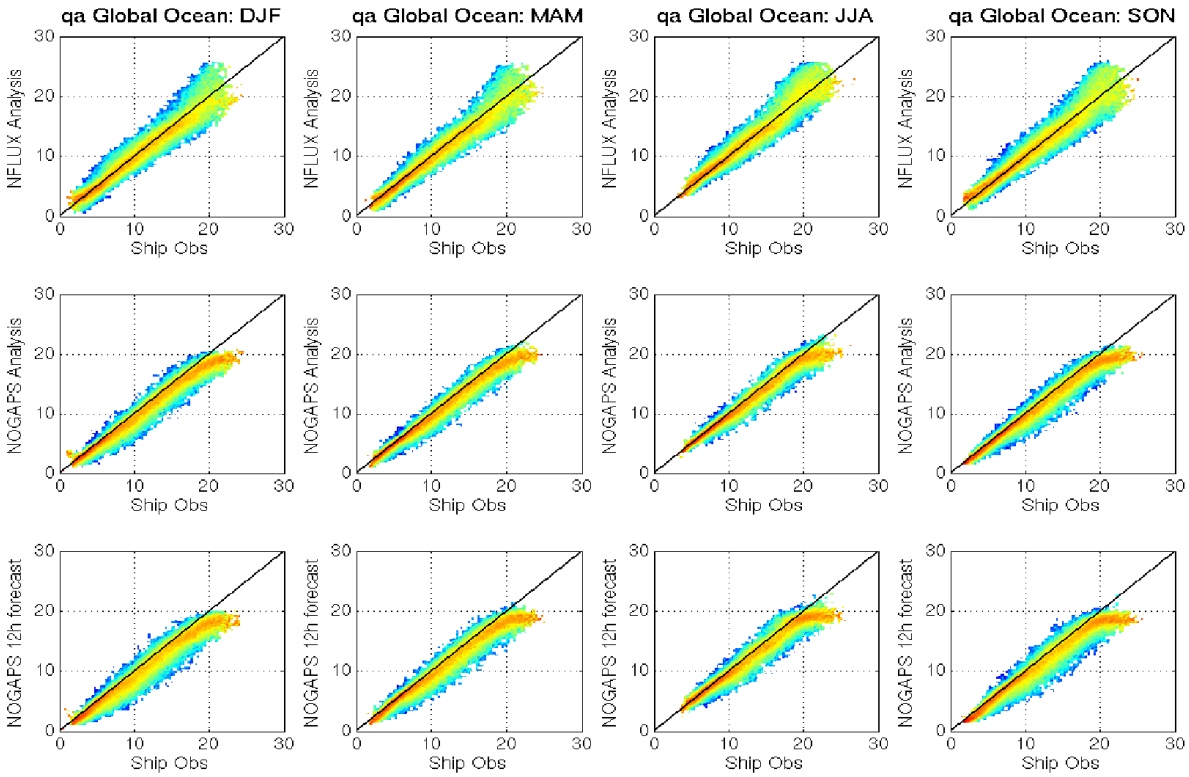

Figure 17: Specific humidity over global open ocean by season using assimilated *in situ* data. Scatterplots of the *in situ* observations versus NFLUX analysis (top), NOGAPS analysis (middle), and NOGAPS 12-hour forecast (bottom) are shown.

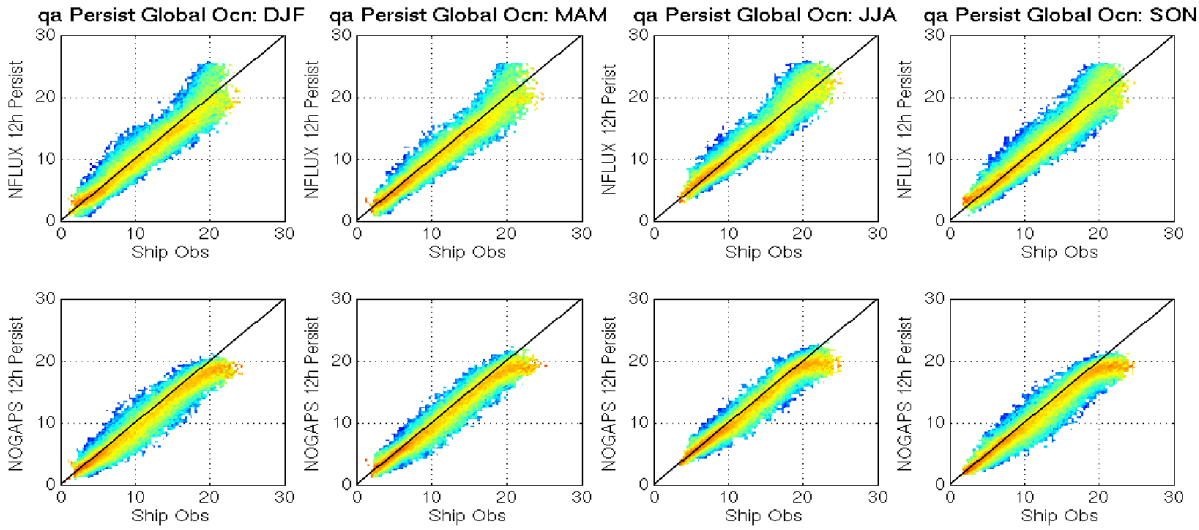

Figure 18: Specific humidity over global open ocean by season using unassimilated *in situ* data. Scatterplots of the *in situ* observations versus NFLUX analysis (top) and NOGAPS analysis (bottom) are shown.

3.3 Wind Speed Results

Figure 19 shows mean wind speed error using unassimilated *in situ* observations of the NFLUX analyses (top) and the NOGAPS analyses (bottom) over the full 2 year data set. The wind speed error has a more random spatial pattern than either air temperature or specific humidity. In general, NFLUX shows a high wind speed bias in the north Atlantic and western Pacific and a slight low wind speed bias in the eastern Pacific. NOGAPS shows an overall low wind speed bias, with the largest differences in the eastern tropical Atlantic and north Pacific.

Figure 20 shows the global 2-year annual wind speed difference between NFLUX and NOGAPS analysis fields (left), with the zonal average of the difference (right). NFLUX shows stronger wind speeds globally compared to NOGAPS, which follows from NOGAPS showing an overall low wind speed bias from Figure 19. Also to note from Figure 20 is the large difference along much of the coastlines. This is due to NOGAPS having a coarser resolution than NFLUX and the relatively smooth topography along the coast.

Wind speed errors using assimilated and unassimilated *in situ* matchups are presented in Table 8. In the open ocean using assimilated and unassimilated matchups, NFLUX shows a smaller mean bias compared to NOGAPS. NOGAPS analysis (NOGAPS 12-hour forecast) shows smaller (larger) errors for the remaining test statistics except for the RMS using unassimilated matchups. Each of the means and standard deviations are significantly different at the 95% confidence interval.

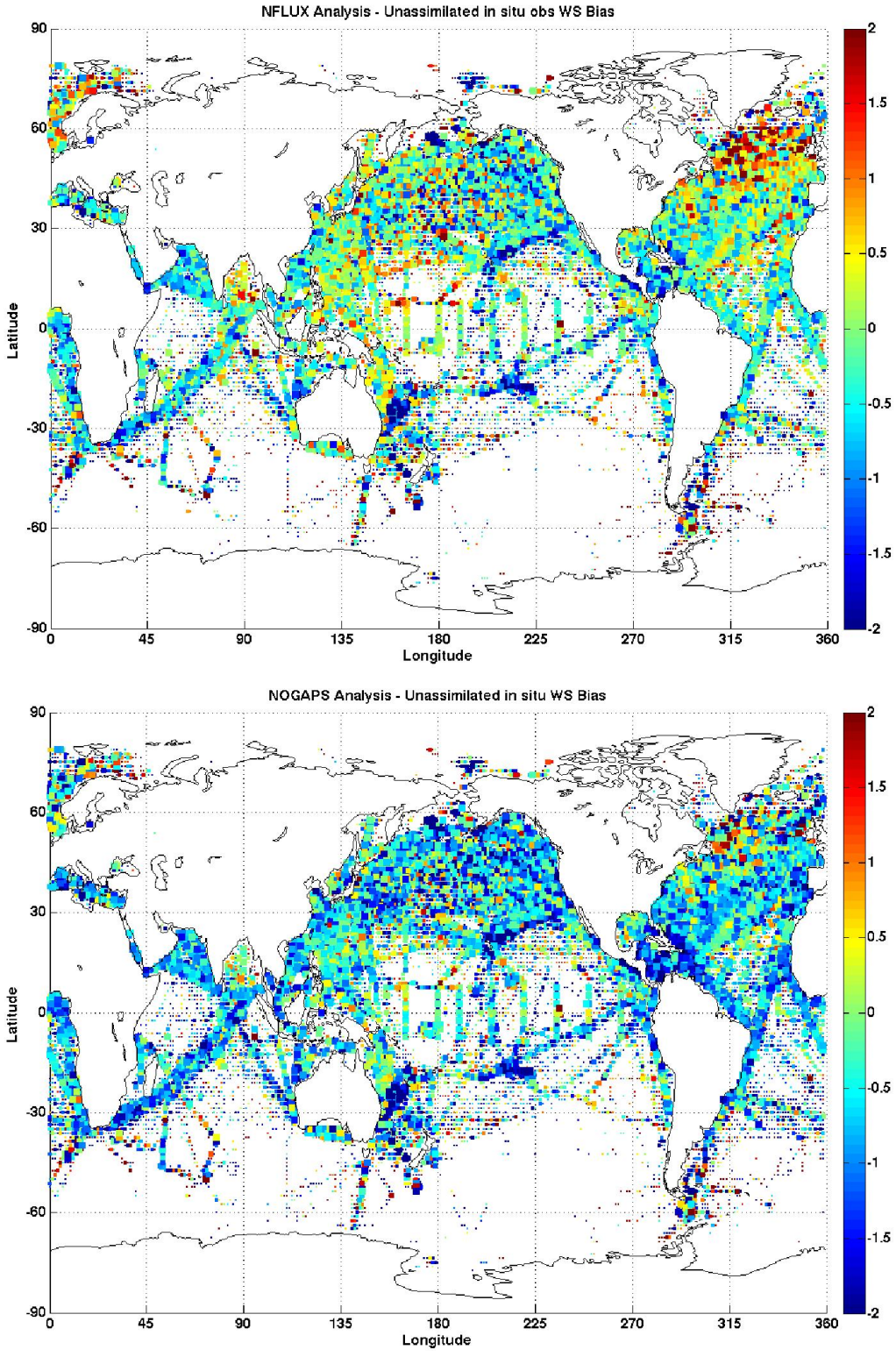

Figure 19: Global 2-year average wind speed bias (m/s). The NFLUX (NOGAPS) bias compared to unassimilated observations is shown in the top (bottom) panel. Colored square sizes represent the number of observations in each grid box, ranging from 5 to 50 observations.

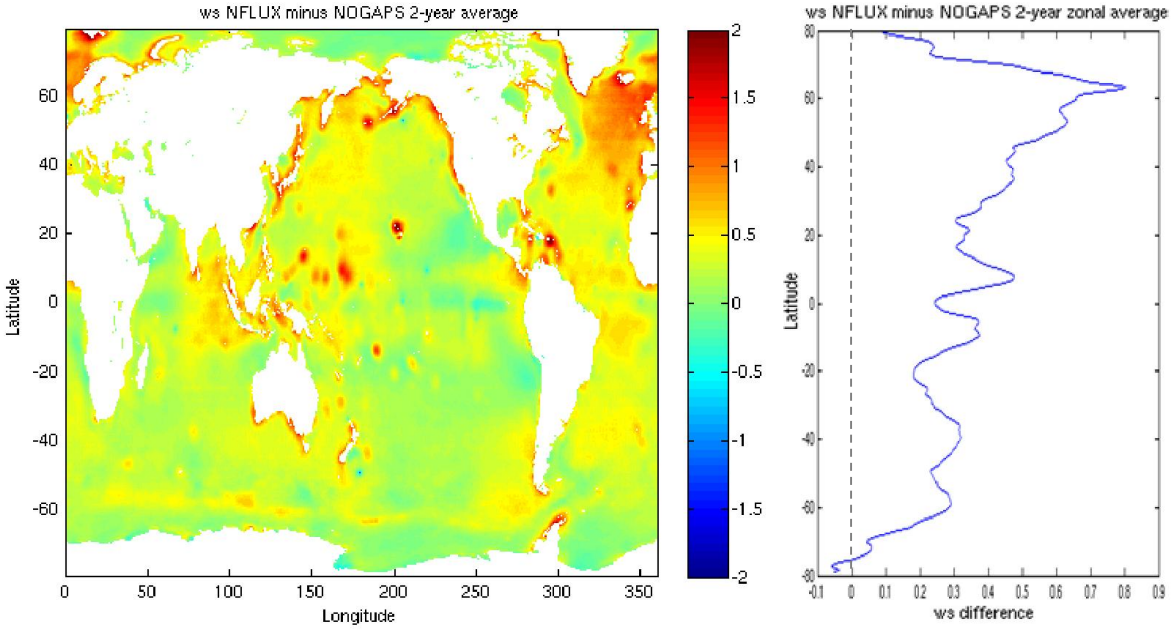

Figure 20: Global 2-year average NFLUX minus NOGAPS wind speed difference (m/s). The left panel shows the global gridded difference. The right panel shows the zonally averaged difference.

Table 8: Wind speed errors over the global ocean. Errors are shown relative to both assimilated (left columns) and unassimilated (right columns) *in situ* observations for all comparisons (global), near land (coastal), and open ocean (ocean). The best test statistic in each column is highlighted in blue. Means and standard deviations that are not significantly different compared to NFLUX at the 95% confidence interval are denoted with an asterisk (*).

	ME	SD	RMSE	R^2		ME	SD	RMSE	R^2
Global		N = 763868							
NFLUX Analysis	-0.1490	2.2148	2.2198	0.6281	NFLUX 12h persist	-0.1526	3.1379	3.1416	0.3297
NOGAPS Analysis	-0.6784	2.1934	2.2959	0.6348	NOGAPS 12h persist	-0.6826	*3.1399	3.2132	0.3282
NOGAPS 12h fcst	-0.5417	2.3316	2.3936	0.5967					
Coastal		N = 343507							
NFLUX Analysis	-0.3360	2.4126	2.4359	0.5927	NFLUX 12h persist	-0.3409	3.3506	3.3679	0.2962
NOGAPS Analysis	-0.9441	*2.4202	2.5978	0.5884	NOGAPS 12h persist	-0.9473	*3.3656	3.4964	0.2854
NOGAPS 12h fcst	-0.7220	2.5515	2.6517	0.5536					
Ocean		N = 420361							
NFLUX Analysis	0.0038	2.0263	2.0263	0.6569	NFLUX 12h persist	0.0012	2.9437	2.9437	0.3479
NOGAPS Analysis	-0.4612	1.9624	2.0159	0.6776	NOGAPS 12h persist	-0.4663	2.9249	2.9618	0.3556
NOGAPS 12h fcst	-0.3944	2.1237	2.1600	0.6310					

Scatterplots of NFLUX and NOGAPS wind speed versus assimilated (unassimilated) *in situ* observations, as well as corresponding histograms of the probability of the mean bias, are shown in Figure 21 (Figure 22). Unlike the scatterplots shown for air temperature and specific humidity which showed a relatively close one-to-one relationship, both NFLUX and NOGAPS show a very large spread in wind speed, with the unassimilated matchups being broader than the assimilated matchups. At low wind speeds, NFLUX and NOGAPS both show a high bias. At high wind speeds, both NFLUX and NOGAPS show a low bias.

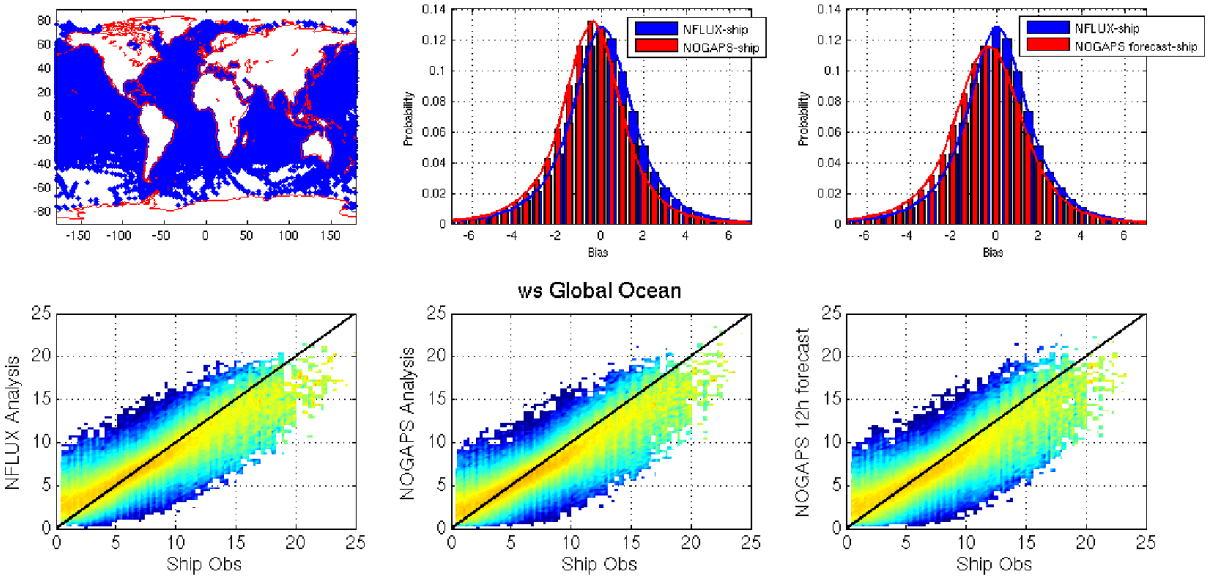

Figure 21: Wind speed over global open ocean using assimilated *in situ* data. The distribution of the matched up observations is shown in the top left panel. The top middle (right) panel shows a histogram of the probability of the mean bias of NFLUX analysis, shown in blue, and NOGAPS analysis (NOGAPS 12-hour forecast), shown in red. The bottom panels show scatterplots of the *in situ* observations versus NFLUX analysis (left), NOGAPS analysis (middle), and NOGAPS 12-hour forecast (right).

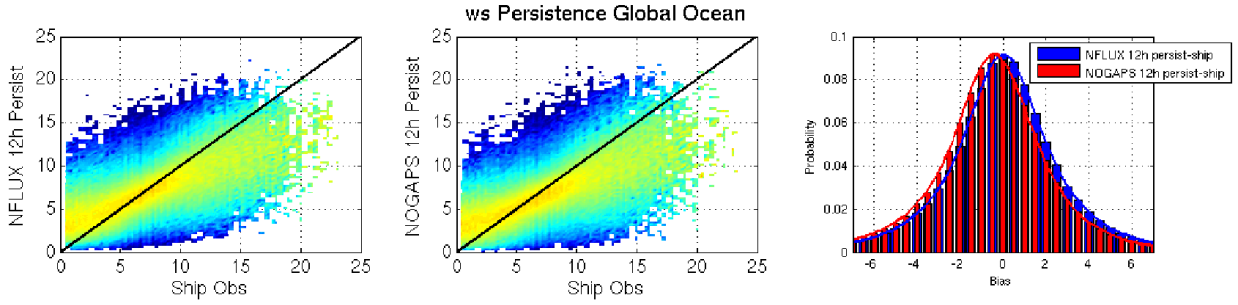

Figure 22: Wind speed over global open ocean using unassimilated *in situ* data. The right panel shows a histogram of the probability of the mean bias of NFLUX analysis (blue) and NOGAPS analysis (red). Scatterplots of the *in situ* observations versus NFLUX analysis (left) and NOGAPS analysis (middle) are also shown.

3.3.1 Latitude Bands

The open ocean wind speed results by latitude band are shown in Table 9. The corresponding scatterplots using assimilated (unassimilated) *in situ* observations shown in Figure 23 (Figure 24). NFLUX has a lower mean bias than NOGAPS in all latitude bands with both assimilated and unassimilated matchups, except for the 45°N to 90°N latitude band using assimilated matchups.

Using assimilated matchups, NFLUX has smaller errors in the remaining test statistics compared to NOGAPS in the tropics, the 15°S to 15°N latitude bands. As seen with the scatterplots (Figure 23), these two latitude bands have wind speeds less than approximately 13 m/s which reduces the low wind speed bias at high wind speeds. In the 15°N to 45°N latitude bands, NFLUX shows a smaller RMS than NOGAPS; however, the NOGAPS analysis has a smaller standard deviation and higher correlation. In the remaining latitude bands, 90°S to 15°S and 45°N to 90°N, the NOGAPS analysis has smaller errors in the remaining test statistics.

Using unassimilated matchups, NFLUX shows improvement over NOGAPS over an extended area, from 15°S to 45°N. Similar to using assimilated matchups, the two poleward latitude bands, 90°S to 15°S and 45°N to 90°N, NOGAPS has smaller errors in the remaining test statistics.

Table 9: Wind speed errors over the global open ocean by latitude band. Errors are shown relative to both assimilated (left columns) and unassimilated (right columns) *in situ* observations. The best test statistic in each column is highlighted in blue. Means and standard deviations that are not significantly different compared to NFLUX at the 95% confidence interval are denoted with an asterisk (*).

	ME	SD	RMSE	R^2		ME	SD	RMSE	R^2
Latitude 45 to 90		N = 104128							
NFLUX Analysis	0.2701	2.2794	2.2953	0.7058	NFLUX 12h persist	0.2755	3.8758	3.8855	0.2695
NOGAPS Analysis	-0.3639	2.0971	2.1284	0.7511	NOGAPS 12h persist	-0.3638	3.8065	3.8238	0.2985
NOGAPS 12h fcst	-0.1356	*2.2912	2.2952	0.7085					
Latitude 30 to 45		N = 64699							
NFLUX Analysis	-0.0601	2.3923	2.3930	0.6203	NFLUX 12h persist	-0.0658	3.6225	3.6230	0.2534
NOGAPS Analysis	-0.5455	2.3577	2.4200	0.6331	NOGAPS 12h persist	-0.5551	*3.6296	3.6718	0.2583
NOGAPS 12h fcst	-0.4678	2.5015	2.5449	0.5955					
Latitude 15 to 30		N = 73890							
NFLUX Analysis	-0.0945	1.8720	1.8743	0.6179	NFLUX 12h persist	-0.1002	2.4621	2.4641	0.3814
NOGAPS Analysis	-0.5232	1.8504	1.9229	0.6263	NOGAPS 12h persist	-0.5311	2.4933	2.5492	0.3688
NOGAPS 12h fcst	-0.4356	1.9849	2.0321	0.5746					
Latitude 0 to 15		N = 86531							
NFLUX Analysis	-0.0095	1.7412	1.7412	0.5511	NFLUX 12h persist	-0.0180	1.9834	1.9835	0.4348
NOGAPS Analysis	-0.4163	1.7692	1.8175	0.5384	NOGAPS 12h persist	-0.4241	2.0096	2.0539	0.4229
NOGAPS 12h fcst	-0.4968	1.9249	1.9880	0.4674					
Latitude -15 to 0		N = 65060							
NFLUX Analysis	-0.0486	1.4708	1.4716	0.5694	NFLUX 12h persist	-0.0517	1.6984	1.6992	0.4450
NOGAPS Analysis	-0.4157	1.4947	1.5514	0.5560	NOGAPS 12h persist	-0.4180	1.7180	1.7681	0.4326
NOGAPS 12h fcst	-0.4236	1.6433	1.6970	0.4802					
Latitude -90 to -15		N = 26053							
NFLUX Analysis	-0.4486	2.3076	2.3507	0.5475	NFLUX 12h persist	-0.4445	3.0303	3.0627	0.2877
NOGAPS Analysis	-0.7270	2.2183	2.3343	0.5793	NOGAPS 12h persist	-0.7322	2.9724	3.0612	0.3043
NOGAPS 12h fcst	-0.7155	2.3662	2.4720	0.5281					

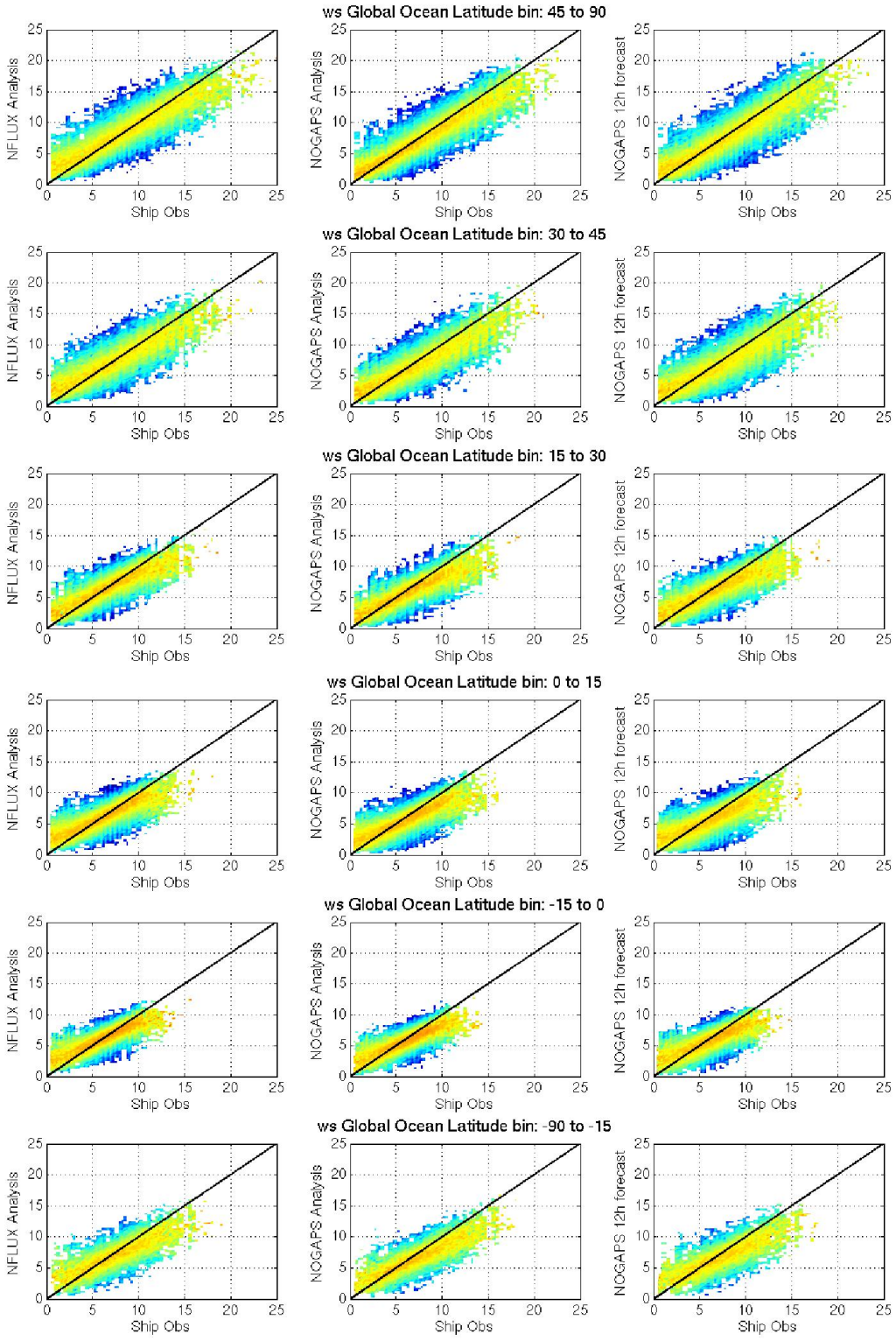

Figure 23: Wind speed over global open ocean by latitude using assimilated *in situ* data. Scatterplots of the *in situ* observations versus NFLUX analysis (left), NOGAPS analysis (middle), and NOGAPS 12-hour forecast (right) are shown.

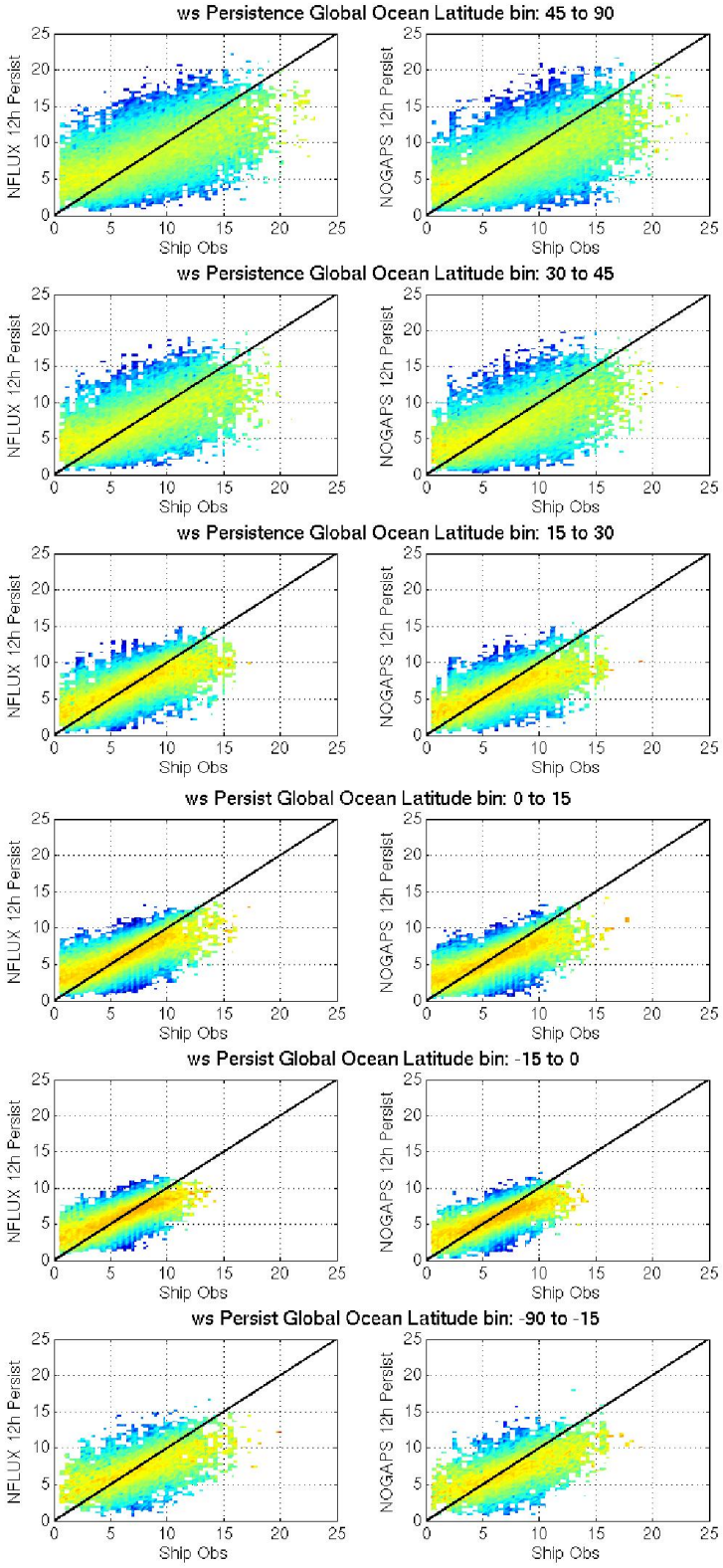

Figure 24: Wind speed over global open ocean by latitude using unassimilated *in situ* data. Scatterplots of the *in situ* observations versus NFLUX analysis (left) and NOGAPS analysis (right) are shown.

3.3.2 Seasonal

The open ocean wind speed results by season are shown in Table 10, with the corresponding scatterplots using assimilated (unassimilated) *in situ* observations shown in Figure 25 (Figure 26). As seen with the latitude banding, NFLUX has improved skill over each of the NOGAPS products for the mean bias in each season. Using assimilated matchups, the NOGAPS analysis has reduced errors in the remaining test statistics than NFLUX; however, NFLUX does show improvement over the NOGAPS 12-hour forecasts. Using the unassimilated matchups, the DJF and MAM seasons do not have significantly different standard deviations at the 95% confidence interval. NFLUX shows a smaller RMS in each season than NOGAPS; however, NOGAPS has smaller standard deviations and larger correlations than NFLUX.

Table 10: Wind speed errors over the global open ocean by season. Errors are shown relative to both assimilated (left columns) and unassimilated (right columns) *in situ* observations. The best test statistic in each column is highlighted in blue. Means and standard deviations that are not significantly different compared to NFLUX at the 95% confidence interval are denoted with an asterisk (*).

	ME	SD	RMSE	R^2		ME	SD	RMSE	R^2
DJF		N = 112196							
NFLUX Analysis	0.0181	2.1997	2.1998	0.6679	NFLUX 12h persist	0.0178	3.2857	3.2857	0.3385
NOGAPS Analysis	-0.4684	2.1365	2.1872	0.6869	NOGAPS 12h persist	-0.4711	*3.2778	3.3115	0.3442
NOGAPS 12h fcst	-0.3886	2.2939	2.3266	0.6469					
MAM		N = 94957							
NFLUX Analysis	0.0105	1.9885	1.9885	0.6389	NFLUX 12h persist	0.0061	2.8659	2.8659	0.3300
NOGAPS Analysis	-0.4398	1.9325	1.9819	0.6570	NOGAPS 12h persist	-0.4467	*2.8483	2.8831	0.3329
NOGAPS 12h fcst	-0.3724	2.0938	2.1266	0.6066					
JJA		N = 102180							
NFLUX Analysis	0.0086	1.8615	1.8615	0.6072	NFLUX 12h persist	0.0052	2.5633	2.5633	0.3223
NOGAPS Analysis	-0.4375	1.8003	1.8527	0.6317	NOGAPS 12h persist	-0.4417	2.5316	2.5698	0.3367
NOGAPS 12h fcst	-0.3965	1.9632	2.0028	0.5708					
SON		N = 111028							
NFLUX Analysis	-0.0209	2.0207	2.0208	0.6681	NFLUX 12h persist	-0.0233	2.9710	2.9710	0.3537
NOGAPS Analysis	-0.4939	1.9466	2.0083	0.6920	NOGAPS 12h persist	-0.5009	2.9485	2.9907	0.3648
NOGAPS 12h fcst	-0.4170	2.1122	2.1529	0.6470					

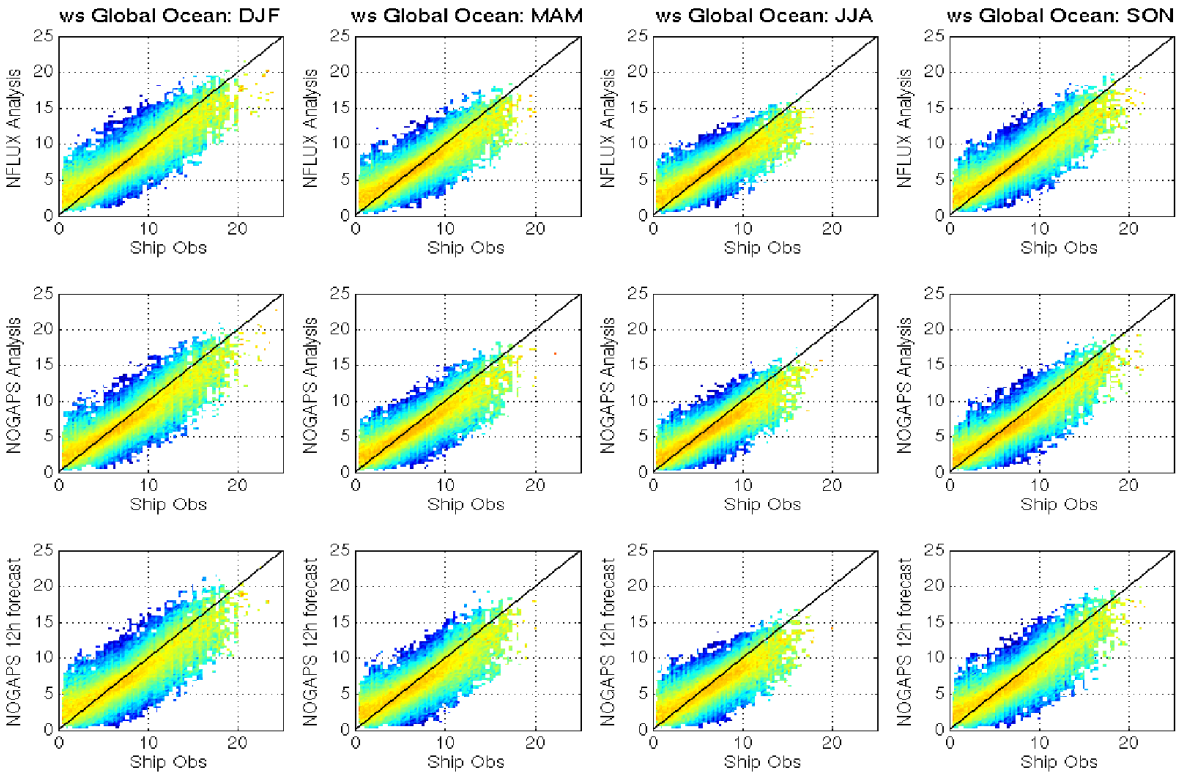

Figure 25: Wind speed over global open ocean by season using assimilated *in situ* data. Scatterplots of the *in situ* observations versus NFLUX analysis (top), NOGAPS analysis (middle), and NOGAPS 12-hour forecast (bottom) are shown.

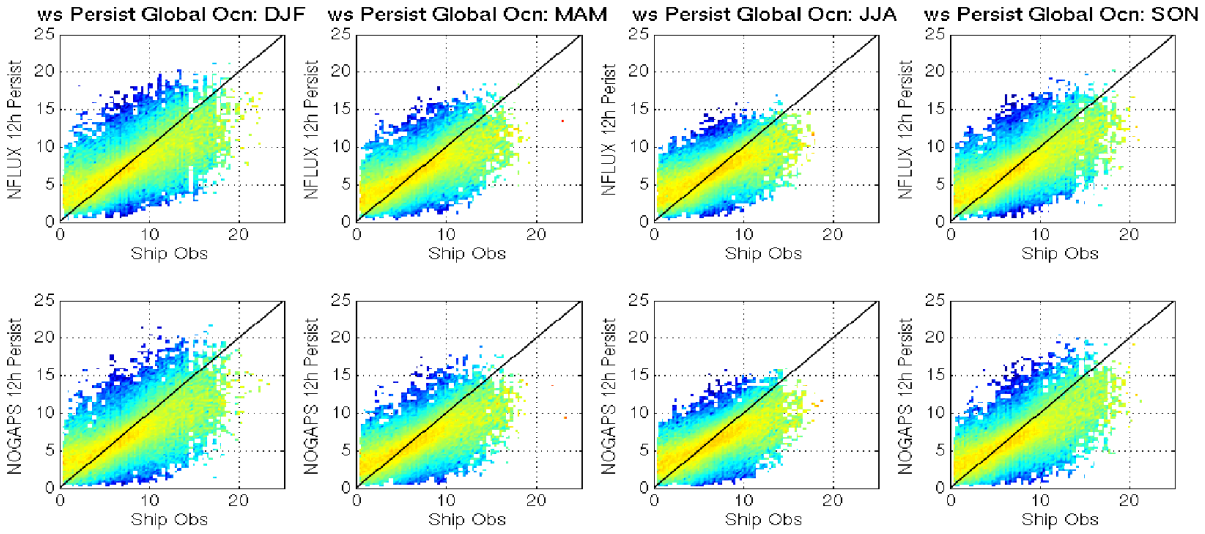

Figure 26: Wind speed over global open ocean by season using unassimilated *in situ* data. Scatterplots of the *in situ* observations versus NFLUX analysis (top) and NOGAPS analysis (bottom) are shown.

4.0 TEST CASE 2: EASTERN PACIFIC

The eastern Pacific domain spans from 160°-114°W and 29°-60°N with a horizontal resolution of .2 degrees. The grid has 231 x 156 grid points. The NFLUX grid domain and resolution matches the eastern Pacific COAMPS domain. The COAMPS 12-hour forecast is blended with the previous NFLUX correction field to generate the background field for the NFLUX analysis. NFLUX analysis performance is compared against both the eastern Pacific COAMPS analysis and 12-hour forecast fields, as well as the global NOGAPS analysis and 12-hour forecast fields over the eastern Pacific. Validation statistics are calculated for both the assimilated and unassimilated *in situ* matchup data.

4.1 Air Temperature Results

Figure 27 shows mean air temperature error over the eastern Pacific using unassimilated *in situ* observations and NFLUX (top), COAMPS (middle left), and NOGAPS (bottom left). Gridded annual differences are also shown for NFLUX versus COAMPS (middle right) and NOGAPS (bottom right). Compared with the *in situ* matchups, both NFLUX and NOGAPS show near neutral to slightly cold biases. Therefore, the annual difference between NFLUX and NOGAPS shows very little change, with the exception of the west coast of Mexico. In this area NFLUX is warmer than NOGAPS. Unlike NFLUX or NOGAPS, COAMPS shows a very noticeable cold bias throughout the entire region compared to the *in situ* observations. This causes NFLUX to be significantly warmer than COAMPS in the annual comparison of the two systems. Similar to the comparison between NFLUX and NOGAPS, the differences between NFLUX and COAMPS are greatest off the west coast of Mexico.

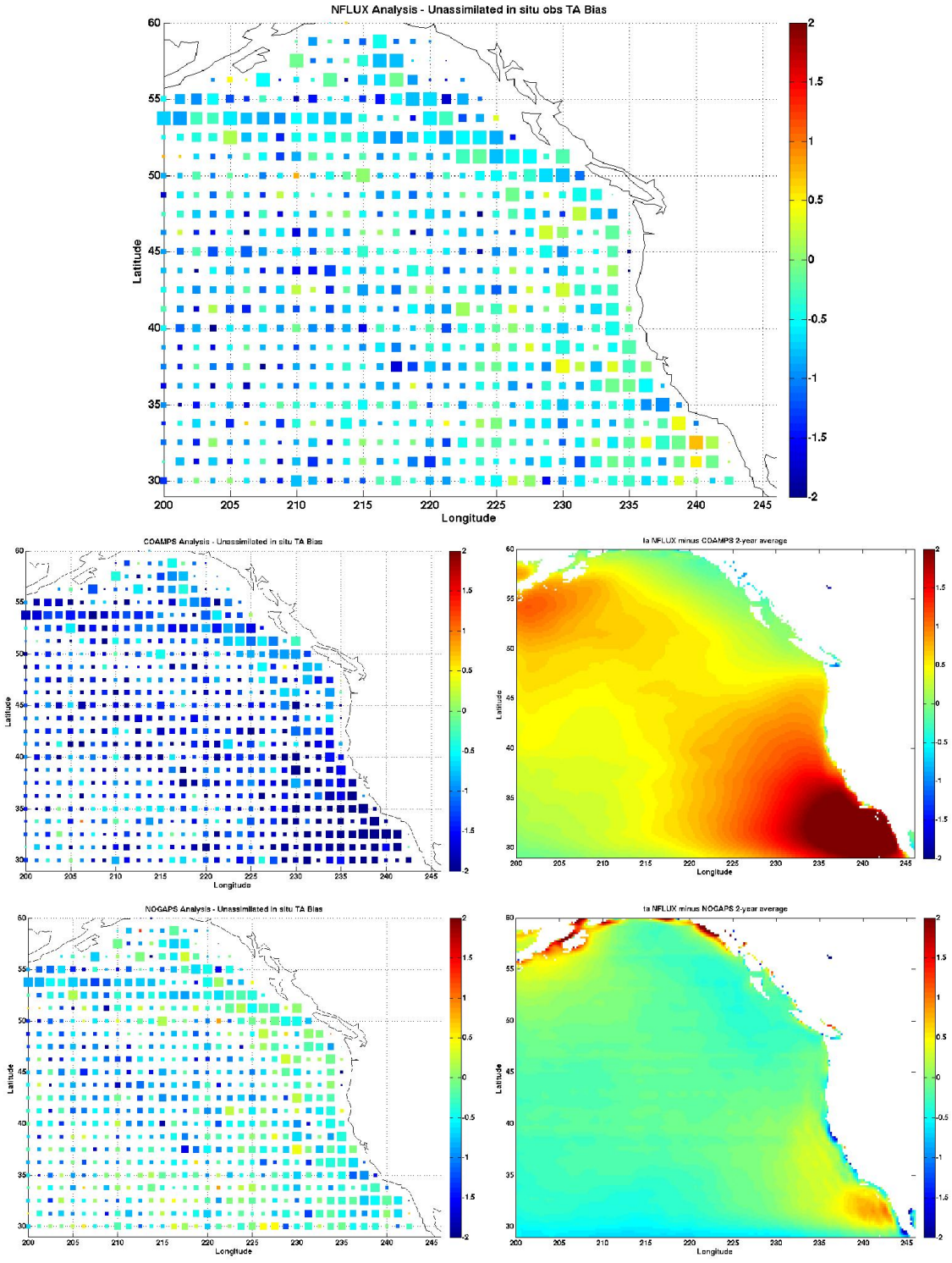

Figure 27: Eastern Pacific 2-year average air temperature bias (°C). The NFLUX (top), COAMPS (middle left), and NOGAPS (bottom left) bias compared to unassimilated observations is shown. Colored square sizes represent the number of observations in each grid box, ranging from 5 to 50 observations. The NFLUX minus COAMPS (NOGAPS) air temperature difference is shown in the middle (bottom) right panel.

Test statistics are calculated for the eastern Pacific region (Table 11) using assimilated (left column) and unassimilated (right column) *in situ* matchup observations. For the open ocean using assimilated matchups, NFLUX shows improvement over COAMPS; however, NOGAPS shows smaller errors than NFLUX. Using unassimilated matchups, NFLUX shows improvement over both COAMPS and NOGAPS in each test statistic except for the mean bias.

Table 11: Air temperature errors over the eastern Pacific Ocean region. Errors are shown relative to both assimilated (left columns) and unassimilated (right columns) *in situ* observations for all comparisons (regional), near land (coastal), and open ocean (ocean). The best test statistic in each column is highlighted in blue. Means and standard deviations that are not significantly different compared to NFLUX at the 95% confidence interval are denoted with an asterisk (*).

	ME	SD	RMSE	R^2		ME	SD	RMSE	R^2
Regional		N = 92425							
NFLUX Analysis	-0.1157	1.4696	1.4741	0.8844	NFLUX 12h persist	-0.1189	1.9201	1.9237	0.8053
COAMPS Analysis	-0.6729	2.0463	2.1541	0.7810	COAMPS 12h persist	-0.6670	2.3782	2.4700	0.7101
COAMPS 12h fcst	-0.5566	1.8236	1.9067	0.8275	NOGAPS 12h persist	0.0311	2.3897	2.3899	0.7389
NOGAPS Analysis	0.0176	1.9761	1.9761	0.8226					
NOGAPS 12h fcst	0.1667	1.9903	1.9972	0.8204					
Coastal		N = 61765							
NFLUX Analysis	-0.0543	1.5927	1.5936	0.8483	NFLUX 12h persist	-0.0512	2.1467	2.1472	0.7260
COAMPS Analysis	-0.5083	2.2381	2.2951	0.7110	COAMPS 12h persist	-0.4987	2.6312	2.6780	0.6085
COAMPS 12h fcst	-0.4046	2.0348	2.0746	0.7724	NOGAPS 12h persist	0.1309	2.7469	2.7500	0.6525
NOGAPS Analysis	0.1087	2.2681	2.2707	0.7728					
NOGAPS 12h fcst	0.2999	2.2871	2.3067	0.7695					
Ocean		N = 30660							
NFLUX Analysis	-0.2392	1.1734	1.1975	0.9413	NFLUX 12h persist	-0.2551	1.3427	1.3667	0.9235
COAMPS Analysis	-1.0045	1.5386	1.8375	0.8989	COAMPS 12h persist	-1.0061	1.7122	1.9859	0.8757
COAMPS 12h fcst	-0.8628	1.2426	1.5127	0.9334	NOGAPS 12h persist	-0.1701	1.3980	1.4083	0.9164
NOGAPS Analysis	-0.1660	*1.1653	1.1770	0.9416					
NOGAPS 12h fcst	-0.1016	1.1383	1.1428	0.9442					

Open ocean air temperature scatterplots of the assimilated (unassimilated) *in situ* observations are shown in the left (bottom) panels of Figure 28 (Figure 29), with the corresponding comparison of the probability of the mean bias in the right (top) panels. The global air temperature test case revealed a capping effect at very high temperatures, above approximately 28°C. NFLUX also showed a slight warm bias at low temperatures, below approximately 4°C.

Unlike the global ocean, air temperature in the eastern Pacific generally remains below 25°C; therefore, the issue at high temperatures is not seen here. The slight warm bias at low temperatures is still present in NFLUX. This feature is not seen in the COAMPS / NOGAPS products. The close linear relationship between the models and *in situ* observations is seen here; however, COAMPS shows a shift in the one-to-one relationship to reveal a consistent cold bias.

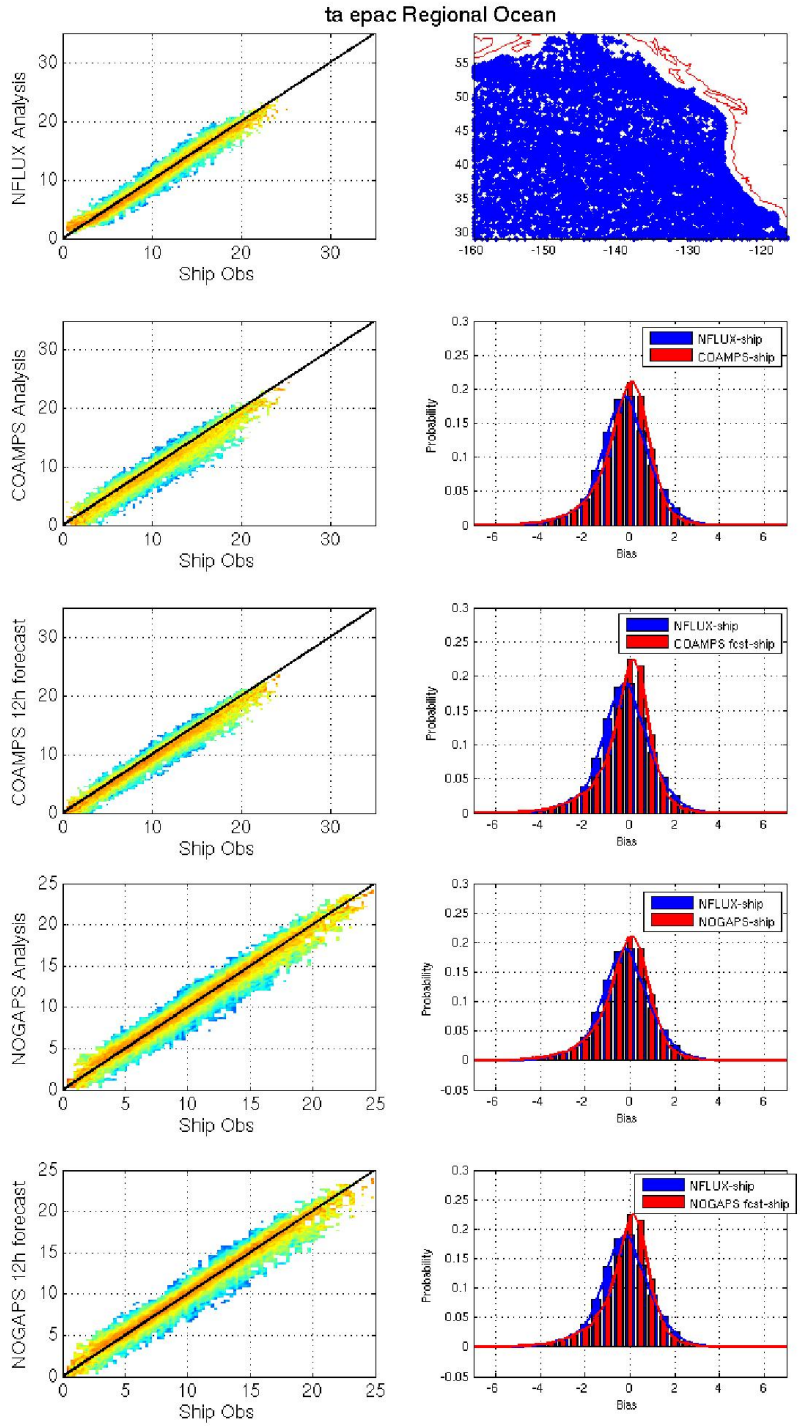

Figure 28: Air temperature over eastern Pacific open ocean using assimilated *in situ* data. The distribution of the matched up observations is shown in the top right panel. The panels on the left show scatterplots of the *in situ* observations versus NFLUX analysis (top), COAMPS analysis (second row), COAMPS 12-hour forecast (third row), NOGAPS analysis (fourth row), and NOGAPS 12-hour forecast (bottom). The right panels show histograms of the probability of the mean bias of NFLUX analysis (blue) and corresponding COAMPS/NOGAPS model (red).

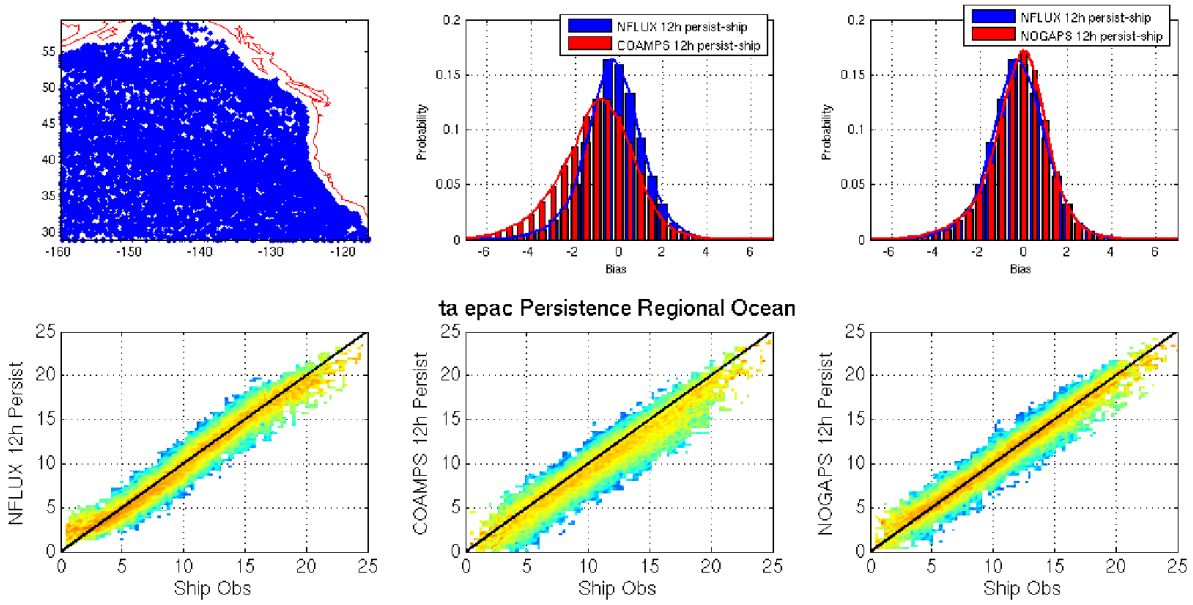

Figure 29: Air temperature over eastern Pacific open ocean using unassimilated *in situ* data. The distribution of the matched up observations is shown in the top left panel. The panels on the bottom show scatterplots of the *in situ* observations versus NFLUX analysis (left), COAMPS analysis (middle), and NOGAPS analysis (right). The top panels show histograms of the probability of the mean bias of NFLUX analysis (blue) and corresponding COAMPS/NOGAPS model (red).

4.1.1 Seasonal

The eastern Pacific open ocean air temperature results by season are shown in Table 12. The corresponding scatterplots using assimilated (unassimilated) matchup observations versus NLFUX, COAMPS, and NOGAPS are shown in Figure 30 (Figure 31). The scatterplots show a larger spread in the COAMPS comparisons than either NFLUX or NOGAPS. Similar to the regional open ocean, NFLUX shows improvement over each COAMPS product in using both assimilated and unassimilated observations.

Comparing NFLUX to NOGAPS shows mixed results. Each NOGAPS product has a lower mean bias in all but the JJA season using both assimilated and unassimilated observations. As seen in the scatterplots, JJA air temperatures are warmer than the other seasons, generally not reaching below 5°C. This eliminates the warm bias at low temperatures that was present in NFLUX, resulting in NFLUX having a smaller mean bias compared to NOGAPS.

Using assimilated observations, NFLUX shows general improvement over NOGAPS in DJF and MAM for the remaining test statistics; although, the NOGAPS 12-hour forecast shows general improvement over NFLUX in JJA and SON. Using unassimilated observations, NFLUX shows overall improvement over NOGAPS in all but the JJA season for the remaining test statistics.

Table 12: Air temperature errors over the eastern Pacific open ocean by season. Errors are shown relative to both assimilated (left columns) and unassimilated (right columns) *in situ* observations. The best test statistic in each column is highlighted in blue. Means and standard deviations that are not significantly different compared to NFLUX at the 95% confidence interval are denoted with an asterisk (*).

	ME	SD	RMSE	R^2		ME	SD	RMSE	R^2
DJF		N = 7982							
NFLUX Analysis	-0.3251	1.1078	1.1545	0.9449	NFLUX 12h persist	-0.3227	1.2812	1.3212	0.9259
COAMPS Analysis	-0.9504	1.5522	1.8200	0.8928	COAMPS 12h persist	-0.9341	1.7554	1.9884	0.8644
COAMPS 12h fcst	-0.7864	1.2396	1.4679	0.9305	NOGAPS 12h persist	-0.0461	1.4151	1.4157	0.9108
NOGAPS Analysis	-0.0719	1.1698	1.1719	0.9386					
NOGAPS 12h fcst	-0.0289	1.1440	1.1443	0.9412					
MAM		N = 6350							
NFLUX Analysis	-0.5735	1.0948	1.2358	0.9390	NFLUX 12h persist	-0.6207	1.2852	1.4271	0.9163
COAMPS Analysis	-1.0095	1.5326	1.8351	0.8801	COAMPS 12h persist	-1.0189	1.6877	1.9713	0.8557
COAMPS 12h fcst	-0.9928	1.2358	1.5851	0.9219	NOGAPS 12h persist	-0.2978	1.3847	1.4162	0.9019
NOGAPS Analysis	-0.2645	1.1454	1.1754	0.9332					
NOGAPS 12h fcst	-0.2026	*1.1176	1.1357	0.9365					
JJA		N = 7677							
NFLUX Analysis	0.1599	1.2450	1.2551	0.8744	NFLUX 12h persist	0.1150	1.3939	1.3985	0.8437
COAMPS Analysis	-1.0152	1.6039	1.8981	0.7906	COAMPS 12h persist	-1.0500	1.6732	1.9753	0.7727
COAMPS 12h fcst	-0.9385	1.2988	1.6023	0.8628	NOGAPS 12h persist	-0.3326	1.3372	1.3779	0.8557
NOGAPS Analysis	-0.3000	*1.2130	1.2495	0.8807					
NOGAPS 12h fcst	-0.2233	1.1954	1.2160	0.8840					
SON		N = 8651							
NFLUX Analysis	-0.2689	1.1232	1.1549	0.9431	NFLUX 12h persist	-0.2527	1.3095	1.3336	0.9229
COAMPS Analysis	-1.0413	1.4686	1.8003	0.9065	COAMPS 12h persist	-1.0242	1.7221	2.0036	0.8727
COAMPS 12h fcst	-0.7705	1.1856	1.4139	0.9363	NOGAPS 12h persist	-0.0466	1.4215	1.4222	0.9101
NOGAPS Analysis	-0.0615	*1.1133	1.1149	0.9443					
NOGAPS 12h fcst	0.0133	1.0776	1.0776	0.9476					

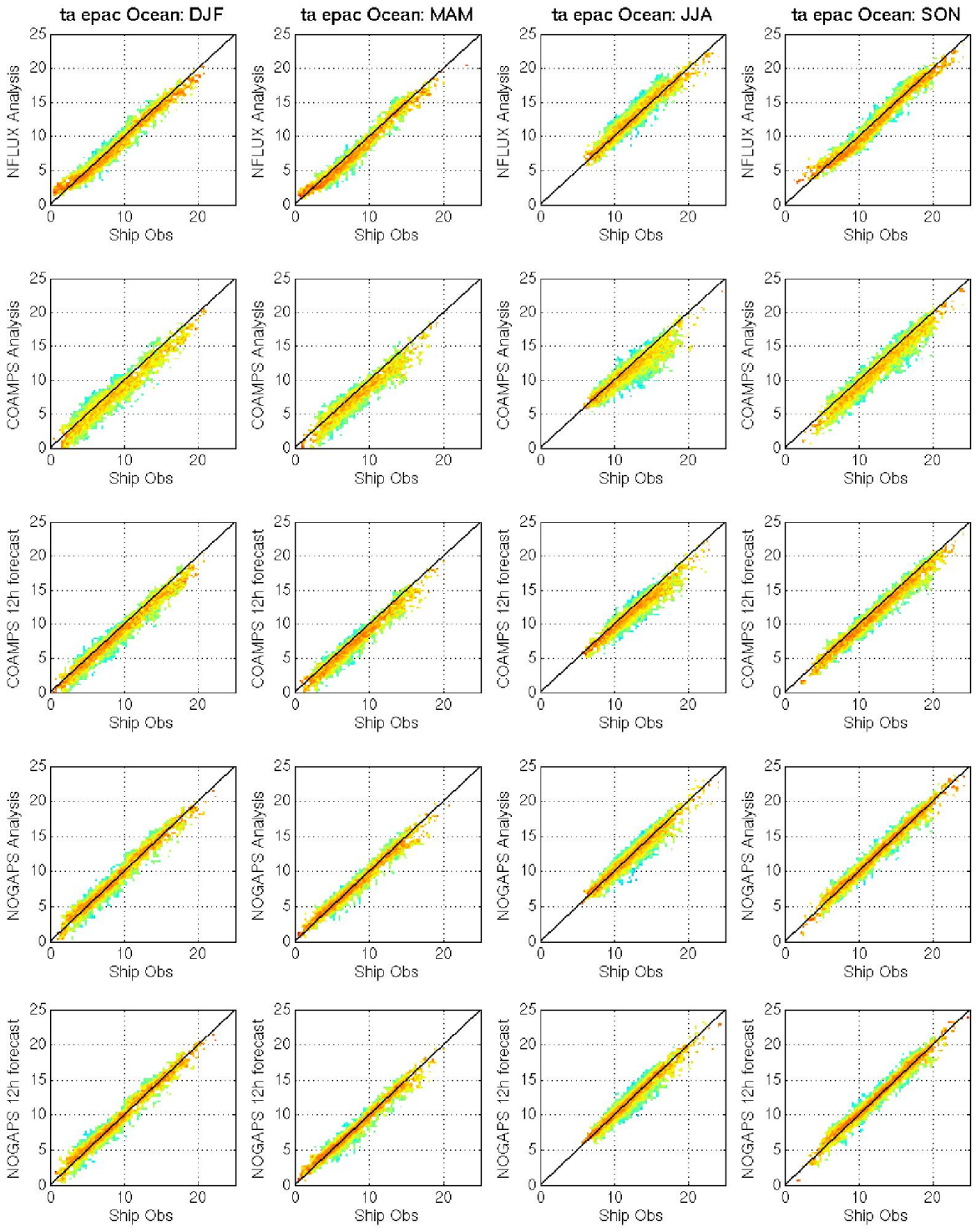

Figure 30: Air temperature over eastern Pacific open ocean by season using assimilated *in situ* data. Scatterplots of the *in situ* observations versus NFLUX analysis (top row), COAMPS analysis (second row), COAMPS 12-hour forecast (third row), NOGAPS analysis (fourth row), and NOGAPS 12-hour forecast (bottom row) are shown.

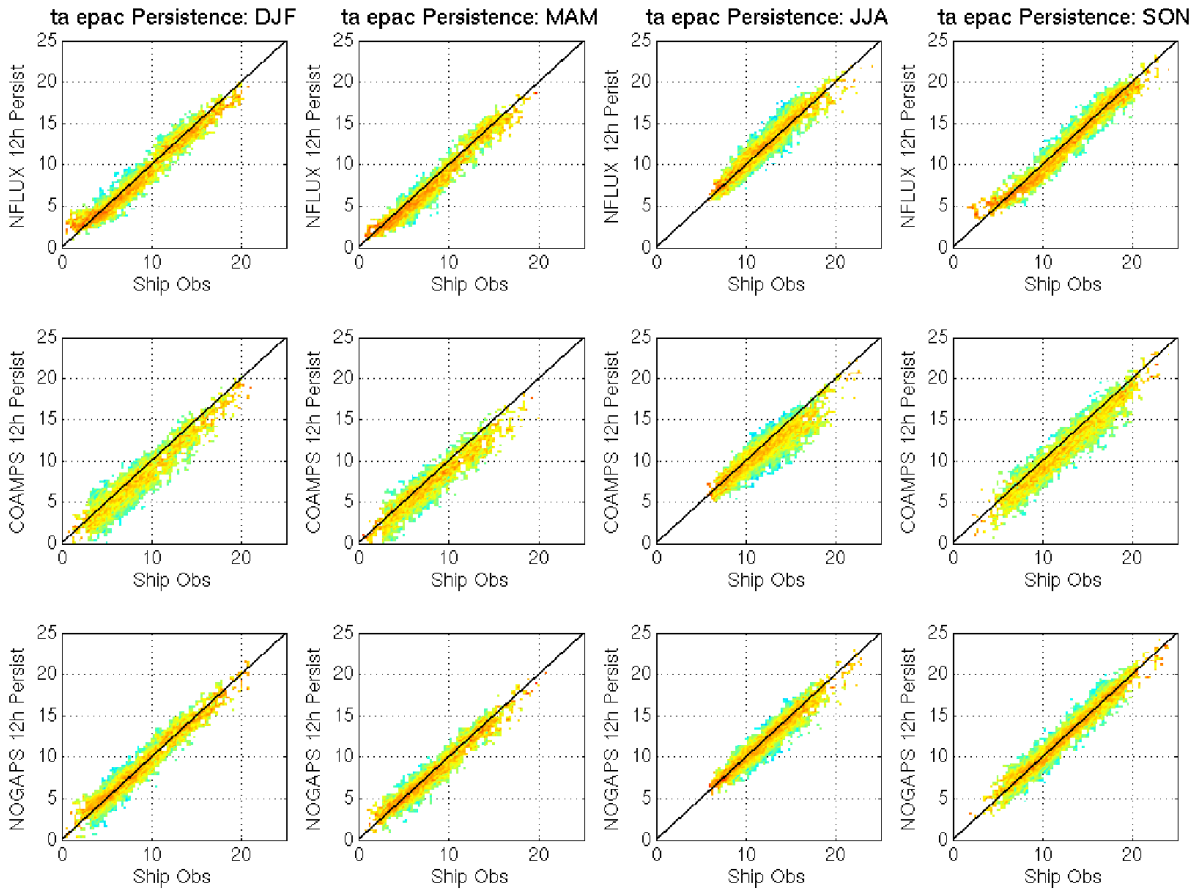

Figure 31: Air temperature over eastern Pacific open ocean by season using unassimilated *in situ* data. Scatterplots of the *in situ* observations versus NFLUX analysis (top row), COAMPS analysis (middle row), and NOGAPS analysis (bottom row) are shown.

4.2 Specific Humidity Results

Figure 32 shows mean specific humidity error over the eastern Pacific using unassimilated *in situ* observations and NFLUX (top), COAMPS (middle left), and NOGAPS (bottom left). Gridded annual differences are also shown for NFLUX versus COAMPS (middle right) and NOGAPS (bottom right). Compared with *in situ* matchups, NFLUX shows a slight dry bias close to the coast with a near neutral to slight moist bias farther from the coast. NOGAPS and COAMPS show a dry bias throughout the region. The annual comparisons of NFLUX versus COAMPS and NOGAPS are very similar with NFLUX being moister over the region.

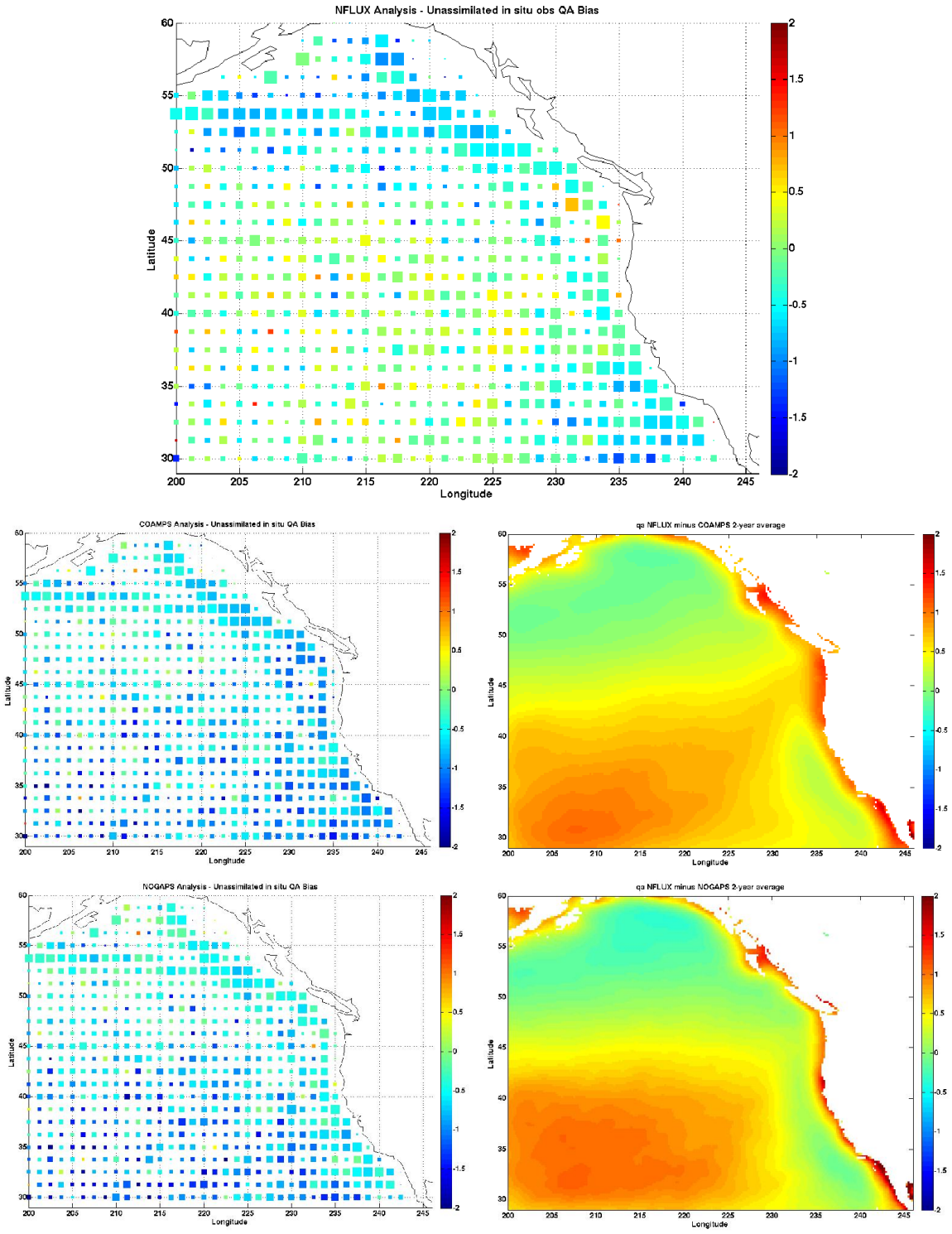

Figure 32: Eastern Pacific 2-year average specific humidity bias (g/kg). The NFLUX (top), COAMPS (middle left), and NOGAPS (bottom left) bias compared to unassimilated observations is shown. Colored square sizes represent the number of observations in each grid box, ranging from 5 to 50 observations. The NFLUX minus COAMPS (NOGAPS) air temperature difference is shown in the middle (bottom) right panel.

Eastern Pacific specific humidity test statistics are shown in Table 13. Over the open ocean NFLUX shows a smaller mean bias than COAMPS and NOGAPS using both assimilated and unassimilated observations. However, NFLUX also shows a larger standard deviation than either COAMPS or NOGAPS. NFLUX shows a lower (higher) correlation over both COAMPS and NOGAPS using assimilated (unassimilated) observations.

Table 13: Specific humidity errors over the eastern Pacific Ocean region. Errors are shown relative to both assimilated (left columns) and unassimilated (right columns) *in situ* observations for all comparisons (regional), near land (coastal), and open ocean (ocean). The best test statistic in each column is highlighted in blue. Means and standard deviations that are not significantly different compared to NFLUX at the 95% confidence interval are denoted with an asterisk (*).

	ME	SD	RMSE	R^2		ME	SD	RMSE	R^2
Regional		N = 29205							
NFLUX Analysis	-0.0371	1.0794	1.0800	0.8261	NFLUX 12h persist	-0.0406	1.2057	1.2064	0.7872
COAMPS Analysis	-0.6743	1.0145	1.2182	0.8281	COAMPS 12h persist	-0.6786	1.1592	1.3433	0.7782
COAMPS 12h fcst	-0.3687	0.9511	1.0200	0.8489	NOGAPS 12h persist	-0.5557	1.1250	1.2548	0.7912
NOGAPS Analysis	-0.5375	0.8659	1.0192	0.8740					
NOGAPS 12h fcst	-0.7179	1.0023	1.2329	0.8359					
Coastal		N = 14236							
NFLUX Analysis	0.1827	0.9724	0.9894	0.8087	NFLUX 12h persist	0.1917	1.1030	1.1195	0.7609
COAMPS Analysis	-0.6752	1.0150	1.2191	0.7716	COAMPS 12h persist	-0.6789	*1.1056	1.2974	0.7309
COAMPS 12h fcst	-0.3343	*0.9545	1.0113	0.8004	NOGAPS 12h persist	-0.5295	1.0178	1.1473	0.7684
NOGAPS Analysis	-0.5321	0.8529	1.0052	0.8347					
NOGAPS 12h fcst	-0.6913	0.9461	1.1717	0.8055					
Ocean		N = 14969							
NFLUX Analysis	-0.2462	1.1332	1.1596	0.8450	NFLUX 12h persist	-0.2615	1.2566	1.2835	0.8117
COAMPS Analysis	-0.6735	1.0141	1.2174	0.8558	COAMPS 12h persist	-0.6784	1.2081	1.3855	0.7979
COAMPS 12h fcst	-0.4014	0.9467	1.0282	0.8742	NOGAPS 12h persist	-0.5806	1.2178	1.3491	0.7967
NOGAPS Analysis	-0.5426	0.8782	1.0323	0.8919					
NOGAPS 12h fcst	-0.7432	1.0523	1.2883	0.8483					

Corresponding open ocean scatterplots using assimilated (unassimilated) matchup observations are shown in Figure 33 (Figure 34), along with histograms comparing the probability of the mean bias. Each of the products shows a linear relationship to the *in situ* matchups; however, NFLUX shows a wider spread in the observations compared to either COAMPS or NOGAPS which leads to a larger standard deviation. The slight moist bias seen at low specific humidity values in the global open ocean, at less than approximately 4 g/kg, can also be seen in this region.

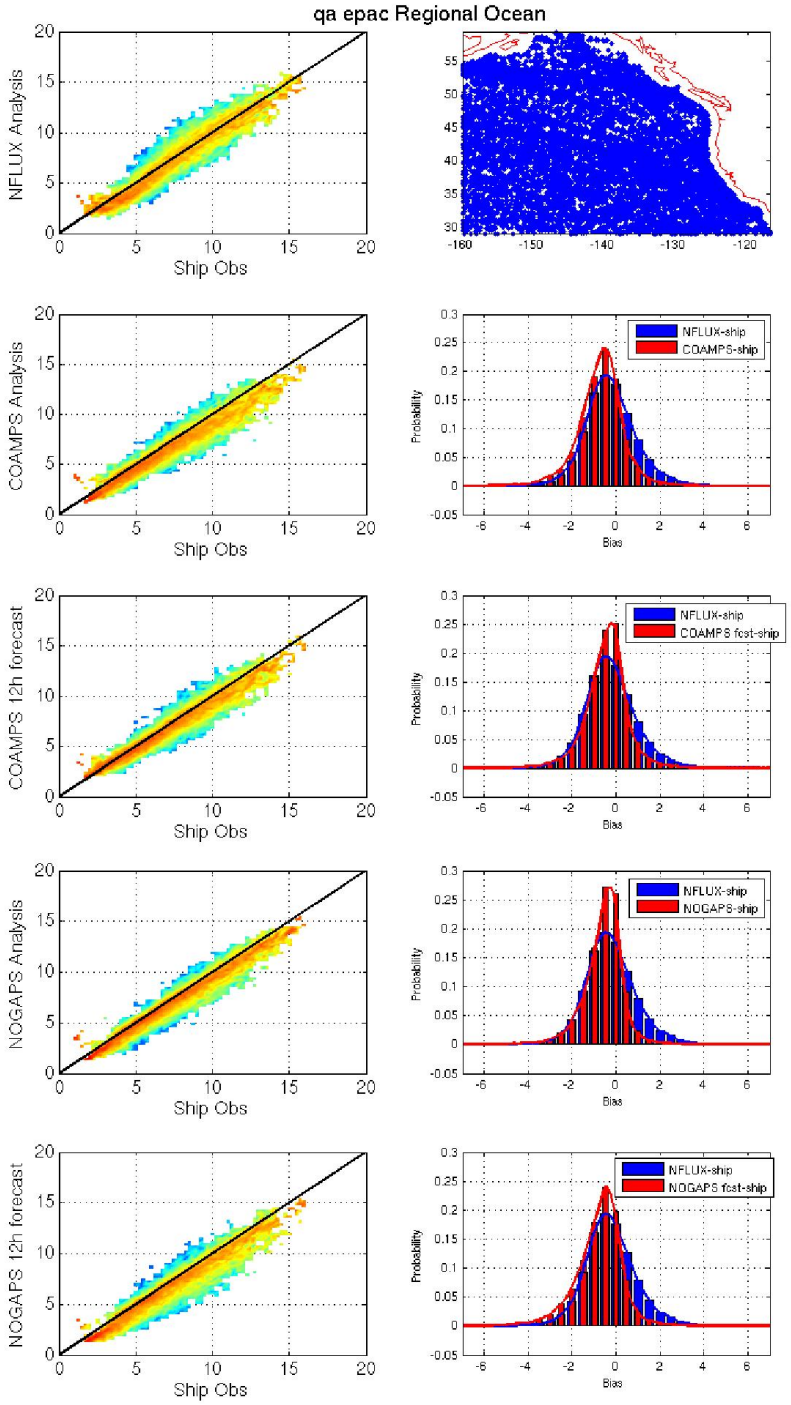

Figure 33: Specific humidity over eastern Pacific open ocean using assimilated *in situ* data. The distribution of the matched up observations is shown in the top right panel. The panels on the left show scatterplots of the *in situ* observations versus NFLUX analysis (top), COAMPS analysis (second row), COAMPS 12-hour forecast (third row), NOGAPS analysis (fourth row), and NOGAPS 12-hour forecast (bottom). The right panels show histograms of the probability of the mean bias of NFLUX analysis (blue) and corresponding COAMPS/NOGAPS model (red).

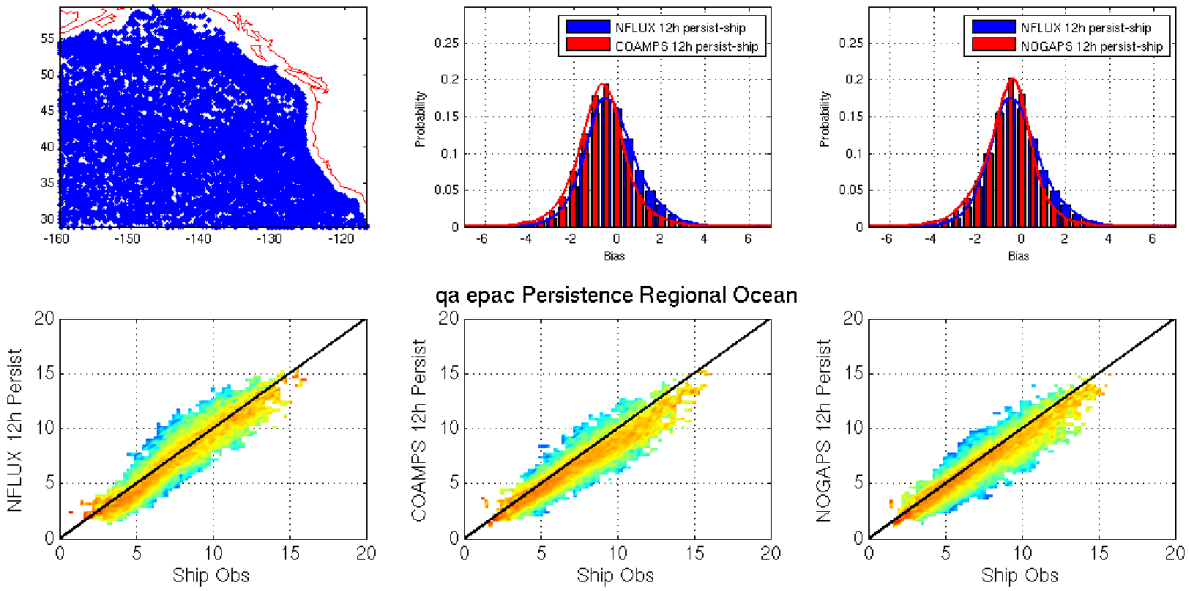

Figure 34: Specific humidity over eastern Pacific open ocean using unassimilated *in situ* data. The distribution of the matched up observations is shown in the top left panel. The panels on the bottom show scatterplots of the *in situ* observations versus NFLUX analysis (left), COAMPS analysis (middle), and NOGAPS analysis (right). The top panels show histograms of the probability of the mean bias of NFLUX analysis (blue) and corresponding COAMPS/NOGAPS model (red).

4.2.1 Seasonal

The eastern Pacific open ocean results by season are given in Table 14. Figure 35 (Figure 36) shows the corresponding scatterplots of NFLUX, COAMPS, and NOGAPS versus assimilated (unassimilated) matchup observations. NFLUX has a smaller mean bias COAMPS or NOGAPS in each season except DJF and MAM using assimilated matchups. As in the total regional open ocean, NFLUX shows a larger spread in the scatterplots. This causes NFLUX to have a larger or no significant difference in the standard deviation for each season. Using assimilated matchups, the NOGAPS analysis shows a higher correlation than NFLUX in each season. Using unassimilated matchups NFLUX shows a higher correlation for each season except JJA.

Table 14: Specific humidity errors over the eastern Pacific open ocean by season. Errors are shown relative to both assimilated (left columns) and unassimilated (right columns) *in situ* observations. The best test statistic in each column is highlighted in blue. Means and standard deviations that are not significantly different compared to NFLUX at the 95% confidence interval are denoted with an asterisk (*).

	ME	SD	RMSE	R^2		ME	SD	RMSE	R^2
DJF		N = 4366							
NFLUX Analysis	-0.5463	1.0399	1.1745	0.8406	NFLUX 12h persist	-0.5488	1.2089	1.3275	0.7926
COAMPS Analysis	-0.6886	0.9942	1.2093	0.8420	COAMPS 12h persist	-0.6725	*1.1961	1.3721	0.7764
COAMPS 12h fcst	-0.4058	0.9340	1.0182	0.8600	NOGAPS 12h persist	-0.6674	*1.2494	1.4163	0.7565
NOGAPS Analysis	-0.6431	0.9212	1.1234	0.8642					
NOGAPS 12h fcst	-0.8579	1.0892	1.3864	0.8143					
MAM		N = 2899							
NFLUX Analysis	-0.4514	1.0471	1.1401	0.8345	NFLUX 12h persist	-0.4944	1.1296	1.2329	0.8061
COAMPS Analysis	-0.5309	0.9714	1.1069	0.8242	COAMPS 12h persist	*-0.5426	*1.1271	1.2507	0.7658
COAMPS 12h fcst	-0.3813	0.9197	0.9954	0.8420	NOGAPS 12h persist	-0.6028	*1.1516	1.2996	0.7556
NOGAPS Analysis	-0.5441	0.8536	1.0122	0.8637					
NOGAPS 12h fcst	-0.7290	*1.0061	1.2422	0.8118					
JJA		N = 3400							
NFLUX Analysis	0.2444	1.1508	1.1763	0.7530	NFLUX 12h persist	0.2040	1.2147	1.2316	0.7281
COAMPS Analysis	-0.7029	1.0095	1.2299	0.7926	COAMPS 12h persist	-0.7479	1.0907	1.3224	0.7587
COAMPS 12h fcst	-0.4382	0.9280	1.0261	0.8246	NOGAPS 12h persist	-0.4365	1.0442	1.1316	0.7776
NOGAPS Analysis	-0.3728	0.7671	0.8528	0.8805					
NOGAPS 12h fcst	-0.4852	0.9184	1.0386	0.8278					
SON		N = 4304							
NFLUX Analysis	-0.1911	1.1280	1.1439	0.8524	NFLUX 12h persist	-0.1810	1.2991	1.3115	0.8076
COAMPS Analysis	-0.7309	1.0567	1.2847	0.8625	COAMPS 12h persist	-0.7210	*1.3461	1.5269	0.7821
COAMPS 12h fcst	-0.3814	0.9904	1.0612	0.8788	NOGAPS 12h persist	-0.5915	*1.3402	1.4648	0.7851
NOGAPS Analysis	-0.5738	0.9122	1.0776	0.8972					
NOGAPS 12h fcst	-0.8404	*1.1069	1.3896	0.8537					

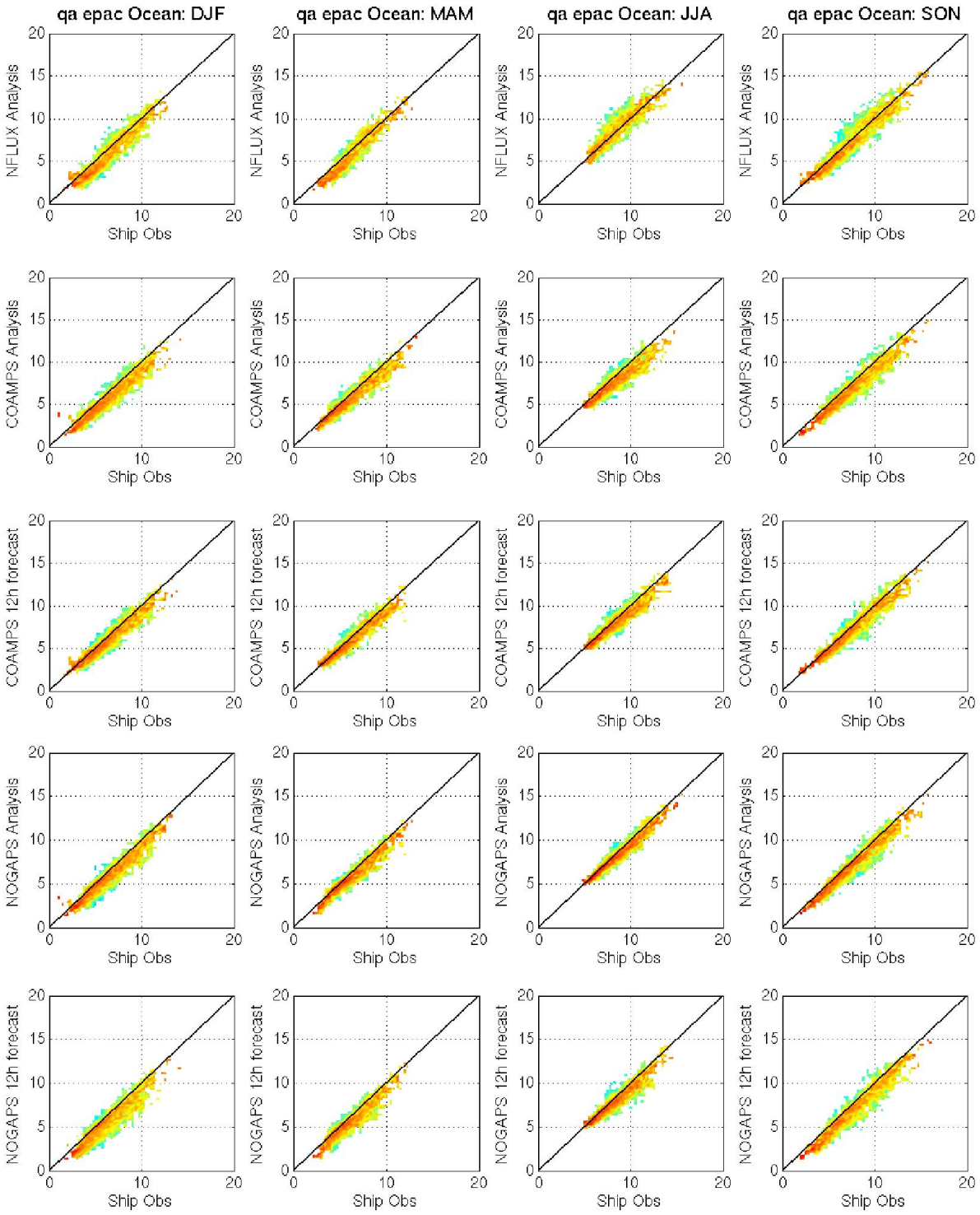

Figure 35: Specific humidity over eastern Pacific open ocean by season using assimilated *in situ* data. Scatterplots of the *in situ* observations versus NFLUX analysis (top row), COAMPS analysis (second row), COAMPS 12-hour forecast (third row), NOGAPS analysis (fourth row), and NOGAPS 12-hour forecast (bottom row) are shown.

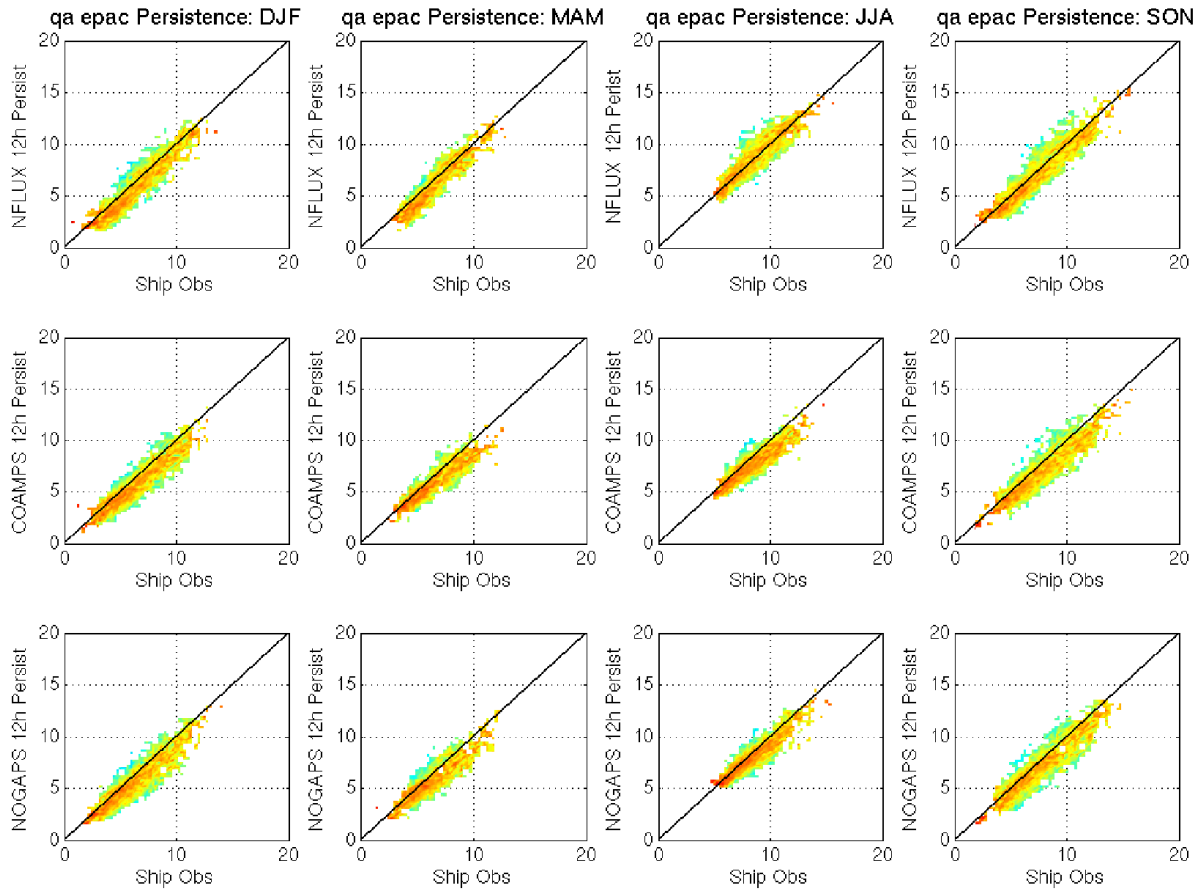

Figure 36: Specific humidity over eastern Pacific open ocean by season using unassimilated *in situ* data. Scatterplots of the *in situ* observations versus NFLUX analysis (top row), COAMPS analysis (middle row), and NOGAPS analysis (bottom row) are shown.

4.3 Wind Speed Results

Figure 37 shows mean wind speed error over the eastern Pacific using unassimilated *in situ* observations and NFLUX (top), COAMPS (middle left), and NOGAPS (bottom left). Gridded annual differences are also shown for NFLUX versus COAMPS (middle right) and NOGAPS (bottom right). Compared to *in situ* observations, NFLUX and COAMPS show higher wind speeds near the coast, and lower wind speeds farther from the coast. This results in the annual difference between NFLUX and COAMPS to be relatively small throughout the region. NOGAPS shows an overall low wind speed bias compared to the *in situ* matchups. This causes much larger differences compared to NFLUX. As discussed with the global test case, NOGAPS also has a coarser resolution than NFLUX or COAMPS. The different resolutions, along with the smooth coastal topography and overall bias differences, cause larger differences between NFLUX and NOGAPS in the coastal region than in the open ocean.

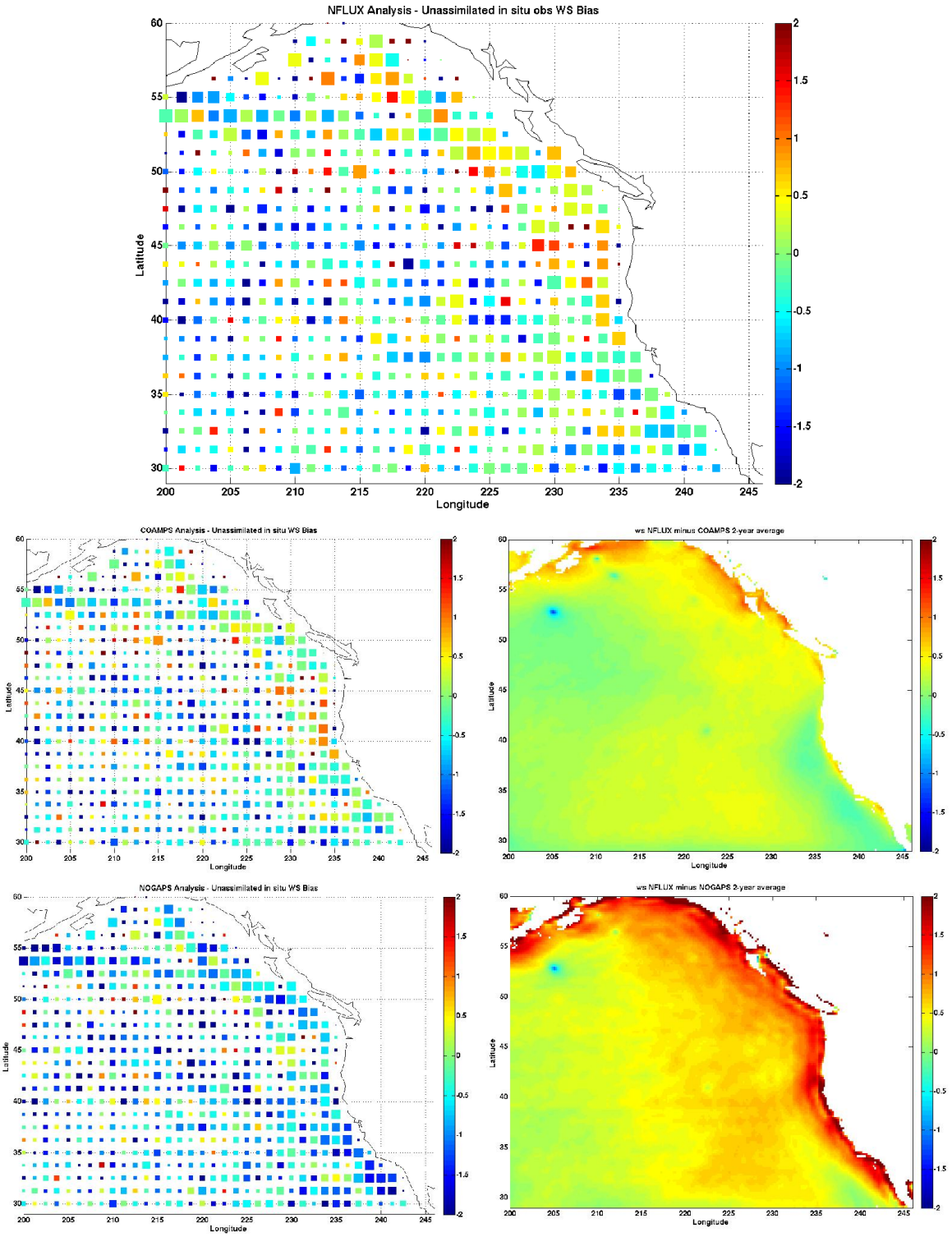

Figure 37: Eastern Pacific 2-year average wind speed bias (m/s). The NFLUX (top), COAMPS (middle left), and NOGAPS (bottom left) bias compared to unassimilated observations is shown. Colored square sizes represent the number of observations in each grid box, ranging from 5 to 50 observations. The NFLUX minus COAMPS (NOGAPS) air temperature difference is shown in the middle (bottom) right panel.

Wind speed test statistics are shown in Table 15 for the eastern Pacific region. Using both assimilated and unassimilated matchups in the open ocean, NFLUX shows a smaller mean bias compared to NOGAPS, but a larger mean bias compared to COAMPS. NFLUX also shows improvement or no statistical difference over each COAMPS and NOGAPS product for the remaining test statistics using both assimilated and unassimilated matchups.

Table 15: Wind speed errors over the eastern Pacific Ocean region. Errors are shown relative to both assimilated (left columns) and unassimilated (right columns) *in situ* observations for all comparisons (regional), near land (coastal), and open ocean (ocean). The best test statistic in each column is highlighted in blue. Means and standard deviations that are not significantly different compared to NFLUX at the 95% confidence interval are denoted with an asterisk (*).

	ME	SD	RMSE	R^2		ME	SD	RMSE	R^2
Regional		N = 90157							
NFLUX Analysis	0.2716	2.2491	2.2655	0.6750	NFLUX 12h persist	0.2658	3.5989	3.6087	0.2898
COAMPS Analysis	-0.0879	2.4779	2.4795	0.6294	COAMPS 12h persist	-0.0995	3.8162	3.8175	0.2583
COAMPS 12h fcst	-0.1103	2.6476	2.6498	0.5831	NOGAPS 12h persist	-1.0974	3.6089	3.7721	0.2940
NOGAPS Analysis	-1.0922	2.3301	2.5734	0.6570					
NOGAPS 12h fcst	-0.7431	2.4936	2.6020	0.6230					
Coastal		N = 61705							
NFLUX Analysis	0.2888	2.3665	2.3840	0.6342	NFLUX 12h persist	0.2949	3.6604	3.6722	0.2585
COAMPS Analysis	-0.1527	2.5808	2.5853	0.5853	COAMPS 12h persist	-0.1511	3.8553	3.8582	0.2251
COAMPS 12h fcst	-0.1028	2.7570	2.7589	0.5397	NOGAPS 12h persist	-1.3660	3.6032	3.8534	0.2579
NOGAPS Analysis	-1.3680	2.4320	2.7903	0.6082					
NOGAPS 12h fcst	-0.9276	2.6344	2.7930	0.5660					
Ocean		N = 28452							
NFLUX Analysis	0.2342	1.9704	1.9842	0.7229	NFLUX 12h persist	0.2026	3.4609	3.4668	0.2827
COAMPS Analysis	0.0527	2.2321	2.2327	0.6738	COAMPS 12h persist	0.0123	3.7277	3.7276	0.2483
COAMPS 12h fcst	-0.1264	2.3931	2.3964	0.6269	NOGAPS 12h persist	-0.5150	3.5524	3.5895	0.2687
NOGAPS Analysis	-0.4939	*1.9632	2.0244	0.7290					
NOGAPS 12h fcst	-0.3430	2.1019	2.1296	0.6981					

Scatterplots and corresponding histograms of the probability of the mean bias for the open ocean using assimilated (unassimilated) matchup observations are shown in Figure 38 (Figure 39). NFLUX shows a closer fit to the *in situ* observations than either COAMPS or NOGAPS. This agrees with NFLUX having a smaller standard deviation and larger correlation. At low wind speeds, less than approximately 5 m/s, each of the products show a high wind speed bias. A high bias at low wind speeds was also identified in the global test case.

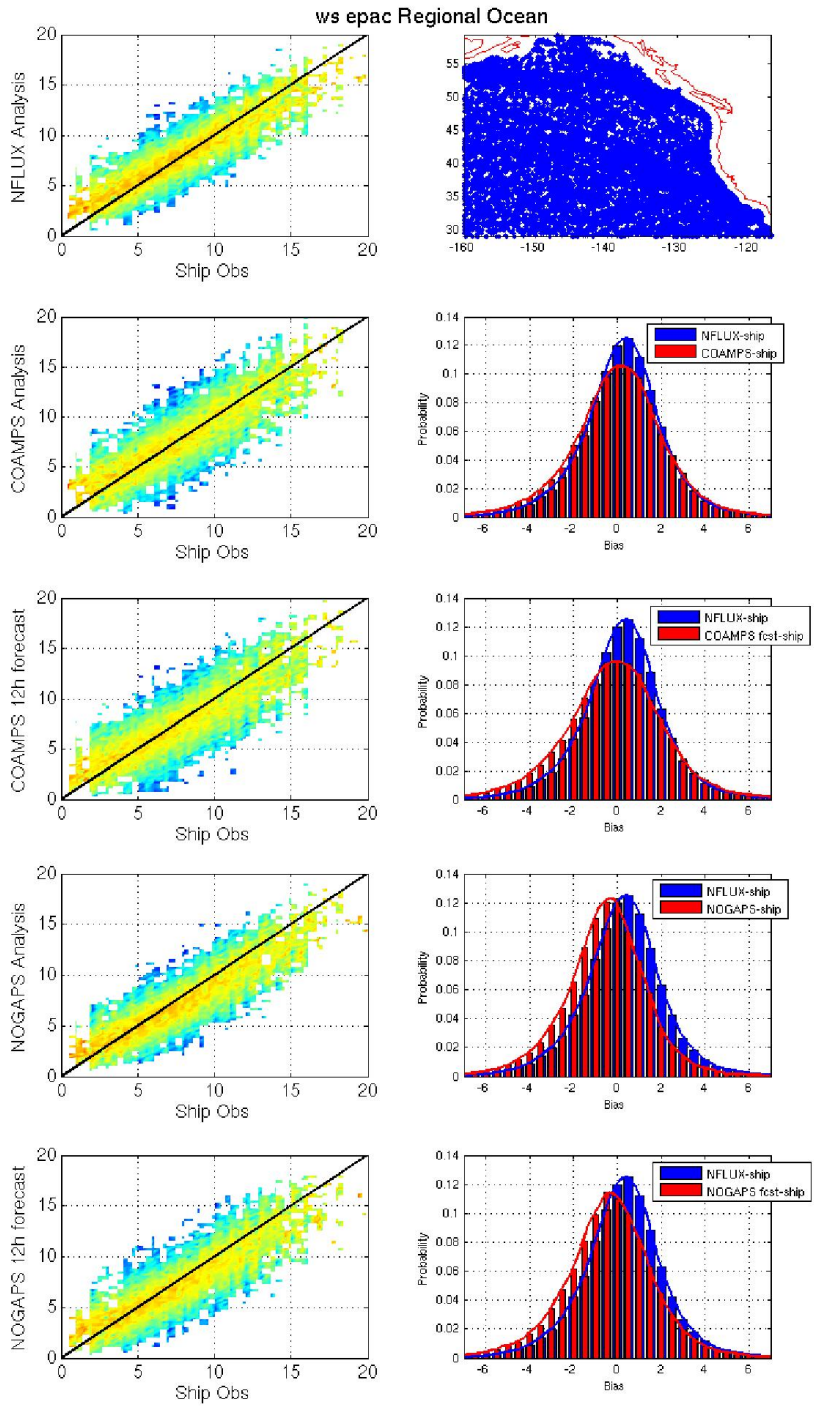

Figure 38: Wind speed over eastern Pacific open ocean using assimilated *in situ* data. The distribution of the matched up observations is shown in the top right panel. The panels on the left show scatterplots of the *in situ* observations versus NFLUX analysis (top), COAMPS analysis (second row), COAMPS 12-hour forecast (third row), NOGAPS analysis (fourth row), and NOGAPS 12-hour forecast (bottom). The right panels show histograms of the probability of the mean bias of NFLUX analysis (blue) and corresponding COAMPS/NOGAPS model (red).

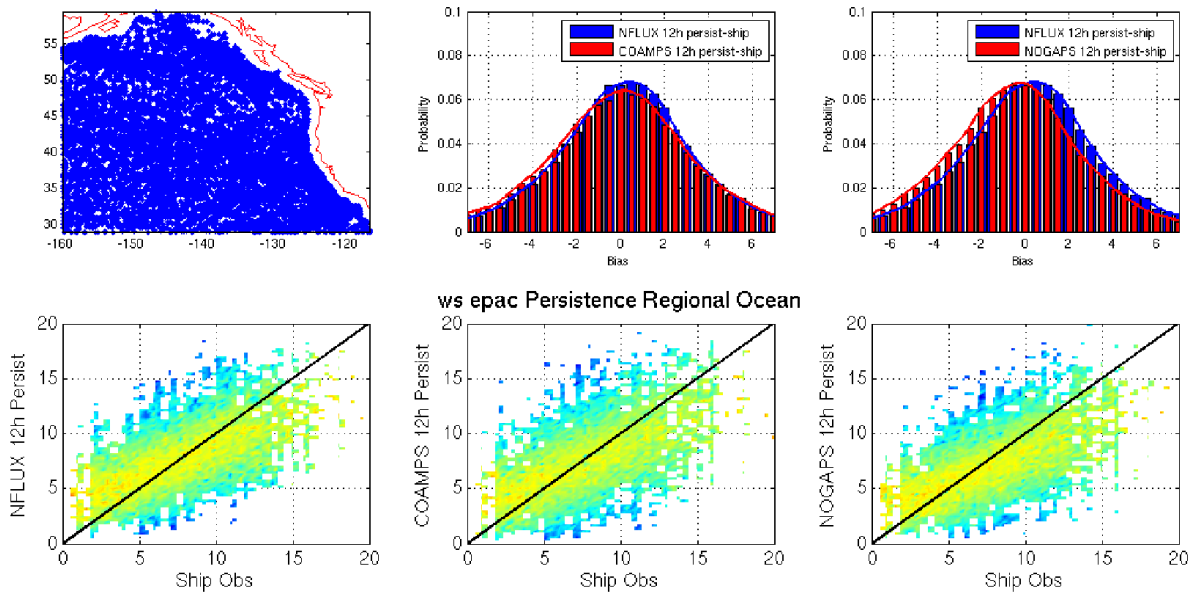

Figure 39: Wind speed over eastern Pacific open ocean using unassimilated *in situ* data. The distribution of the matched up observations is shown in the top left panel. The panels on the bottom show scatterplots of the *in situ* observations versus NFLUX analysis (left), COAMPS analysis (middle), and NOGAPS analysis (right). The top panels show histograms of the probability of the mean bias of NFLUX analysis (blue) and corresponding COAMPS/NOGAPS model (red).

4.3.1 Seasonal

The eastern Pacific open ocean results by season are shown in Table 16, with corresponding scatterplots of wind speed versus assimilated (unassimilated) *in situ* matchups shown in Figure 40 (Figure 41). NFLUX shows improvement over COAMPS using both assimilated and unassimilated matchups in all seasons. NFLUX also shows improvement or no significant difference compared to NOGAPS in all seasons except SON using assimilated matchups.

As mentioned before, the north Pacific is known for frequent storm tracks year round, with the peak in storm activity from December through March (Graham and Diaz, 2001). Higher wind speeds are associated with these storms. As seen in the scatterplots, the observed wind speed range is reduced in JJA, when the north Pacific storms are less frequent. The high wind speed bias at low wind speeds is still present in each season, with the most noticeable bias in JJA when the average wind speed is lower than the other seasons.

Table 16: Wind speed errors over the eastern Pacific open ocean by season. Errors are shown relative to both assimilated (left columns) and unassimilated (right columns) *in situ* observations. The best test statistic in each column is highlighted in blue. Means and standard deviations that are not significantly different compared to NFLUX at the 95% confidence interval are denoted with an asterisk (*).

	ME	SD	RMSE	R^2		ME	SD	RMSE	R^2
DJF		N = 7388							
NFLUX Analysis	0.2122	2.2313	2.2412	0.6884	NFLUX 12h persist	0.1949	3.9257	3.9303	0.2161
COAMPS Analysis	0.0550	2.5653	2.5658	0.6205	COAMPS 12h persist	*0.0447	4.2417	4.2416	0.1793
COAMPS 12h fcst	-0.1089	2.7200	2.7220	0.5775	NOGAPS 12h persist	-0.4409	*4.0187	4.0425	0.2070
NOGAPS Analysis	-0.4327	*2.1726	2.2152	0.7086					
NOGAPS 12h fcst	-0.3035	2.3506	2.3699	0.6686					
MAM		N = 5583							
NFLUX Analysis	0.2587	1.9899	2.0065	0.6969	NFLUX 12h persist	0.2557	3.4515	3.4606	0.2571
COAMPS Analysis	-0.2045	2.3351	2.3438	0.6194	COAMPS 12h persist	-0.1955	3.6869	3.6918	0.2248
COAMPS 12h fcst	-0.1412	2.4142	2.4181	0.5964	NOGAPS 12h persist	-0.5620	*3.5257	3.5699	0.2411
NOGAPS Analysis	-0.5609	*1.9969	2.0740	0.6985					
NOGAPS 12h fcst	-0.3580	2.1240	2.1537	0.6688					
JJA		N = 7306							
NFLUX Analysis	0.2088	1.6179	1.6312	0.6784	NFLUX 12h persist	0.1631	2.5268	2.5318	0.3078
COAMPS Analysis	0.0609	1.8506	1.8515	0.6171	COAMPS 12h persist	0.0075	2.7045	2.7043	0.2879
COAMPS 12h fcst	-0.2840	1.9631	1.9834	0.5538	NOGAPS 12h persist	-0.5774	*2.6031	2.6662	0.2855
NOGAPS Analysis	-0.5467	1.7373	1.8212	0.6362					
NOGAPS 12h fcst	-0.4350	1.8087	1.8601	0.6097					
SON		N = 8175							
NFLUX Analysis	0.2601	1.9921	2.0089	0.7499	NFLUX 12h persist	0.2087	3.7309	3.7365	0.2712
COAMPS Analysis	*0.2189	2.1300	2.1411	0.7387	COAMPS 12h persist	*0.1293	4.0303	4.0321	0.2364
COAMPS 12h fcst	0.0086	2.4048	2.4046	0.6712	NOGAPS 12h persist	-0.4942	*3.8440	3.8754	0.2559
NOGAPS Analysis	-0.4562	1.9284	1.9815	0.7686					
NOGAPS 12h fcst	-0.2863	2.0898	2.1092	0.7390					

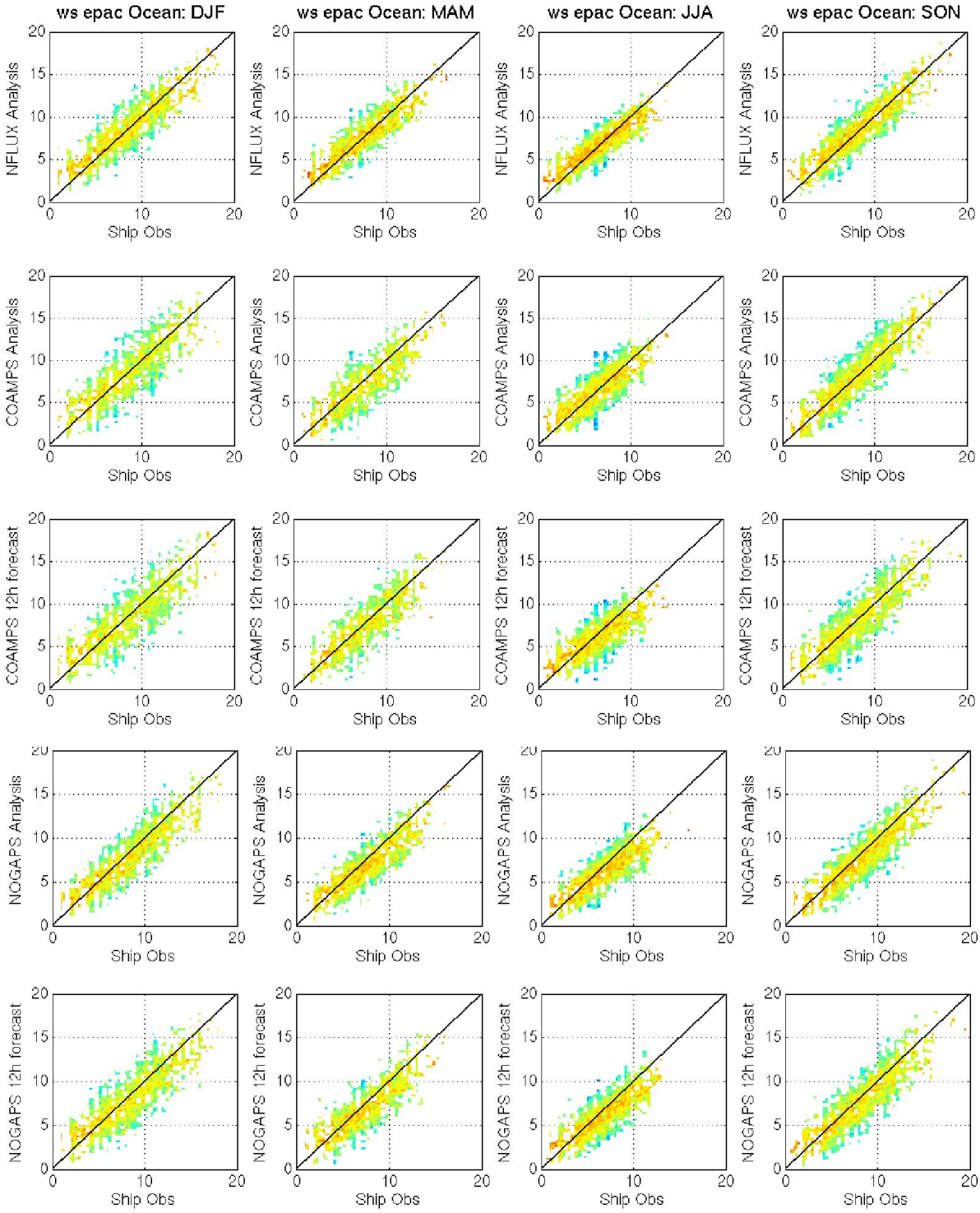

Figure 40: Wind speed over eastern Pacific open ocean by season using assimilated *in situ* data. Scatterplots of the *in situ* observations versus NFLUX analysis (top row), COAMPS analysis (second row), COAMPS 12-hour forecast (third row), NOGAPS analysis (fourth row), and NOGAPS 12-hour forecast (bottom row) are shown.

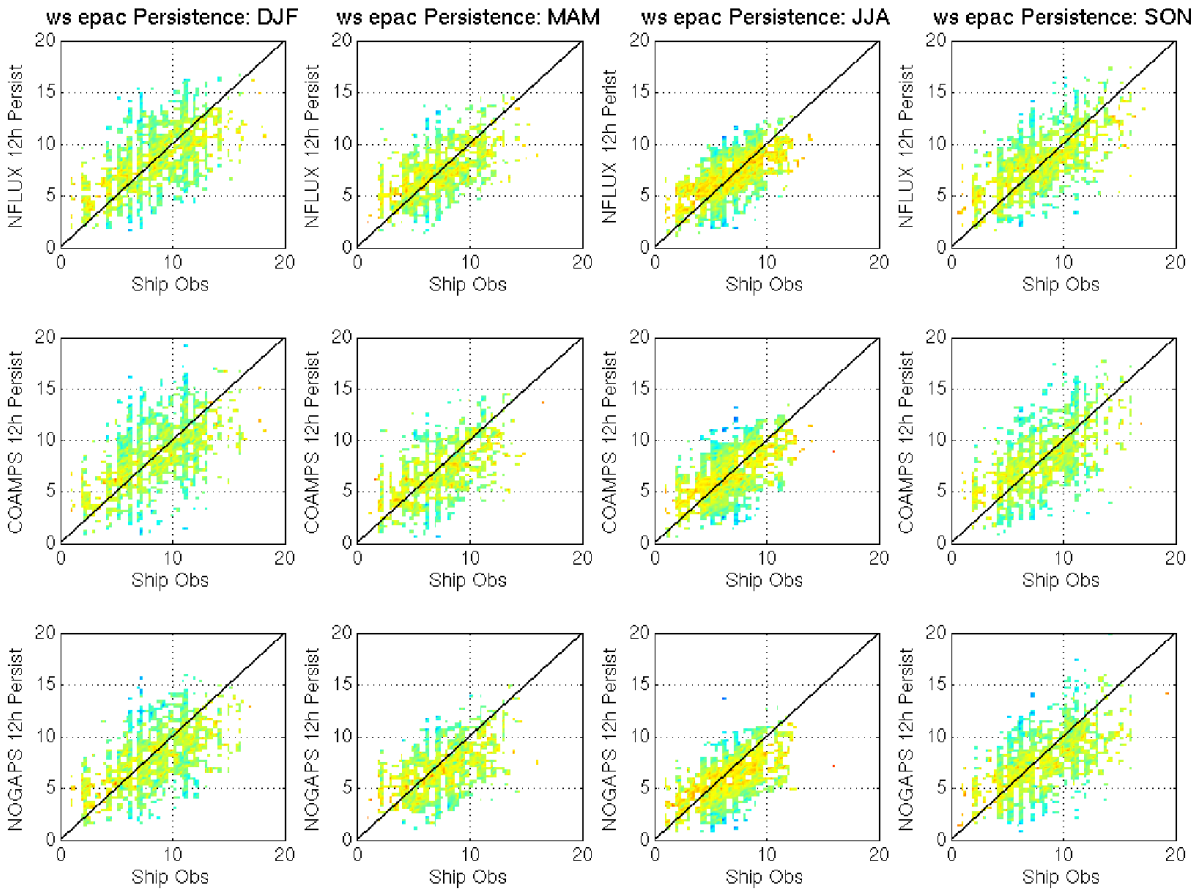

Figure 41: Wind speed over eastern Pacific open ocean by season using unassimilated *in situ* data. Scatterplots of the *in situ* observations versus NFLUX analysis (top row), COAMPS analysis (middle row), and NOGAPS analysis (bottom row) are shown.

5.0 TEST CASE 3: WESTERN PACIFIC

The western Pacific domain spans from 95°-180°E and 7°S-45°N with a horizontal resolution of .2 degrees. The grid has 426 x 261 grid points. The NFLUX grid domain and resolution matches the western Pacific COAMPS domain. The COAMPS 12-hour forecast is blended with the previous NFLUX correction field to generate the background field for the NFLUX analysis. NFLUX analysis performance is compared against both the western Pacific COAMPS analysis and 12-hour forecast fields, as well as the NOGAPS analysis and 12-hour forecast fields over the western Pacific. Validation statistics are calculated for both the assimilated and unassimilated *in situ* matchup data.

5.1 Air Temperature Results

Figure 42 shows mean air temperature error over the western Pacific using unassimilated *in situ* observations and NFLUX (top), COAMPS (middle left), and NOGAPS (bottom left).

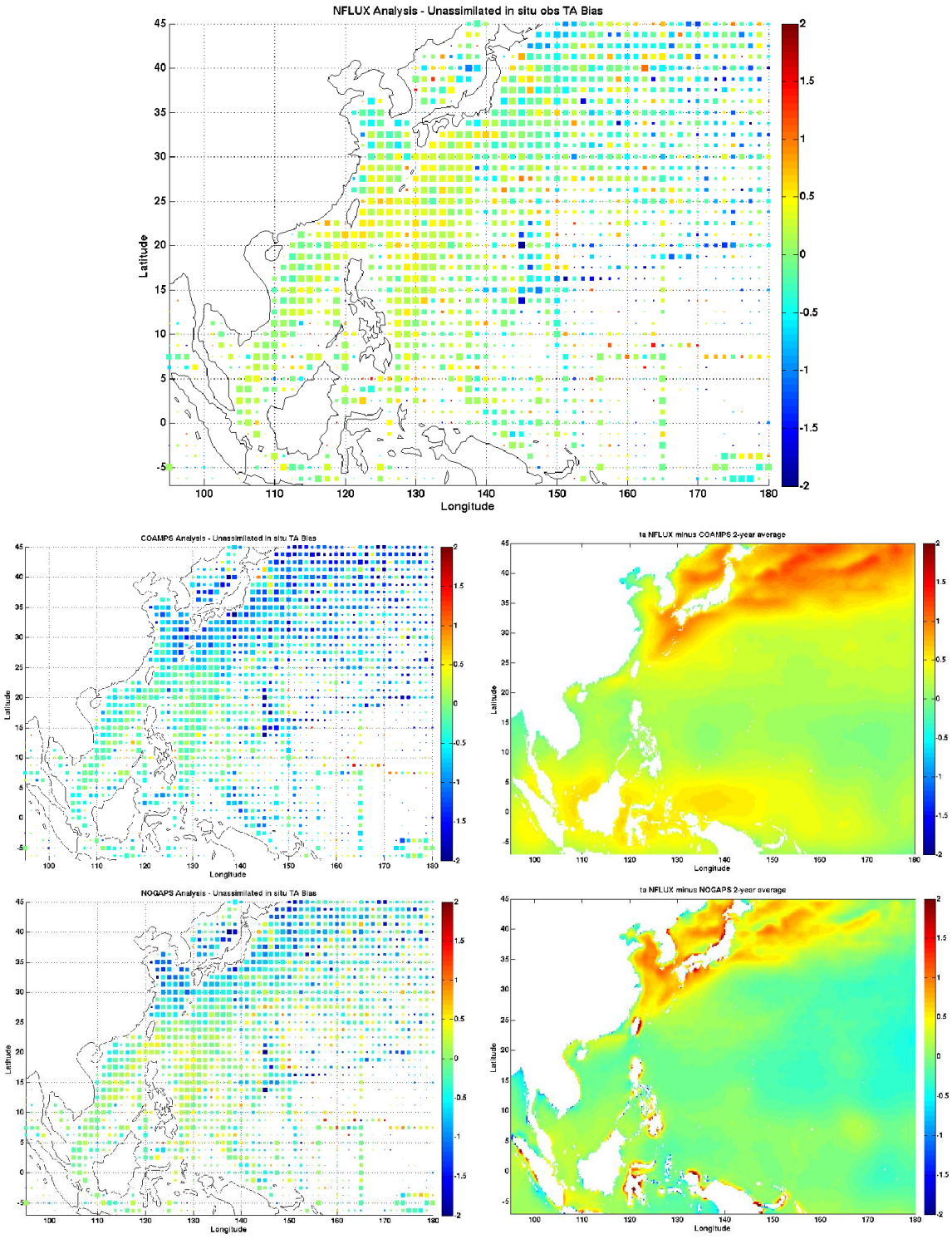

Figure 42: Western Pacific 2-year average air temperature bias (°C). The NFLUX (top), COAMPS (middle left), and NOGAPS (bottom left) bias compared to unassimilated observations is shown. Colored square sizes represent the number of observations in each grid box, ranging from 5 to 50 observations. The NFLUX minus COAMPS (NOGAPS) air temperature difference is shown in the middle (bottom) right panel.

Gridded annual differences are also shown for NFLUX versus COAMPS (middle right) and NOGAPS (bottom right). Compared with the *in situ* matchups, NFLUX shows an overall warm bias throughout the region with the largest differences along the Kuroshio Current. Both COAMPS and NOGAPS show a cold bias in the northern part of the region and a warm bias in the south western part of the region. The annual difference comparisons show the largest differences along the Kuroshio Current. The NFLUX and COAMPS annual comparison also shows a large difference along the equator; this is due to COAMPS showing a cold bias and NFLUX showing a warm bias in this area.

Air temperature test statistics over the western Pacific are shown in Table 17 using assimilated and unassimilated *in situ* matchups. NFLUX shows improvement over both COAMPS and NOGAPS in all test statistics using both assimilated and unassimilated matchups. It is interesting to note that NOGAPS performs better than COAMPS, as in the eastern Pacific.

Table 17: Air temperature errors over the western Pacific Ocean region. Errors are shown relative to both assimilated (left columns) and unassimilated (right columns) *in situ* observations for all comparisons (regional), near land (coastal), and open ocean (ocean). The best test statistic in each column is highlighted in blue. Means and standard deviations that are not significantly different compared to NFLUX at the 95% confidence interval are denoted with an asterisk (*).

	ME	SD	RMSE	R^2		ME	SD	RMSE	R^2
Regional		N = 70980							
NFLUX Analysis	-0.1290	1.1252	1.1326	0.9779	NFLUX 12h persist	-0.1475	1.4867	1.4940	0.9614
COAMPS Analysis	-0.5444	1.4502	1.5490	0.9653	COAMPS 12h persist	-0.5324	1.6968	1.7784	0.9526
COAMPS 12h fcst	-0.7131	1.3584	1.5342	0.9694	NOGAPS 12h persist	-0.2732	1.6395	1.6621	0.9560
NOGAPS Analysis	-0.2780	1.3702	1.3981	0.9697					
NOGAPS 12h fcst	-0.2202	1.3772	1.3947	0.9691					
Coastal		N = 20797							
NFLUX Analysis	-0.1476	1.3984	1.4062	0.9751	NFLUX 12h persist	-0.1717	1.9184	1.9261	0.9532
COAMPS Analysis	-0.5466	1.7907	1.8722	0.9612	COAMPS 12h persist	-0.5263	2.1705	2.2333	0.9432
COAMPS 12h fcst	-0.8450	1.6797	1.8802	0.9651	NOGAPS 12h persist	-0.3641	2.1828	2.2129	0.9449
NOGAPS Analysis	-0.3796	1.7749	1.8150	0.9637					
NOGAPS 12h fcst	-0.3217	1.7901	1.8188	0.9627					
Ocean		N = 50183							
NFLUX Analysis	-0.1212	0.9901	0.9975	0.9738	NFLUX 12h persist	-0.1375	1.2652	1.2727	0.9573
COAMPS Analysis	-0.5435	1.2829	1.3933	0.9595	COAMPS 12h persist	-0.5349	1.4560	1.5512	0.9478
COAMPS 12h fcst	-0.6584	1.1960	1.3653	0.9642	NOGAPS 12h persist	-0.2355	1.3501	1.3704	0.9543
NOGAPS Analysis	-0.2359	1.1593	1.1831	0.9663					
NOGAPS 12h fcst	-0.1782	1.1614	1.1749	0.9659					

The western Pacific open ocean scatterplots using assimilated (unassimilated) matchups and the corresponding histograms of the probability of the mean bias are shown in Figure 43 (Figure 44).

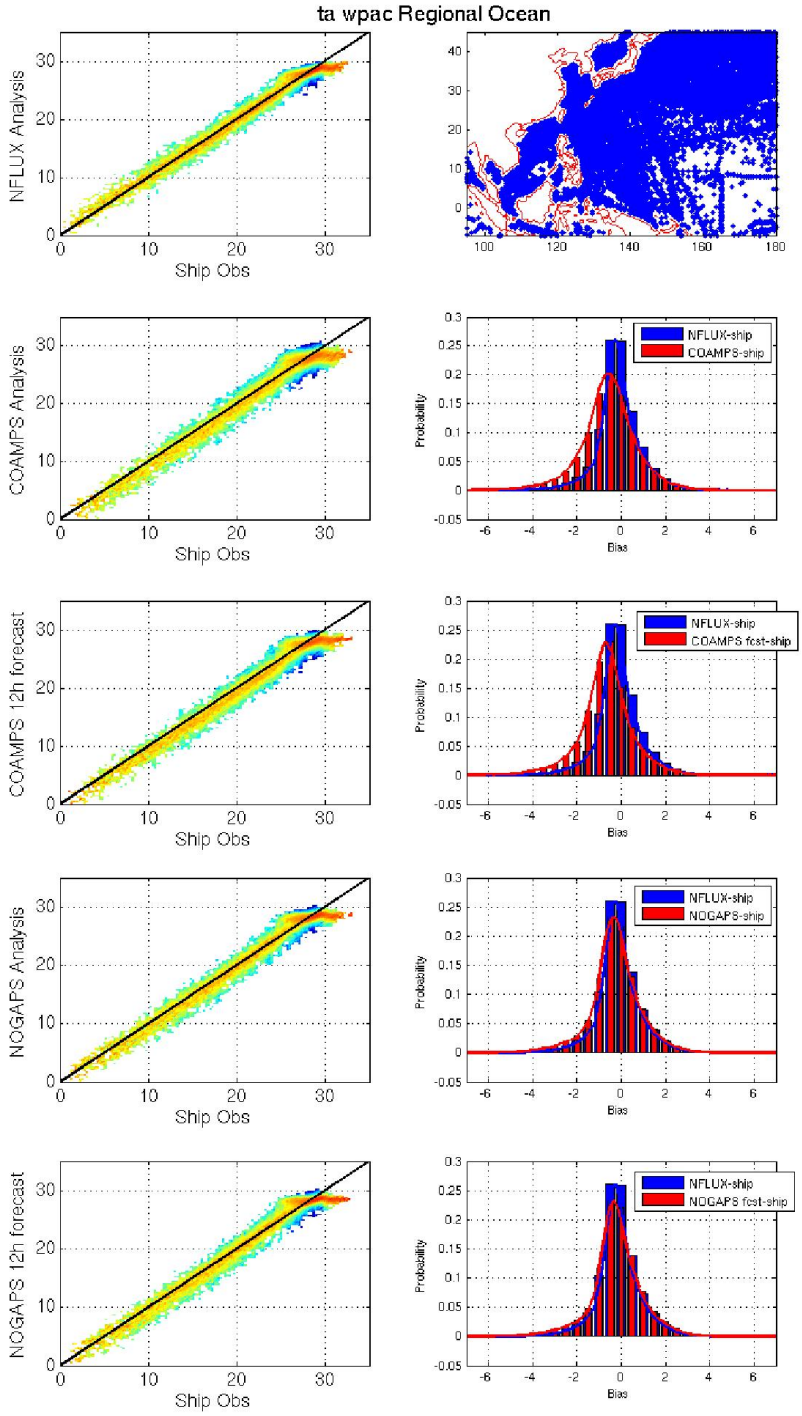

Figure 43: Air temperature over western Pacific open ocean using assimilated *in situ* data. The distribution of the matched up observations is shown in the top right panel. The panels on the left show scatterplots of the *in situ* observations versus NFLUX analysis (top), COAMPS analysis (second row), COAMPS 12-hour forecast (third row), NOGAPS analysis (fourth row), and NOGAPS 12-hour forecast (bottom). The right panels show histograms of the probability of the mean bias of NFLUX analysis (blue) and corresponding COAMPS/NOGAPS model (red).

As discussed in the global test case, the models are not able to properly resolve temperatures above approximately 30°C, even if the *in situ* observations are warmer. This same feature is seen in the western Pacific, causing a capping effect at high temperatures. The warm bias that was seen at low temperatures with NFLUX in the global test case is not seen in the western Pacific.

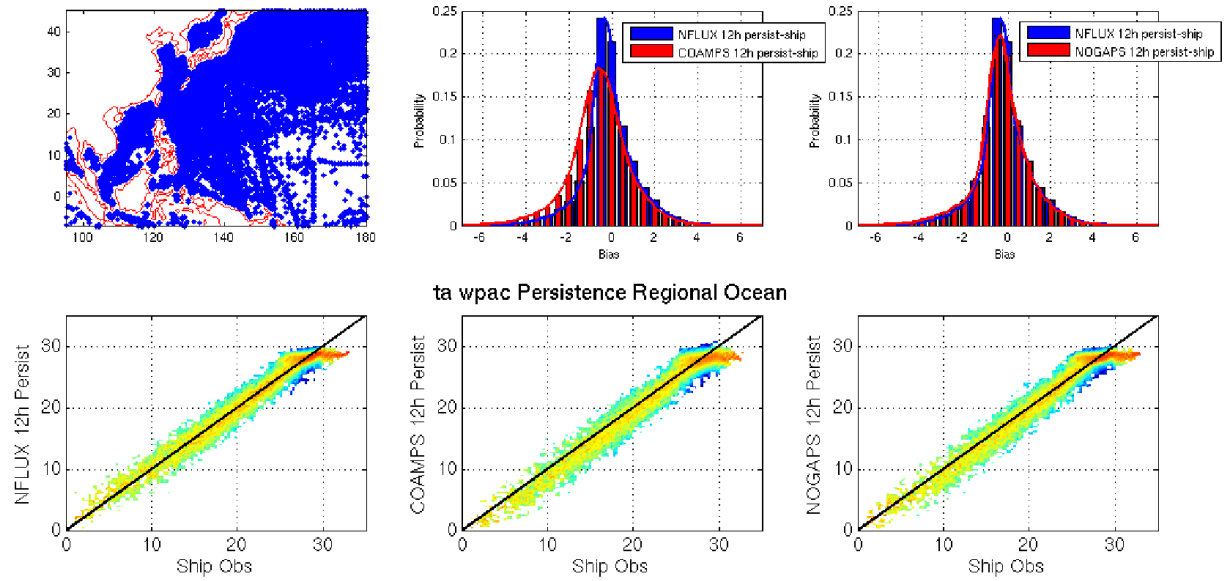

Figure 44: Air temperature over western Pacific open ocean using unassimilated *in situ* data. The distribution of the matched up observations is shown in the top left panel. The panels on the bottom show scatterplots of the *in situ* observations versus NFLUX analysis (left), COAMPS analysis (middle), and NOGAPS analysis (right). The top panels show histograms of the probability of the mean bias of NFLUX analysis (blue) and corresponding COAMPS/NOGAPS model (red).

In the 25° to 30°C *in situ* temperature range, an extended area of relatively constant temperatures can be seen for each of the models in the scatterplots. This feature is present in the western Pacific; however, it was not seen in either the global or eastern Pacific test cases. The western Pacific test case contains a feature called the western Pacific warm pool (Cravatte et al., 2009; Dayem et al., 2007). The warm pool is defined as an area with SSTs greater than 28.5°C, typically found within 10°S to 10°N and 130°E to 170°E. By focusing only on the warm pool region, the feature can easily be seen with each of the models in the top panels of Figure 45. The bottom panels of Figure 45 compare the SST fields used in each of the models to the *in situ* SST. The extended area of constant model temperatures is also seen in the SST matchups. By removing the warm pool from our matchup observations (Figure 46), the extended constant temperatures feature is no longer present

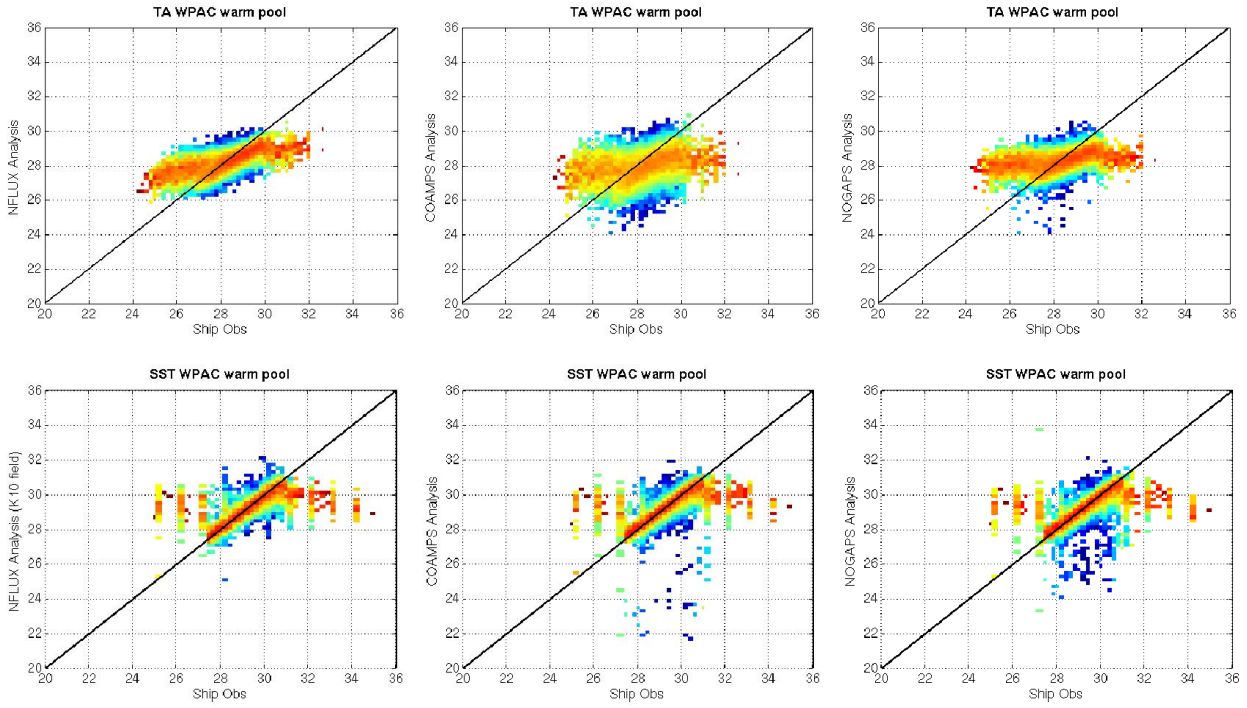

Figure 45: Air temperature and SST over western Pacific warm pool using assimilated *in situ* data. Scatterplots of the *in situ* observations of air temperature (top) and SST (bottom) versus NFLUX analysis (left), COAMPS analysis (middle), and NOGAPS analysis (right) are shown.

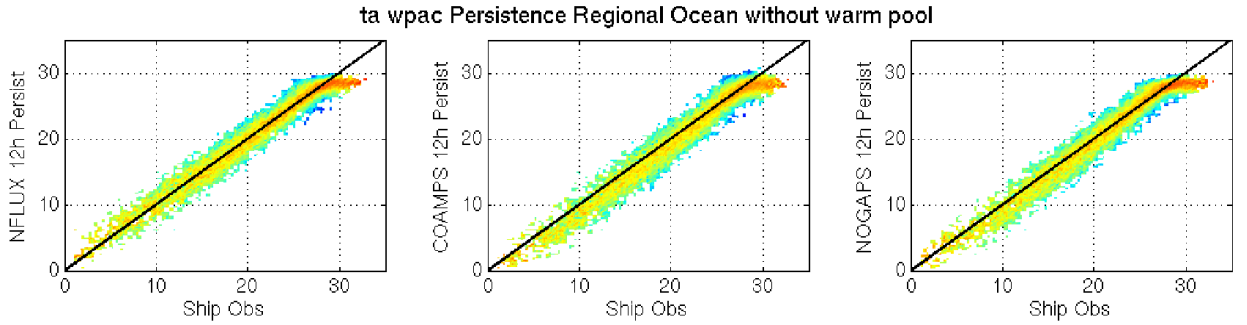

Figure 46: Air temperature over western Pacific open ocean excluding the warm pool using unassimilated *in situ* data. Scatterplots of the *in situ* observations versus NFLUX analysis (left), COAMPS analysis (middle), and NOGAPS analysis (right) are shown.

5.1.1 Seasonal

The western Pacific open ocean air temperature results by season are shown in Table 18. The corresponding scatterplots of air temperature versus assimilated (unassimilated) *in situ* observations are shown in Figure 47 (Figure 48). As in the regional open ocean, NFLUX consistently outperforms or is not statistically different from COAMPS or NOGAPS using both assimilated and unassimilated matchups. The seasonal scatterplots are for the entire western

Pacific region, including the warm pool. The extended relatively constant temperature feature between 25° and 30°C is seen in each season for each product.

Table 18: Air temperature errors over the western Pacific open ocean by season. Errors are shown relative to both assimilated (left columns) and unassimilated (right columns) *in situ* observations. The best test statistic in each column is highlighted in blue. Means and standard deviations that are not significantly different compared to NFLUX at the 95% confidence interval are denoted with an asterisk (*).

	ME	SD	RMSE	R^2		ME	SD	RMSE	R^2
DJF		N = 13467							
NFLUX Analysis	-0.0494	1.0560	1.0571	0.9801	NFLUX 12h persist	-0.0324	1.3491	1.3495	0.9672
COAMPS Analysis	-0.7427	1.3476	1.5386	0.9718	COAMPS 12h persist	-0.7059	1.5883	1.7380	0.9596
COAMPS 12h fcst	-0.7652	1.2205	1.4405	0.9755	NOGAPS 12h persist	-0.2956	1.4667	1.4962	0.9644
NOGAPS Analysis	-0.3126	1.2031	1.2430	0.9764					
NOGAPS 12h fcst	-0.2001	1.1997	1.2162	0.9766					
MAM		N = 11677							
NFLUX Analysis	-0.1974	1.0033	1.0225	0.9789	NFLUX 12h persist	-0.2568	1.3224	1.3470	0.9641
COAMPS Analysis	-0.5756	1.2566	1.3822	0.9678	COAMPS 12h persist	-0.5994	1.4742	1.5914	0.9562
COAMPS 12h fcst	-0.7076	1.2172	1.4078	0.9703	NOGAPS 12h persist	*-0.2979	1.3830	1.4147	0.9620
NOGAPS Analysis	-0.2722	1.1474	1.1792	0.9737					
NOGAPS 12h fcst	*-0.2284	1.1536	1.1760	0.9732					
JJA		N = 11821							
NFLUX Analysis	-0.1086	0.9523	0.9584	0.9403	NFLUX 12h persist	-0.1384	1.1549	1.1631	0.9131
COAMPS Analysis	-0.4173	1.2467	1.3146	0.9020	COAMPS 12h persist	-0.4187	1.3120	1.3771	0.8928
COAMPS 12h fcst	-0.5457	1.2005	1.3187	0.9099	NOGAPS 12h persist	*-0.1596	1.2070	1.2174	0.9091
NOGAPS Analysis	-0.1476	1.1493	1.1587	0.9166					
NOGAPS 12h fcst	-0.1490	1.1650	1.1745	0.9144					
SON		N = 13218							
NFLUX Analysis	-0.1384	0.9351	0.9453	0.9625	NFLUX 12h persist	-0.1383	1.2092	1.2171	0.9376
COAMPS Analysis	-0.4249	1.2428	1.3134	0.9383	COAMPS 12h persist	-0.4076	1.3994	1.4575	0.9220
COAMPS 12h fcst	-0.6070	1.1348	1.2870	0.9470	NOGAPS 12h persist	-0.1871	1.3120	1.3252	0.9293
NOGAPS Analysis	-0.2047	1.1265	1.1449	0.9477					
NOGAPS 12h fcst	*-0.1375	1.1225	1.1308	0.9476					

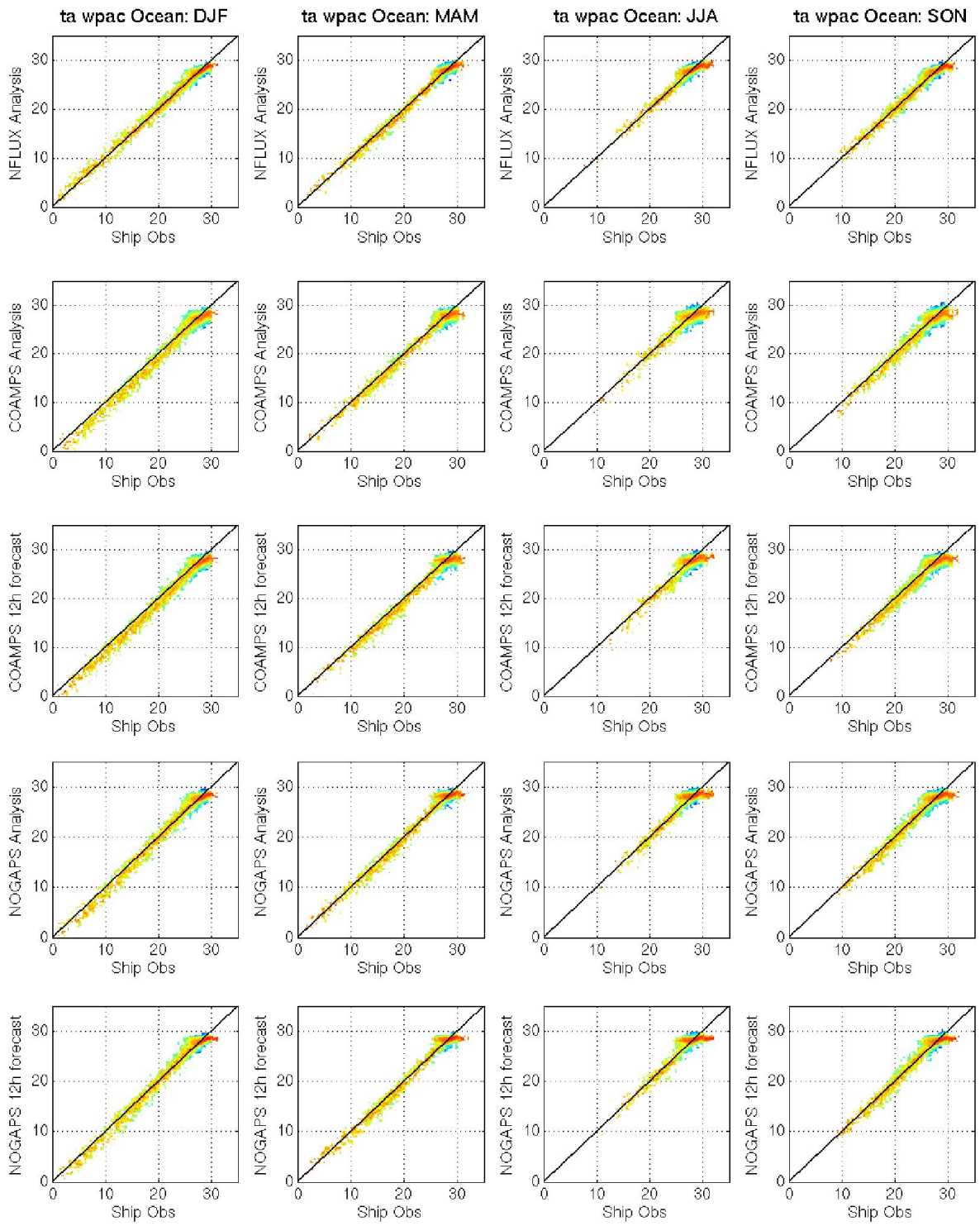

Figure 47: Air temperature over western Pacific open ocean by season using assimilated *in situ* data. Scatterplots of the *in situ* observations versus NFLUX analysis (top row), COAMPS analysis (second row), COAMPS 12-hour forecast (third row), NOGAPS analysis (fourth row), and NOGAPS 12-hour forecast (bottom row) are shown.

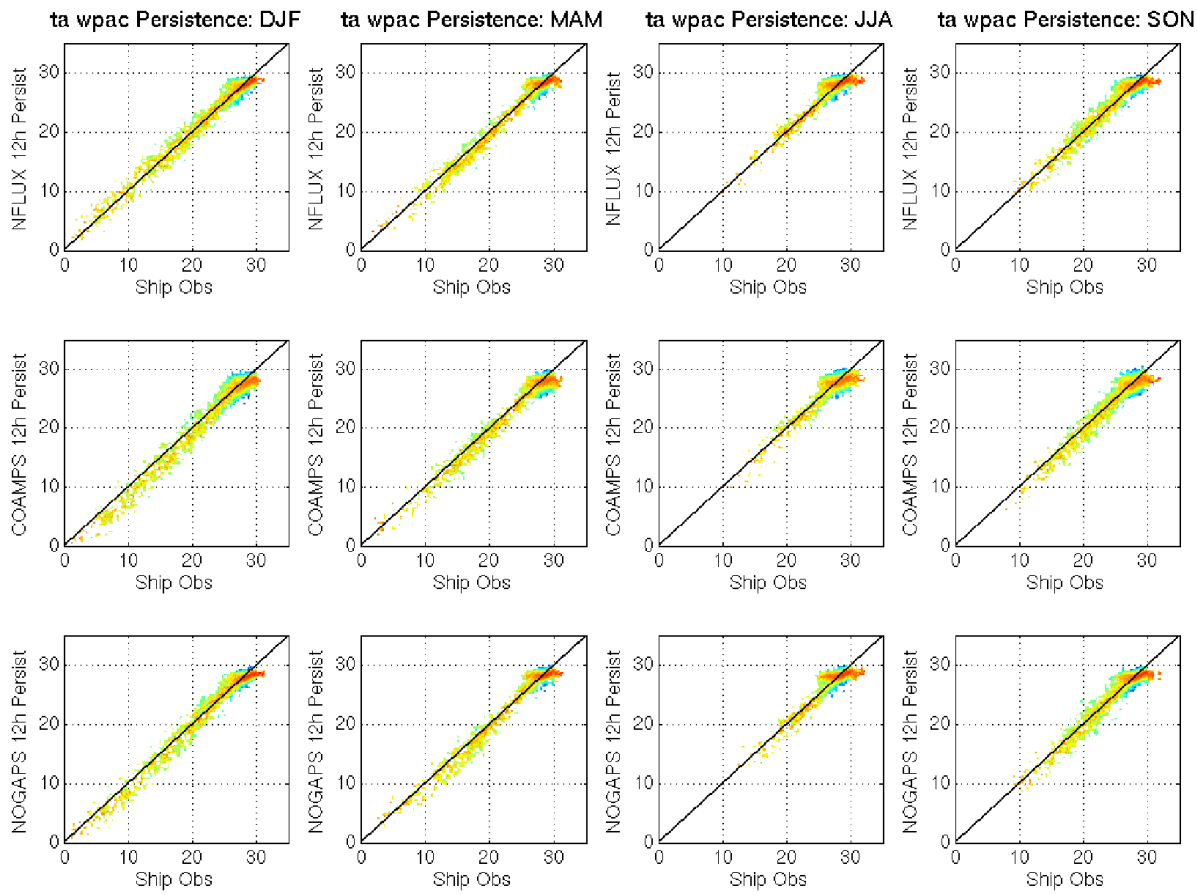

Figure 48: Air temperature over western Pacific open ocean by season using unassimilated *in situ* data. Scatterplots of the *in situ* observations versus NFLUX analysis (top row), COAMPS analysis (middle row), and NOGAPS analysis (bottom row) are shown.

5.2 Specific Humidity Results

Figure 49 shows mean specific humidity error over the eastern Pacific using unassimilated *in situ* observations and NFLUX (top), COAMPS (middle left), and NOGAPS (bottom left). Gridded annual differences are also shown for NFLUX versus COAMPS (middle right) and NOGAPS (bottom right). Compared with the *in situ* matchups, NFLUX shows a moist bias with the most significant differences just north of the equator. NOGAPS and COAMPS show a dry bias throughout the region with the most significant differences along the Kuroshio Current. The annual comparisons of NFLUX versus COAMPS and NOGAPS are very similar with NFLUX being moister over the region with the most noticeable differences along the equator. These differences agree well with the differences seen in the global test case.

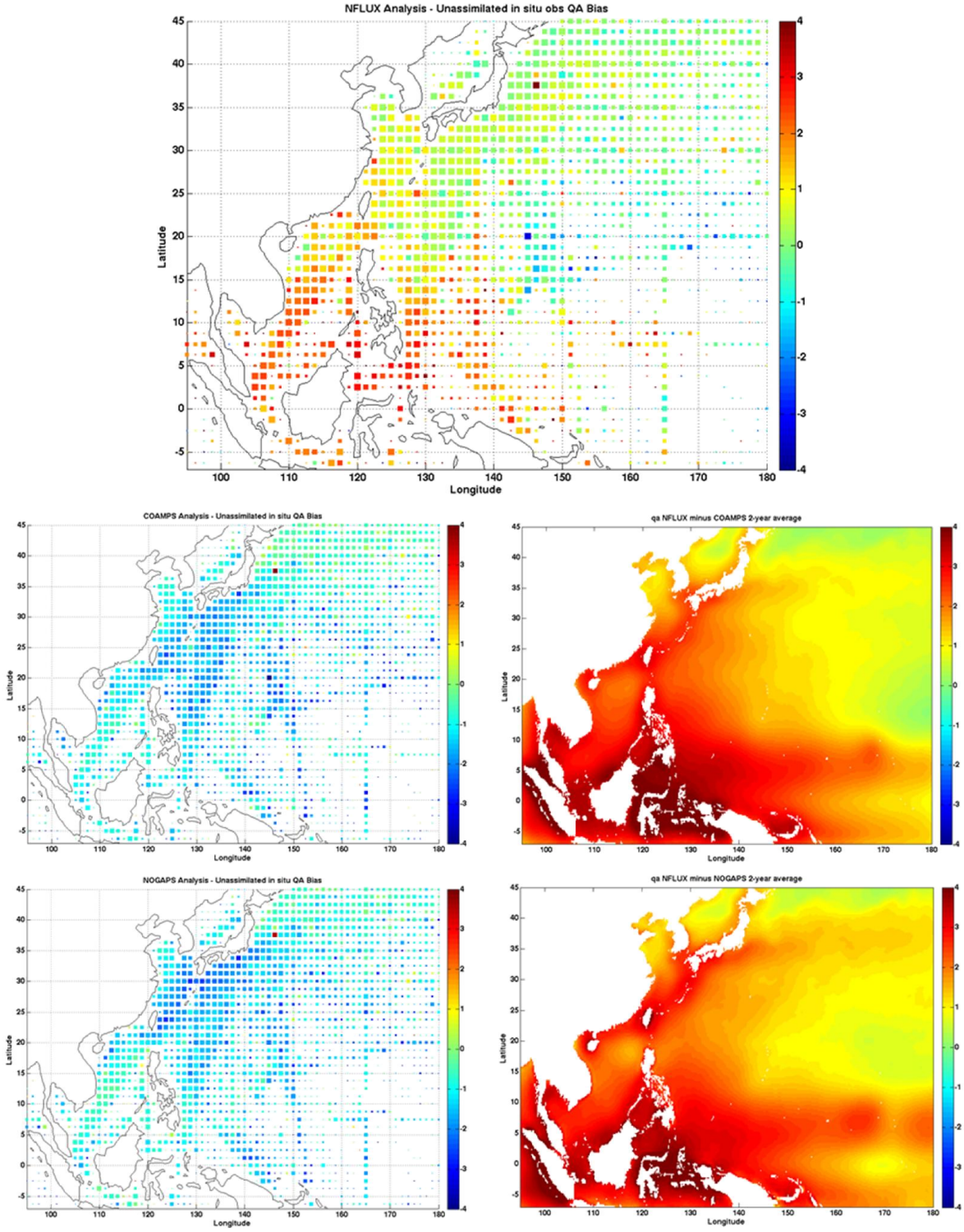

Figure 49: Western Pacific 2-year average specific humidity bias (g/kg). The NFLUX (top), COAMPS (middle left), and NOGAPS (bottom left) bias compared to unassimilated observations is shown. Colored square sizes represent the number of observations in each grid box, ranging from 5 to 50 observations. The NFLUX minus COAMPS (NOGAPS) air temperature difference is shown in the middle (bottom) right panel.

The test statistics for specific humidity in the western Pacific are shown in Table 19. Over the open ocean, NFLUX shows a smaller mean bias compared to each of the COAMPS and NOGAPS products, with the exception of the COAMPS 12-hour forecast using assimilated observations. Each of the COAMPS and NOGAPS products outperforms NFLUX in the remaining test statistics using both assimilated and unassimilated observations. Interesting to note is that NFLUX shows a positive mean bias (NFLUX is moister than the observations) while each of the COAMPS and NOGAPS products shows a negative mean bias (COAMPS and NOGAPS are dryer than the observations). This agrees with the mean error shown in Figure 49.

Table 19: Specific humidity errors over the western Pacific Ocean region. Errors are shown relative to both assimilated (left columns) and unassimilated (right columns) *in situ* observations for all comparisons (regional), near land (coastal), and open ocean (ocean). The best test statistic in each column is highlighted in blue. Means and standard deviations that are not significantly different compared to NFLUX at the 95% confidence interval are denoted with an asterisk (*).

	ME	SD	RMSE	R^2		ME	SD	RMSE	R^2
Regional		N = 32046							
NFLUX Analysis	0.9579	2.1503	2.3540	0.8901	NFLUX 12h persist	1.0300	2.3761	2.5897	0.8670
COAMPS Analysis	-1.2818	1.7345	2.1567	0.9101	COAMPS 12h persist	-1.2570	1.8834	2.2644	0.8943
COAMPS 12h fcst	-0.7592	1.6295	1.7976	0.9206	NOGAPS 12h persist	-1.2584	1.8034	2.1990	0.9047
NOGAPS Analysis	-1.2704	1.4995	1.9653	0.9334					
NOGAPS 12h fcst	-1.5811	1.6436	2.2806	0.9197					
Coastal		N = 10432							
NFLUX Analysis	1.3136	2.1580	2.5263	0.8973	NFLUX 12h persist	1.4096	2.3686	2.7562	0.8777
COAMPS Analysis	-1.4706	1.7805	2.3093	0.9131	COAMPS 12h persist	-1.4572	1.8934	2.3891	0.9019
COAMPS 12h fcst	-0.9161	1.6786	1.9122	0.9227	NOGAPS 12h persist	-1.3960	1.7894	2.2695	0.9133
NOGAPS Analysis	-1.4248	1.5538	2.1081	0.9341					
NOGAPS 12h fcst	-1.6949	1.6639	2.3751	0.9241					
Ocean		N = 21614							
NFLUX Analysis	0.7862	2.1255	2.2662	0.8875	NFLUX 12h persist	0.8468	2.3579	2.5053	0.8626
COAMPS Analysis	-1.1906	1.7044	2.0790	0.9091	COAMPS 12h persist	-1.1604	1.8710	2.2016	0.8910
COAMPS 12h fcst	-0.6835	1.5998	1.7396	0.9200	NOGAPS 12h persist	-1.1919	1.8064	2.1642	0.9005
NOGAPS Analysis	-1.1958	1.4668	1.8925	0.9335					
NOGAPS 12h fcst	-1.5262	1.6309	2.2336	0.9177					

Scatterplots of the western Pacific open ocean specific humidity versus assimilated (unassimilated) matchups along with the corresponding histograms of the probability of the mean bias are shown in Figure 50 (Figure 51). As noted in the global test case, NOGAPS showed an upper limit of approximately 20 g/kg even when the *in situ* observations reached 25 g/kg. Both COAMPS and NOGAPS show this same feature in the western Pacific. NFLUX applies a correction to high specific humidity values that eliminates the 20 g/kg capping effect. This creates a larger spread in NFLUX, which increases the standard deviation; however, NFLUX represents a closer one-to-one fit with *in situ* match ups than COAMPS or NOGAPS.

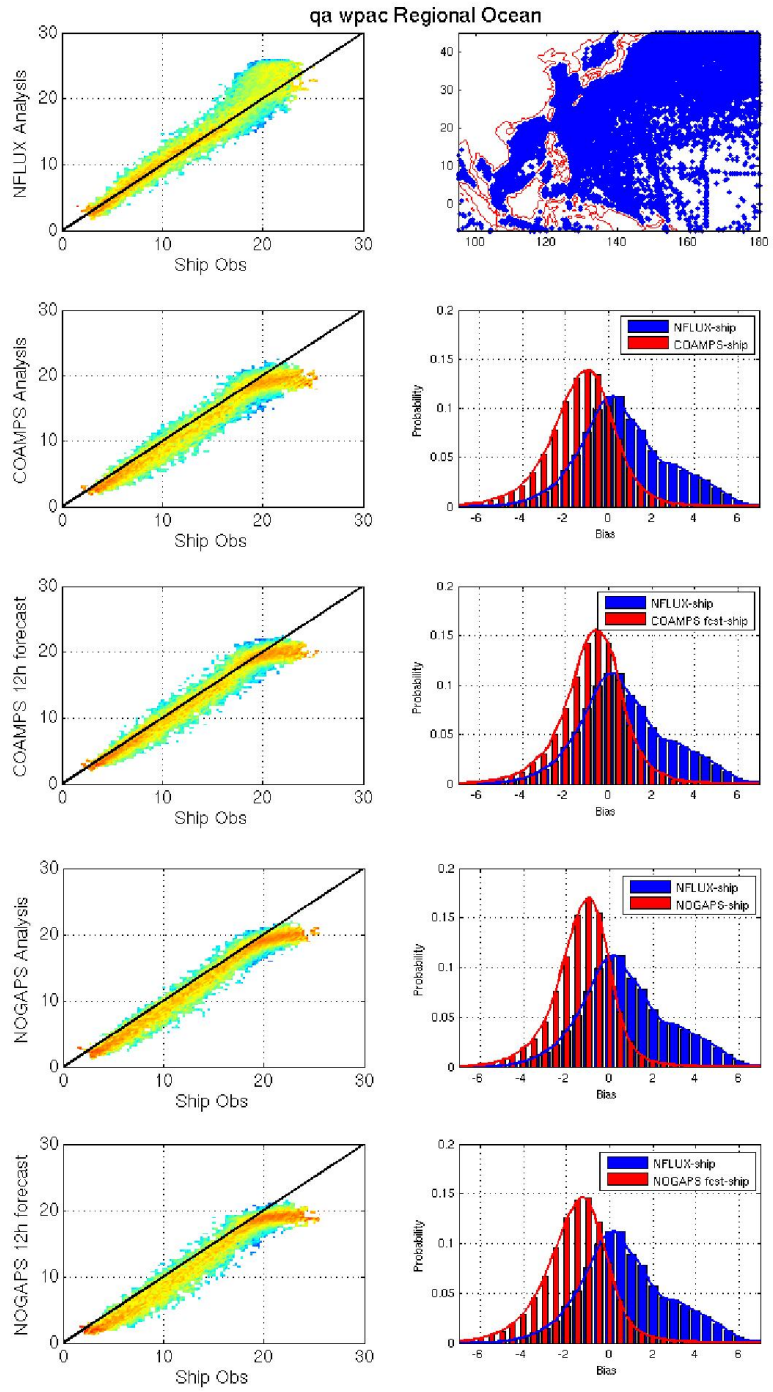

Figure 50: Specific humidity over western Pacific open ocean using assimilated *in situ* data. The distribution of the matched up observations is shown in the top right panel. The panels on the left show scatterplots of the *in situ* observations versus NFLUX analysis (top), COAMPS analysis (second row), COAMPS 12-hour forecast (third row), NOGAPS analysis (fourth row), and NOGAPS 12-hour forecast (bottom). The right panels show histograms of the probability of the mean bias of NFLUX analysis (blue) and corresponding COAMPS/NOGAPS model (red).

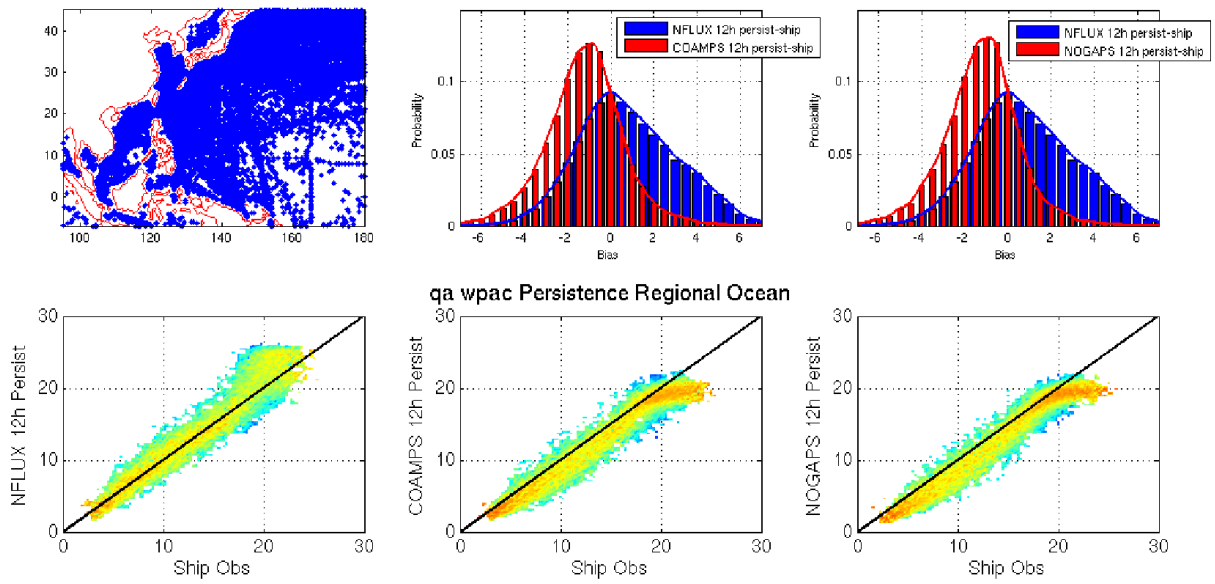

Figure 51: Specific humidity over western Pacific open ocean using unassimilated *in situ* data. The distribution of the matched up observations is shown in the top left panel. The panels on the bottom show scatterplots of the *in situ* observations versus NFLUX analysis (left), COAMPS analysis (middle), and NOGAPS analysis (right). The top panels show histograms of the probability of the mean bias of NFLUX analysis (blue) and corresponding COAMPS/NOGAPS model (red).

5.2.1 Seasonal

The western Pacific open ocean specific humidity results by season are shown in Table 20. The corresponding scatterplots of NFLUX, COAMPS, and NOGAPS compared to assimilated (unassimilated) observations are shown in Figure 52 (Figure 53). Using assimilated observations, NFLUX shows a smaller mean bias in DJF and MAM; however, the COAMPS 12-hour forecast shows a smaller mean bias in JJA and SON. Using unassimilated observations, NFLUX shows a smaller mean bias in each season except JJA. For each of the seasons using both assimilated and unassimilated matchups, NFLUX shows a larger standard deviation, which results in a lower correlation compared to either COAMPS or NOGAPS. The large standard deviation is due to the adjustment at high specific humidity values to remove the capping effect seen in the COAMPS and NOGAPS models.

At high specific humidity values, both COAMPS and NOGAPS display a capping effect. NFLUX applies a correction at high specific humidity values to partially remove this effect. The NFLUX seasonal scatterplots show a more extreme high specific humidity correction than anticipated from the regional open ocean results. Part of this may be attributed to the western Pacific warm pool; however, further investigation is required.

Table 20: Specific humidity errors over the western Pacific open ocean by season. Errors are shown relative to both assimilated (left columns) and unassimilated (right columns) *in situ* observations. The best test statistic in each column is highlighted in blue. Means and standard deviations that are not significantly different compared to NFLUX at the 95% confidence interval are denoted with an asterisk (*).

	ME	SD	RMSE	R^2		ME	SD	RMSE	R^2
DJF		N = 6248							
NFLUX Analysis	0.4557	1.9291	1.9821	0.9019	NFLUX 12h persist	0.5306	2.1707	2.2344	0.8772
COAMPS Analysis	-1.4143	1.5866	2.1254	0.9215	COAMPS 12h persist	-1.3695	1.8143	2.2730	0.8983
COAMPS 12h fcst	-0.8556	1.4884	1.7166	0.9308	NOGAPS 12h persist	-1.3699	1.7646	2.2338	0.9082
NOGAPS Analysis	-1.3917	1.4160	1.9853	0.9404					
NOGAPS 12h fcst	-1.7647	1.5481	2.3474	0.9284					
MAM		N = 4515							
NFLUX Analysis	0.2903	2.0172	2.0378	0.8970	NFLUX 12h persist	0.2955	2.2715	2.2904	0.8720
COAMPS Analysis	-0.9958	1.7089	1.9777	0.9168	COAMPS 12h persist	-1.0093	1.8816	2.1350	0.8987
COAMPS 12h fcst	-0.6557	1.6103	1.7385	0.9260	NOGAPS 12h persist	-1.0112	1.7792	2.0463	0.9103
NOGAPS Analysis	-0.9886	1.4256	1.7347	0.9419					
NOGAPS 12h fcst	-1.3204	1.5771	2.0567	0.9288					
JJA		N = 4529							
NFLUX Analysis	1.4014	2.1062	2.5297	0.7965	NFLUX 12h persist	1.4910	2.2962	2.7376	0.7647
COAMPS Analysis	-1.0112	1.6418	1.9281	0.8456	COAMPS 12h persist	-0.9778	1.6812	1.9448	0.8380
COAMPS 12h fcst	-0.5026	1.5285	1.6088	0.8660	NOGAPS 12h persist	-0.9851	1.5873	1.8680	0.8559
NOGAPS Analysis	-0.9883	1.3182	1.6474	0.9026					
NOGAPS 12h fcst	-1.2240	1.5147	1.9473	0.8724					
SON		N = 6322							
NFLUX Analysis	1.0264	2.2523	2.4750	0.8519	NFLUX 12h persist	1.0917	2.4938	2.7221	0.8173
COAMPS Analysis	-1.2373	1.8238	2.2037	0.8735	COAMPS 12h persist	-1.1926	2.0197	2.3453	0.8458
COAMPS 12h fcst	-0.6628	1.7269	1.8496	0.8862	NOGAPS 12h persist	-1.2933	1.9797	2.3646	0.8558
NOGAPS Analysis	-1.2990	1.6029	2.0631	0.9036					
NOGAPS 12h fcst	-1.6541	1.7714	2.4235	0.8828					

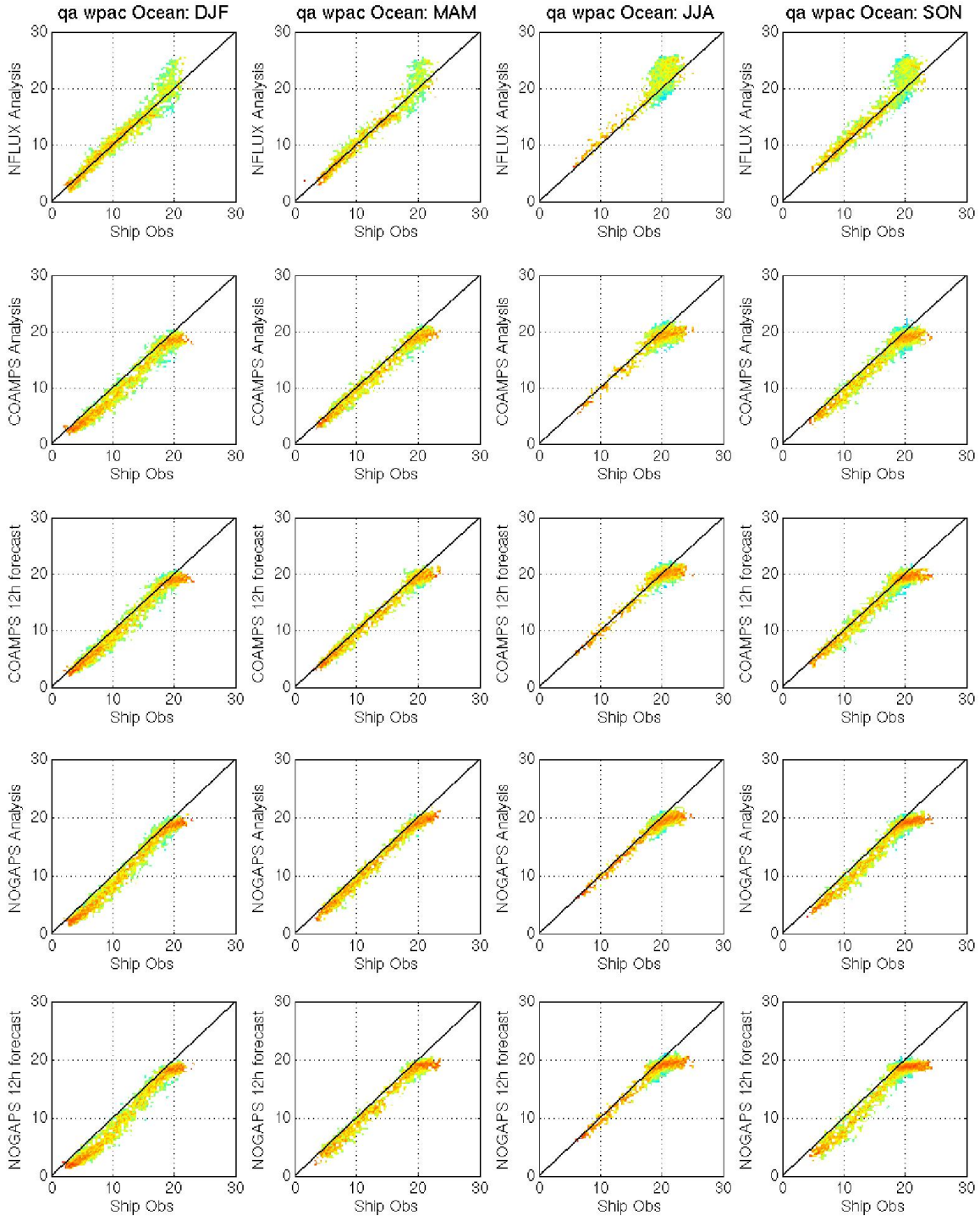

Figure 52: Specific humidity over western Pacific open ocean by season using assimilated *in situ* data. Scatterplots of the *in situ* observations versus NFLUX analysis (top row), COAMPS analysis (second row), COAMPS 12-hour forecast (third row), NOGAPS analysis (fourth row), and NOGAPS 12-hour forecast (bottom row) are shown.

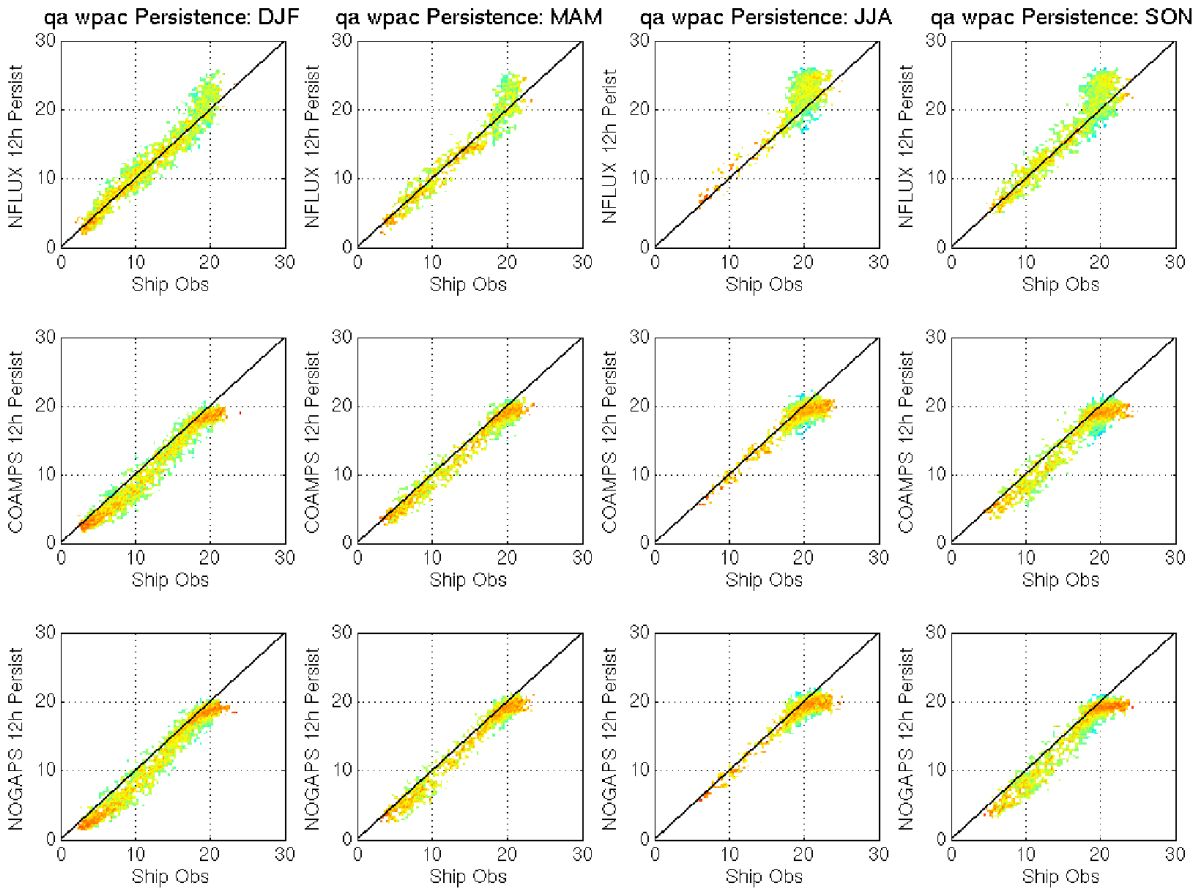

Figure 53: Specific humidity over western Pacific open ocean by season using unassimilated *in situ* data. Scatterplots of the *in situ* observations versus NFLUX analysis (top row), COAMPS analysis (middle row), and NOGAPS analysis (bottom row) are shown.

5.3 Wind Speed Results

Figure 54 shows mean wind speed error over the eastern Pacific using unassimilated *in situ* observations and NFLUX (top), COAMPS (middle left), and NOGAPS (bottom left). Gridded annual differences are also shown for NFLUX versus COAMPS (middle right) and NOGAPS (bottom right). Compared to *in situ* observations, NFLUX shows an overall high bias throughout the region. COAMPS shows a high bias in the center of the region, with a low bias in the southern and northern areas of the region. NOGAPS shows a general low bias throughout the region. As in the other two test cases, a combination of the low bias, coarse resolution, and smooth coastal topography causes enhanced differences between NOGAPS and NFLUX in the coastal areas.

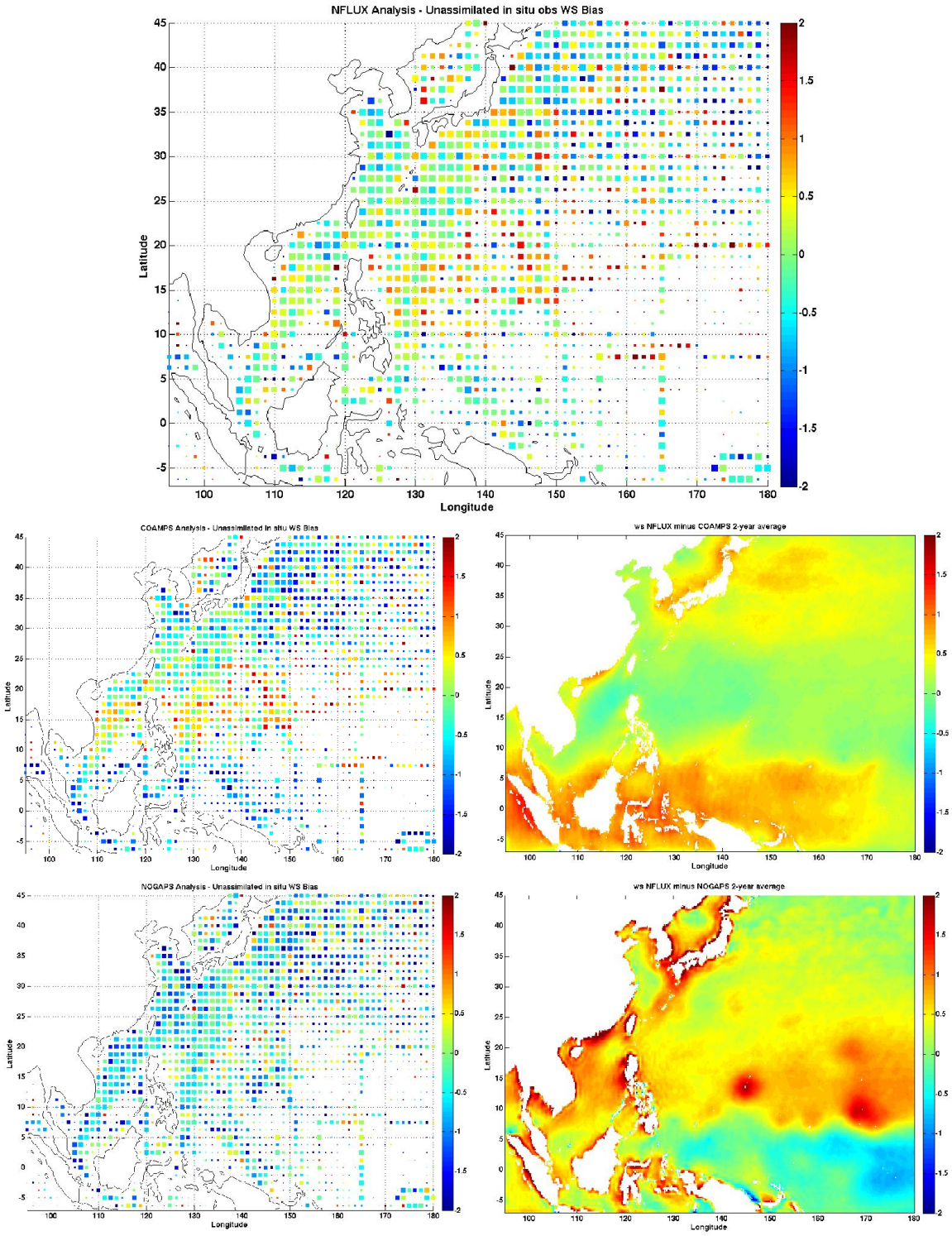

Figure 54: Western Pacific 2-year average wind speed bias (m/s). The NFLUX (top), COAMPS (middle left), and NOGAPS (bottom left) bias compared to unassimilated observations is shown. Colored square sizes represent the number of observations in each grid box, ranging from 5 to 50 observations. The NFLUX minus COAMPS (NOGAPS) air temperature difference is shown in the middle (bottom) right panel.

The wind speed test statistics for the western Pacific are shown in Table 21. For the open ocean, NFLUX shows better or not significantly different statistics compared to both COAMPS and NOGAPS using both assimilated and unassimilated observations. The corresponding scatterplots of wind speed versus assimilated (unassimilated) *in situ* matchups along with the corresponding histograms of the probability of the mean bias are shown in Figure 55 (Figure 56). Each of the model products show a relatively large spread compared to what is seen with air temperature and specific humidity. Each of the products show the high bias at low wind speeds, less than approximately 4 m/s, that was discussed in the global test case.

Table 21: Wind speed errors over the western Pacific Ocean region. Errors are shown relative to both assimilated (left columns) and unassimilated (right columns) *in situ* observations for all comparisons (regional), near land (coastal), and open ocean (ocean). The best test statistic in each column is highlighted in blue. Means and standard deviations that are not significantly different compared to NFLUX at the 95% confidence interval are denoted with an asterisk (*).

	ME	SD	RMSE	R^2		ME	SD	RMSE	R^2
Regional		N = 67381							
NFLUX Analysis	-0.2956	2.5732	2.5901	0.5852	NFLUX 12h persist	-0.3044	3.3093	3.3232	0.3528
COAMPS Analysis	-0.8109	2.8894	3.0010	0.4962	COAMPS 12h persist	-0.8214	3.5176	3.6122	0.3103
COAMPS 12h fcst	-0.8893	2.9983	3.1273	0.4624	NOGAPS 12h persist	-0.8719	3.3800	3.4906	0.3173
NOGAPS Analysis	-0.8767	2.7492	2.8856	0.5265					
NOGAPS 12h fcst	-0.7956	2.8395	2.9488	0.4969					
Coastal		N = 20539							
NFLUX Analysis	-0.6520	3.2231	3.2883	0.5677	NFLUX 12h persist	-0.6613	4.0973	4.1502	0.3212
COAMPS Analysis	-1.2629	3.5039	3.7245	0.4877	COAMPS 12h persist	-1.2795	4.2857	4.4725	0.2758
COAMPS 12h fcst	-1.2360	3.5815	3.7887	0.4662	NOGAPS 12h persist	-1.7983	4.1949	4.5640	0.2768
NOGAPS Analysis	-1.8074	3.5069	3.9452	0.4903					
NOGAPS 12h fcst	-1.5694	3.5631	3.8933	0.4699					
Ocean		N = 46842							
NFLUX Analysis	-0.1393	2.2113	2.2157	0.6073	NFLUX 12h persist	-0.1479	2.8831	2.8868	0.3812
COAMPS Analysis	-0.6126	2.5490	2.6216	0.5193	COAMPS 12h persist	-0.6206	3.1006	3.1620	0.3454
COAMPS 12h fcst	-0.7372	2.6891	2.7883	0.4712	NOGAPS 12h persist	-0.4657	*2.8595	2.8971	0.3799
NOGAPS Analysis	-0.4686	*2.2212	2.2701	0.6015					
NOGAPS 12h fcst	-0.4563	2.3777	2.4211	0.5481					

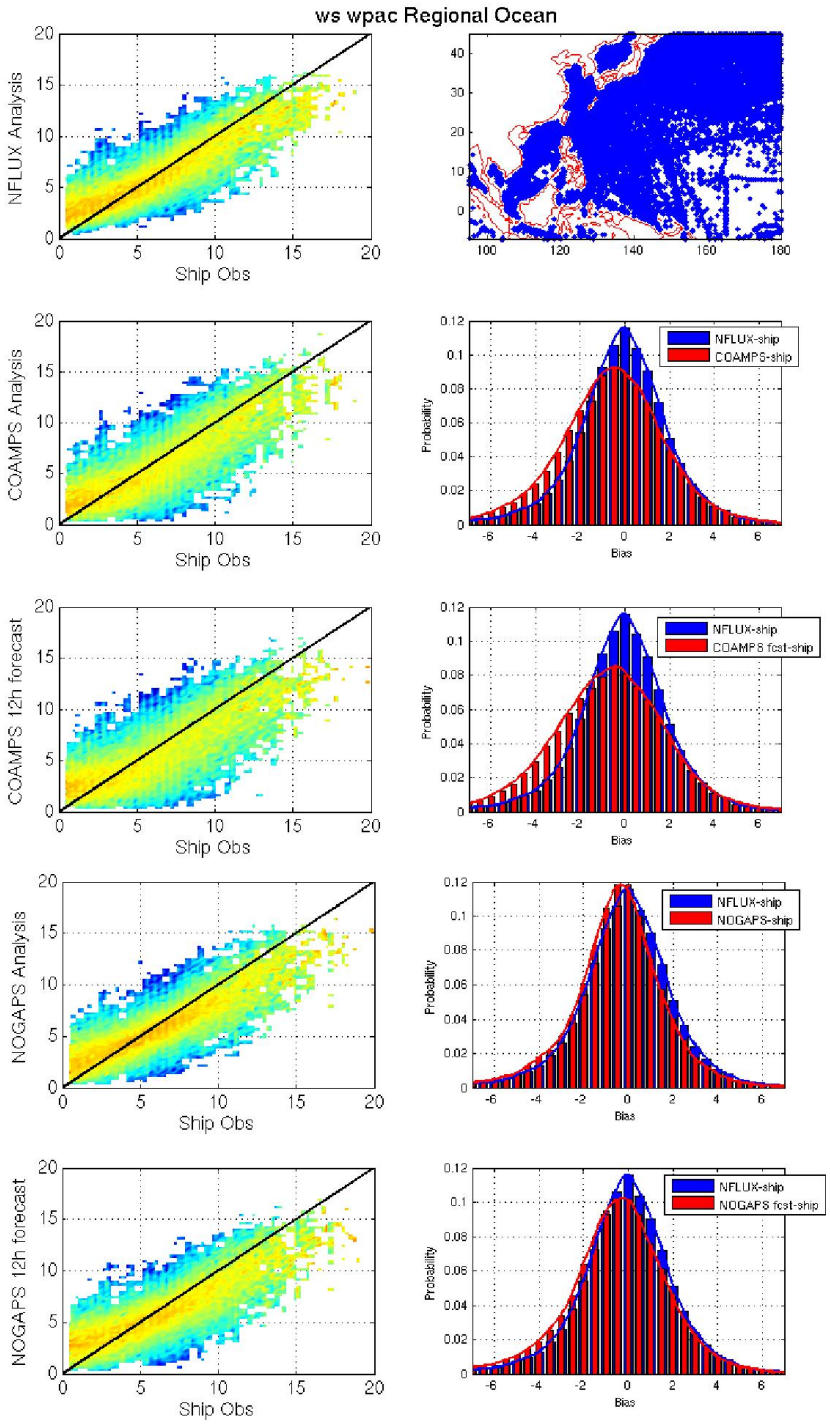

Figure 55: Wind speed over western Pacific open ocean using assimilated *in situ* data. The distribution of the matched up observations is shown in the top right panel. The panels on the left show scatterplots of the *in situ* observations versus NFLUX analysis (top), COAMPS analysis (second row), COAMPS 12-hour forecast (third row), NOGAPS analysis (fourth row), and NOGAPS 12-hour forecast (bottom). The right panels show histograms of the probability of the mean bias of NFLUX analysis (blue) and corresponding COAMPS/NOGAPS model (red).

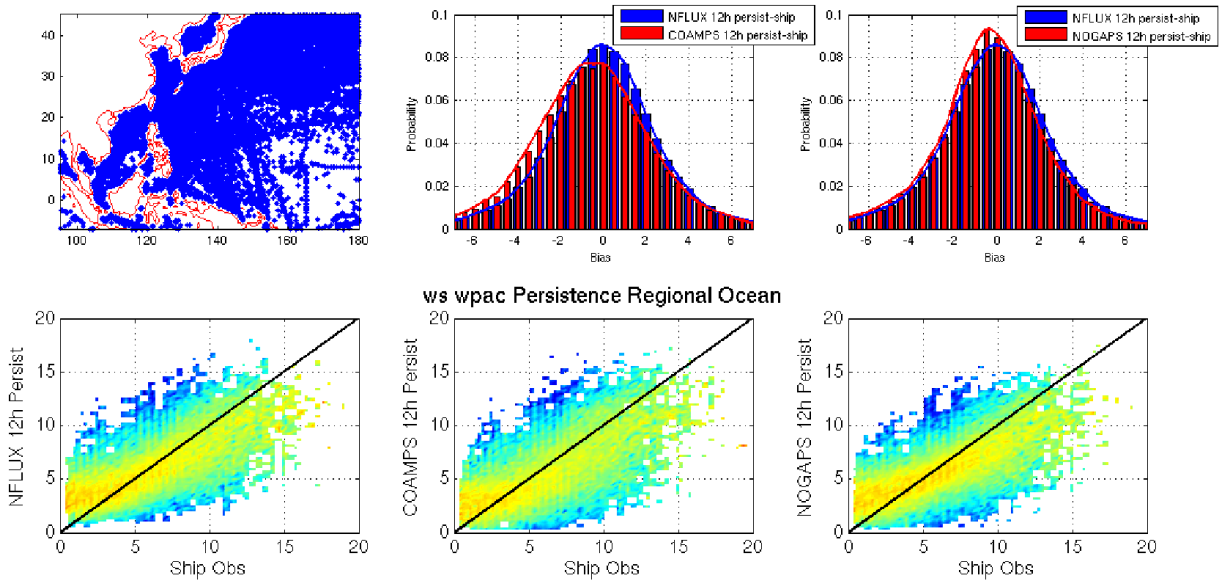

Figure 56: Wind speed over western Pacific open ocean using unassimilated *in situ* data. The distribution of the matched up observations is shown in the top left panel. The panels on the bottom show scatterplots of the *in situ* observations versus NFLUX analysis (left), COAMPS analysis (middle), and NOGAPS analysis (right). The top panels show histograms of the probability of the mean bias of NFLUX analysis (blue) and corresponding COAMPS/NOGAPS model (red).

5.3.1 Seasonal

The open ocean wind speed results in the western Pacific by season are shown in Table 22. The corresponding scatterplots of NFLUX, COAMPS, and NOGAPS compared to assimilated (unassimilated) observations are shown in Figure 57 (Figure 58). The results are similar to those presented for the regional open ocean. Using both assimilated and unassimilated observations, NFLUX shows improvement or no significant difference compared to both COAMPS and NOGAPS.

Table 22: Wind speed errors over the western Pacific open ocean by season. Errors are shown relative to both assimilated (left columns) and unassimilated (right columns) *in situ* observations. The best test statistic in each column is highlighted in blue. Means and standard deviations that are not significantly different compared to NFLUX at the 95% confidence interval are denoted with an asterisk (*).

	ME	SD	RMSE	R^2		ME	SD	RMSE	R^2
DJF		N = 12298							
NFLUX Analysis	-0.0587	2.3676	2.3682	0.6385	NFLUX 12h persist	-0.0474	3.1725	3.1728	0.3982
COAMPS Analysis	-0.3981	2.7974	2.8254	0.5309	COAMPS 12h persist	-0.3882	3.4315	3.4533	0.3511
COAMPS 12h fcst	-0.4914	2.9051	2.9462	0.4974	NOGAPS 12h persist	-0.4530	*3.1267	3.1592	0.4011
NOGAPS Analysis	-0.4729	*2.3863	2.4326	0.6307					
NOGAPS 12h fcst	-0.4097	2.5224	2.5553	0.5895					
MAM		N = 10905							
NFLUX Analysis	-0.1156	2.1475	2.1506	0.5967	NFLUX 12h persist	-0.1392	2.9244	2.9276	0.3190
COAMPS Analysis	-0.7936	2.6172	2.7347	0.4540	COAMPS 12h persist	-0.8103	3.1325	3.2354	0.2788
COAMPS 12h fcst	-0.8006	2.6508	2.7690	0.4455	NOGAPS 12h persist	-0.3981	*2.9116	2.9385	0.3134
NOGAPS Analysis	-0.3797	2.2033	2.2357	0.5744					
NOGAPS 12h fcst	-0.3635	2.3605	2.3882	0.5167					
JJA		N = 10965							
NFLUX Analysis	-0.2589	2.0977	2.1135	0.4936	NFLUX 12h persist	-0.2474	2.5259	2.5379	0.3098
COAMPS Analysis	-0.7681	2.3033	2.4279	0.4352	COAMPS 12h persist	-0.7695	2.6965	2.8040	0.2859
COAMPS 12h fcst	-0.9863	2.4924	2.6804	0.3466	NOGAPS 12h persist	-0.4493	*2.5461	2.5854	0.3017
NOGAPS Analysis	-0.4545	*2.0909	2.1397	0.4974					
NOGAPS 12h fcst	-0.5185	2.2699	2.3282	0.4160					
SON		N = 12674							
NFLUX Analysis	-0.1346	2.2002	2.2042	0.5971	NFLUX 12h persist	-0.1667	2.8389	2.8437	0.3809
COAMPS Analysis	-0.5308	2.4164	2.4739	0.5511	COAMPS 12h persist	-0.5540	3.0441	3.0940	0.3540
COAMPS 12h fcst	-0.7059	2.6461	2.7386	0.4705	NOGAPS 12h persist	-0.5503	*2.7966	2.8502	0.3870
NOGAPS Analysis	-0.5531	*2.1764	2.2455	0.6025					
NOGAPS 12h fcst	-0.5276	2.3352	2.3940	0.5487					

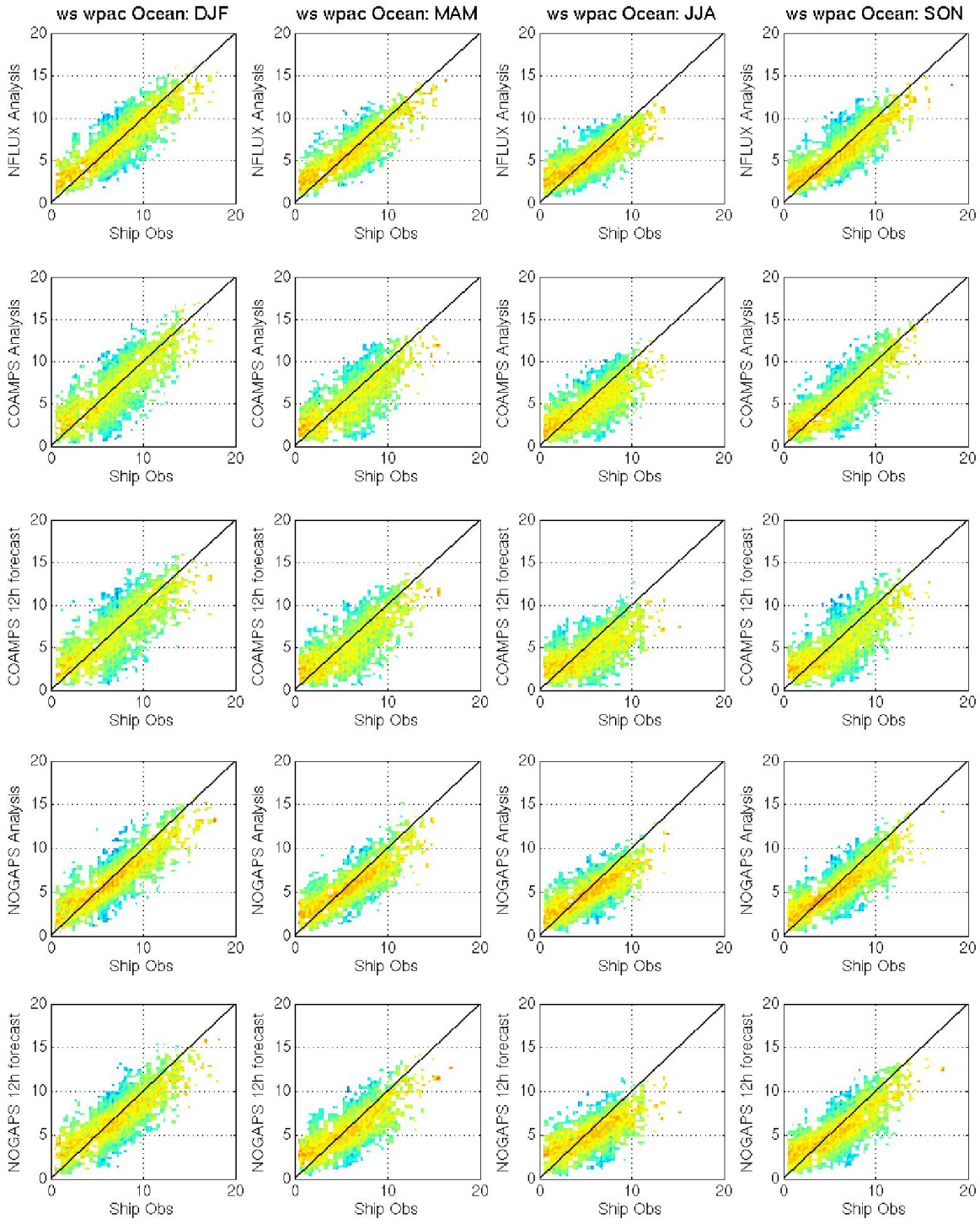

Figure 57: Wind speed over western Pacific open ocean by season using assimilated *in situ* data. Scatterplots of the *in situ* observations versus NFLUX analysis (top row), COAMPS analysis (second row), COAMPS 12-hour forecast (third row), NOGAPS analysis (fourth row), and NOGAPS 12-hour forecast (bottom row) are shown.

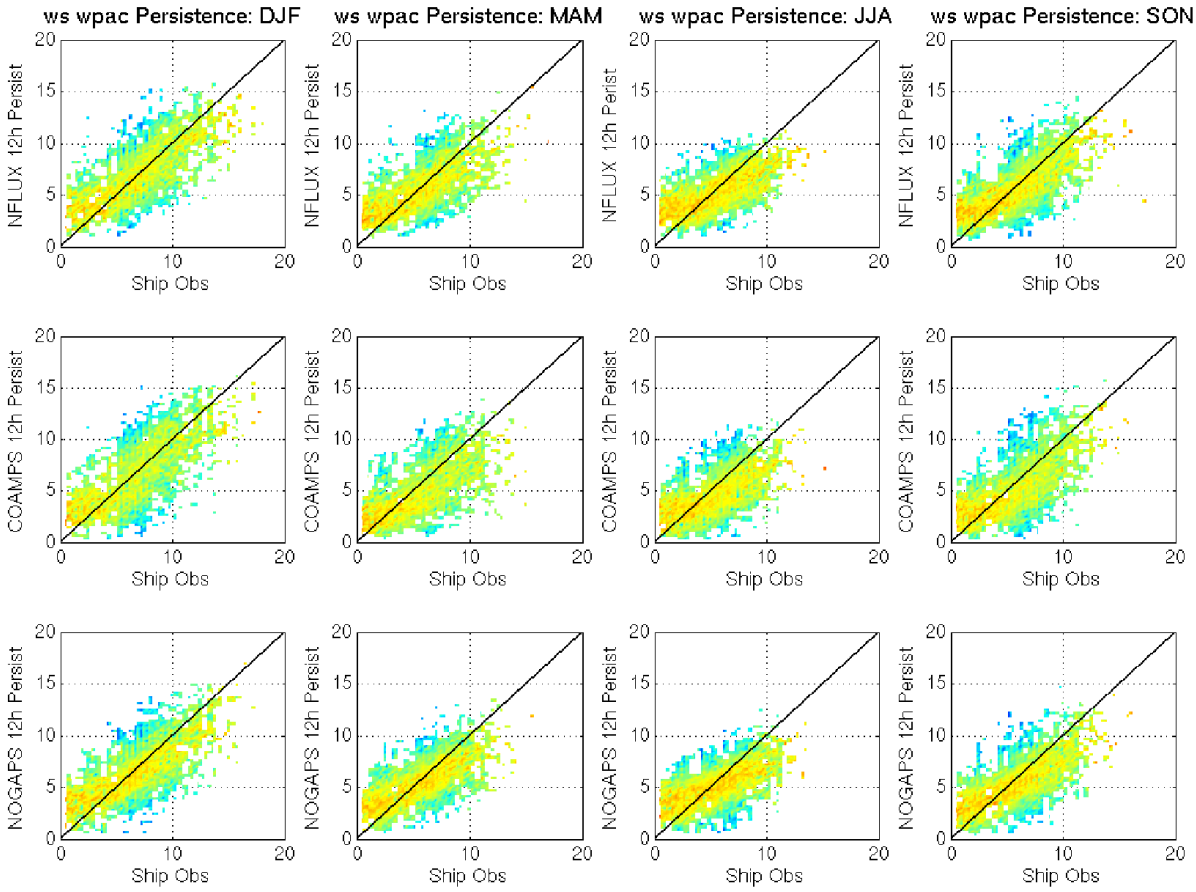

Figure 58: Wind speed over western Pacific open ocean by season using unassimilated *in situ* data. Scatterplots of the *in situ* observations versus NFLUX analysis (top row), COAMPS analysis (middle row), and NOGAPS analysis (bottom row) are shown.

6.0 APPLICATION OF REGION-SPECIFIC RETRIEVALS

The NFLUX version 1 system was built using global satellite retrieval algorithms. Current work with the NFLUX system allows for region-specific retrieval algorithms to be utilized. To demonstrate the capability of region-specific retrievals, four areas of Navy interest were chosen: the California Current System (1), the Arabian Sea (2), the South China Sea (3), and the Okinawa Trough (4). A map outlining the boundaries of each region is shown in Figure 59.

The size of each of these regions was determined based on both the amount of data available for algorithm development and the extent of relatively homogeneous conditions seen in the NFLUX analyses. Each region represents an area with different atmospheric characteristics. The California Current System has an eastern boundary, with NFLUX showing warmer temperatures than NOGAPS. The NFLUX analyses in the Arabian Sea shows similar characteristics to NOGAPS. The South China Sea is in the tropics and represents an area with typical warm and

moist atmospheric conditions. The Okinawa Trough has a western boundary with NFLUX sowing higher temperatures and specific humidity values than NOGAPS.

As presented with the global test case, large scale biases can be identified in the air temperature and specific humidity fields (Figure 3 and Figure 11). The global wind speed biases are more random, causing region-specific retrievals difficult to determine. The domains presented here will include new results only for the air temperature and specific humidity fields; wind speed has not been modified.

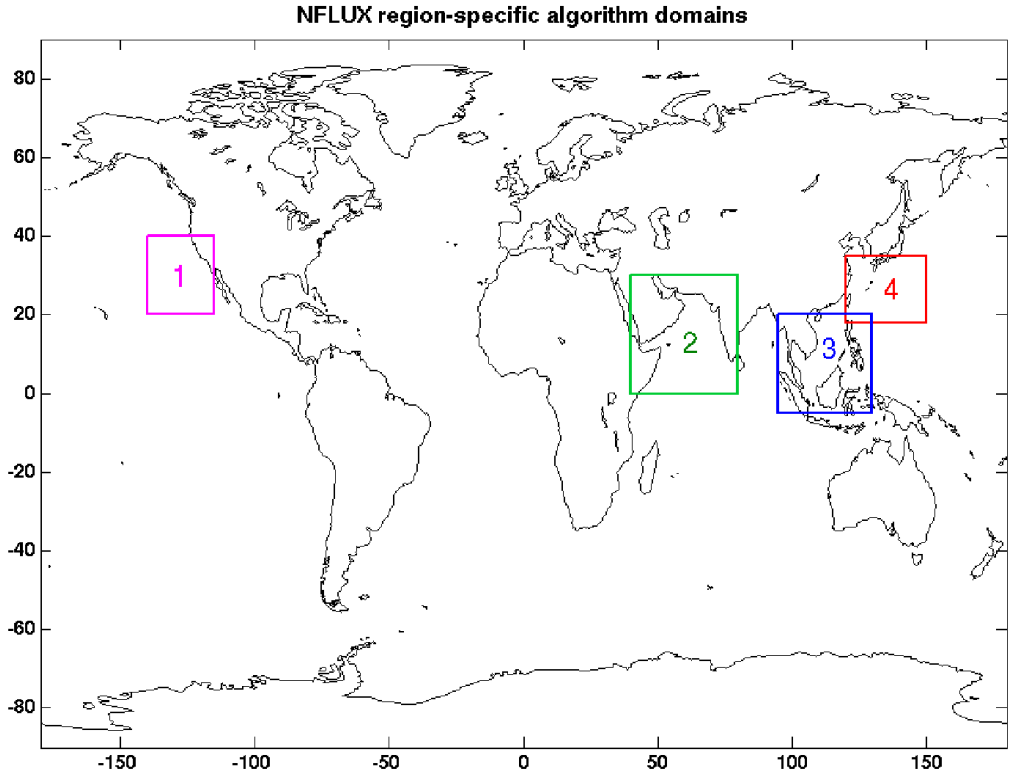

Figure 59: Region-specific satellite retrieval domains. Four regions of interest were chosen to determine performance.

In the Western and Eastern Pacific regional test cases discussed before, COAMPS analysis fields were blended with the previous NFLUX analysis increment field to produce the background fields. In each of the regional test cases, we found NOGAPS had a better comparison with the *in situ* observations than COAMPS. Therefore, for these new modified regions, we use the NOGAPS analysis fields as opposed to the COAMPS analysis fields to form the background fields.

In addition to the four test statistics presented before, an overall skill score (SS) will also be included for each comparison. SS is a non-dimensional quantity based on the correlation coefficient (first term on the right hand side), conditional bias (middle term on the right hand side), and unconditional bias (last term on the right hand side) (Murphy, 1988). The conditional

bias is associated with the differences in the standard deviations and reflects the extent to which the slope of the regression line differs from unity. The unconditional bias is a measure of the difference between the means. A SS of 1.0 is perfect, while a SS of 0.0 is no skill. A positive SS represents improved skill and a negative SS represents reduced skill.

$$SS = R^2 - \left[R - \left(\frac{\sigma_Y}{\sigma_X}\right)\right]^2 - [(\bar{Y} - \bar{X})/\sigma_X]^2, \quad \textbf{(8)}$$

where $\bar{X}$ and σ_X are the mean and standard deviation of the *in situ* observations, $\bar{Y}$ and σ_Y are the mean and standard deviation of the model product, and R is the correlation coefficient.

6.1 California Current System

Figure 60 shows mean air temperature (left) and specific humidity (right) error over the California Current System using unassimilated *in situ* observations and global NFLUX (top), region-specific NFLUX (middle), and NOGAPS (bottom). For the air temperature bias, each of the models shows a similar spatial pattern. For the specific humidity bias, the region-specific NFLUX shows a more negative (dry) bias than the global NFLUX over the central area of the region, while NOGAPS shows an overall dry bias throughout the entire region.

Air temperature and specific humidity test statistics over the California Current System are shown in Table 23 and Table 24 using assimilated and unassimilated *in situ* matchups. The corresponding open ocean scatterplots using unassimilated matchups are shown in Figure 61. The air temperature results for the global and region-specific NFLUX are very similar, with the region-specific retrievals showing a lower ME. However, NOGAPS shows improvement in the other statistics. For specific humidity, the global NFLUX shows improved results over the region-specific NFLUX retrievals and most of the NOGAPS statistics.

In the California Current region, the region-specific retrievals showed similar to worse results compared to the global retrievals. This could be a result of too few observations being used to develop the region-specific algorithms. Over the 2 years, there are 6783 (4584) ship to satellite matchups over the open ocean for air temperature (specific humidity).

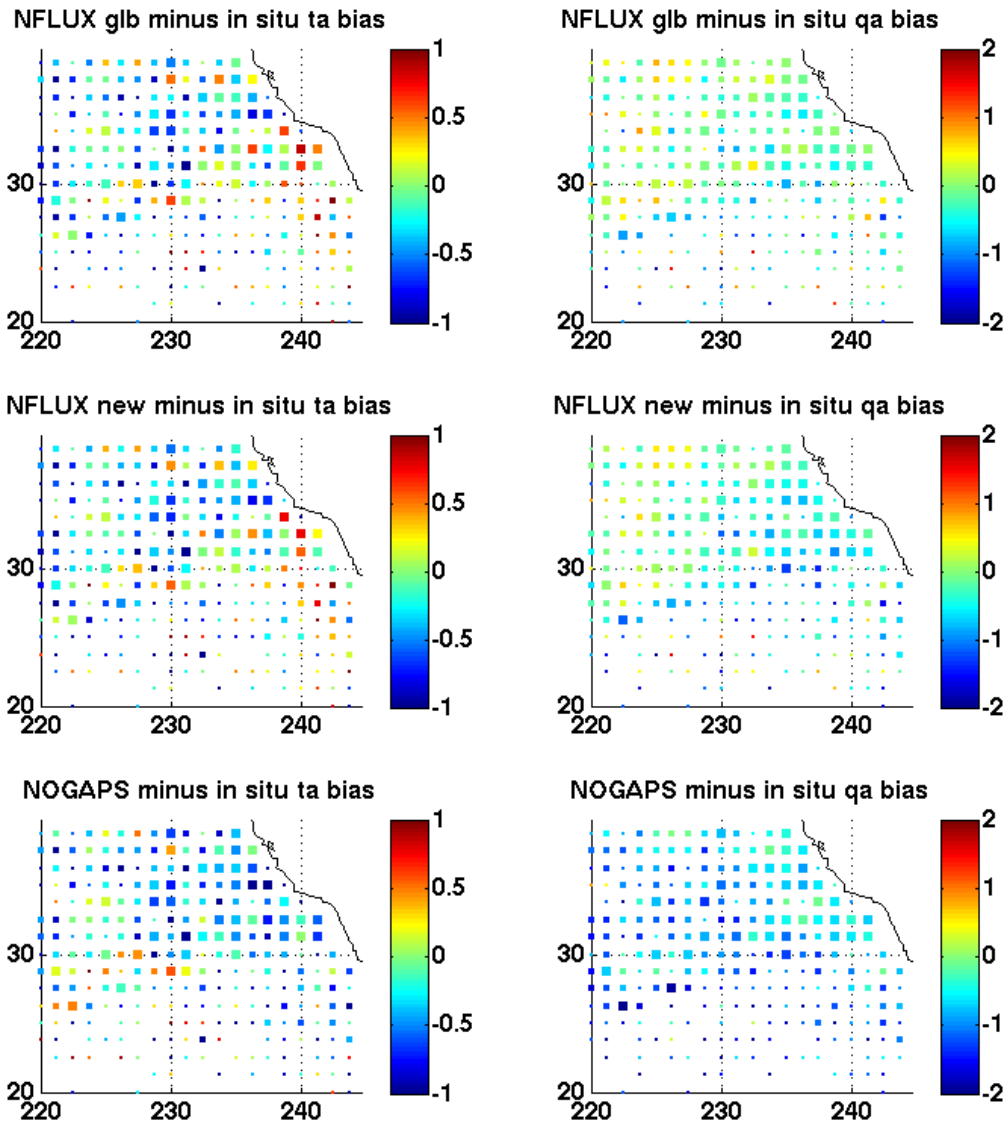

Figure 60: California Current 2-year average air temperature (°C) and specific humidity (g/kg) bias. The global NFLUX (top), new regional NFLUX (middle), and NOGAPS (bottom) bias compared to unassimilated observations is shown for both air temperature (left) and specific humidity (right). Colored square sizes represent the number of observations in each grid box, ranging from 5 to 50 observations.

Table 23: Air temperature errors over the California Current region. Errors are shown relative to both assimilated (left columns) and unassimilated (right columns) *in situ* observations for all comparisons (regional), near land (coastal), and open ocean (ocean). The best test statistic in each column is highlighted in blue. Means and standard deviations that are not significantly different compared to NFLUX at the 95% confidence interval are denoted with an asterisk (*).

	ME	SD	RMSE	R^2	SS		ME	SD	RMSE	R^2	SS
Regional		N = 27177									
NFLUX global	0.8055	2.0000	2.1561	0.5747	0.3537	NFLUX 12h persist glb	0.8109	2.3622	2.4975	0.4354	0.1329
NFLUX new	0.6940	2.0101	2.1265	0.5867	0.3714	NFLUX 12h persist new	0.6973	2.4139	2.5126	0.4326	0.1223
NOGAPS Analysis	0.6619	2.3541	2.4454	0.4855	0.1687	NOGAPS 12h persist	0.6678	2.7554	2.8351	0.3330	-0.1175
NOGAPS 12h fcst	0.8531	2.2990	2.4522	0.4894	0.1640						
Coastal		N = 20394									
NFLUX global	1.0468	2.1159	2.3606	0.4737	-0.2417	NFLUX 12h persist glb	1.0549	2.5469	2.7566	0.2770	-0.6933
NFLUX new	0.9095	2.1476	2.3322	0.4894	-0.2120	NFLUX 12h persist new	0.9169	2.6187	2.7745	0.2745	-0.7154
NOGAPS Analysis	0.9618	2.5412	2.7170	0.3842	-0.6450	NOGAPS 12h persist	0.9686	3.0116	3.1635	0.1826	-1.2300
NOGAPS 12h fcst	1.1719	2.4695	2.7334	0.3932	-0.6648						
Ocean		N = 6783									
NFLUX global	0.0802	1.3655	1.3678	0.7950	0.7927	NFLUX 12h persist glb	0.0773	1.4622	1.4641	0.7660	0.7625
NFLUX new	0.0461	1.3275	1.3282	0.8063	0.8045	NFLUX 12h persist new	0.0373	1.4655	1.4659	0.7656	0.7619
NOGAPS Analysis	-0.2399	1.3060	1.3277	0.8130	0.8047	NOGAPS 12h persist	-0.2366	1.4354	1.4547	0.7756	0.7655
NOGAPS 12h fcst	-0.1053	1.2720	1.2762	0.8209	0.8195						

Table 24: Specific humidity errors over the California Current region. Errors are shown relative to both assimilated (left columns) and unassimilated (right columns) *in situ* observations for all comparisons (regional), near land (coastal), and open ocean (ocean). The best test statistic in each column is highlighted in blue. Means and standard deviations that are not significantly different compared to NFLUX at the 95% confidence interval are denoted with an asterisk (*).

	ME	SD	RMSE	R^2	SS		ME	SD	RMSE	R^2	SS
Regional		N = 7198									
NFLUX global	-0.1068	1.1917	1.1964	0.6591	0.6139	NFLUX 12h persist glb	-0.1232	1.3359	1.3415	0.5817	0.5146
NFLUX new	-0.2514	1.2499	1.2749	0.6262	0.5616	NFLUX 12h persist new	-0.2680	1.3670	1.3929	0.5600	0.4766
NOGAPS Analysis	-0.7642	1.0562	1.3036	0.7176	0.5416	NOGAPS 12h persist	-0.8027	1.3418	1.5635	0.5647	0.3407
NOGAPS 12h fcst	-0.9326	1.2286	1.5424	0.6379	0.3583						
Coastal		N = 2614									
NFLUX global	-0.0606	1.1329	1.1343	0.5751	0.4623	NFLUX 12h persist glb	-0.0814	1.2662	1.2686	0.4943	0.3275
NFLUX new	-0.1028	1.2048	1.2089	0.5293	0.3892	NFLUX 12h persist new	-0.0976	1.2840	1.2875	0.4754	0.3073
NOGAPS Analysis	-0.6850	1.0630	1.2645	0.5822	0.3319	NOGAPS 12h persist	-0.6814	1.2383	1.4132	0.4604	0.1654
NOGAPS 12h fcst	-0.6892	1.1115	1.3076	0.5709	0.2855						
Ocean		N = 4584									
NFLUX global	-0.1332	1.2233	1.2304	0.6676	0.6304	NFLUX 12h persist glb	-0.1470	1.3737	1.3813	0.5880	0.5341
NFLUX new	-0.3362	1.2673	1.3110	0.6458	0.5804	NFLUX 12h persist new	-0.3652	1.4030	1.4496	0.5733	0.4869
NOGAPS Analysis	-0.8094	1.0497	1.3254	0.7463	0.5711	NOGAPS 12h persist	-0.8718	1.3928	1.6430	0.5762	0.3409
NOGAPS 12h fcst	-1.0714	1.2701	1.6616	0.6532	0.3260						

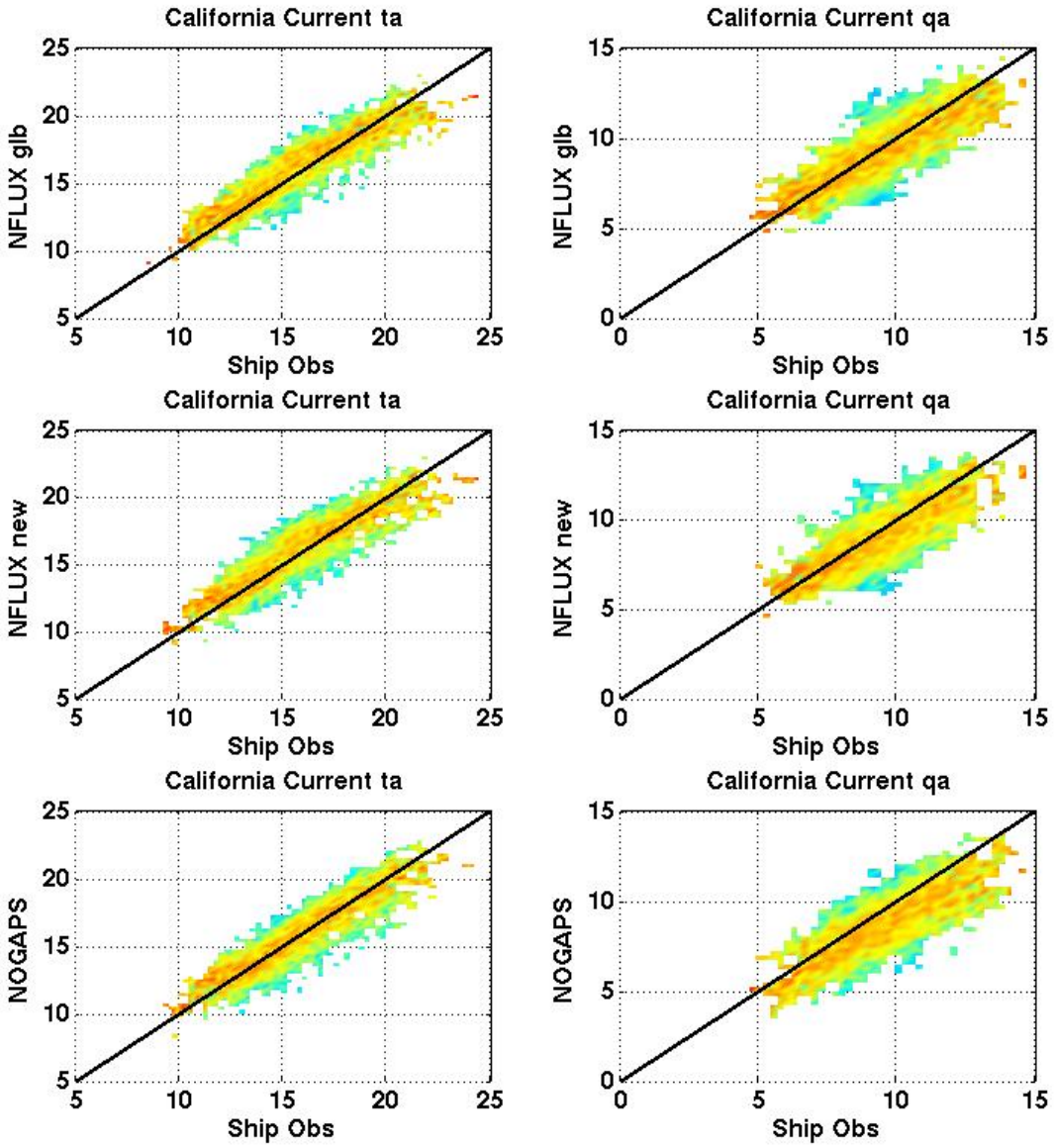

Figure 61: Air temperature and specific humidity over the California Current open ocean region using unassimilated *in situ* data. Scatterplots of the *in situ* observations versus global NFLUX analysis (top), new regional NFLUX analysis (middle), and NOGAPS analysis (bottom) are shown for both air temperature (left) and specific humidity (right).

6.2 Arabian Sea

Figure 62 shows mean air temperature (left) and specific humidity (right) error over the Arabian Sea using unassimilated *in situ* observations and global NFLUX (top), region-specific NFLUX (middle), and NOGAPS (bottom). For the air temperature bias, the region-specific NFLUX shows a near neutral overall bias, while both the global NFLUX and NOGAPS shows a dominantly cold bias. For the specific humidity bias, each of the models shows a similar spatial

pattern with the majority of the region showing a dry bias. The models differ off the western coast of India however. The global and region-specific NFLUX shows a near neutral bias, while NOGAPS continues to show a dry bias.

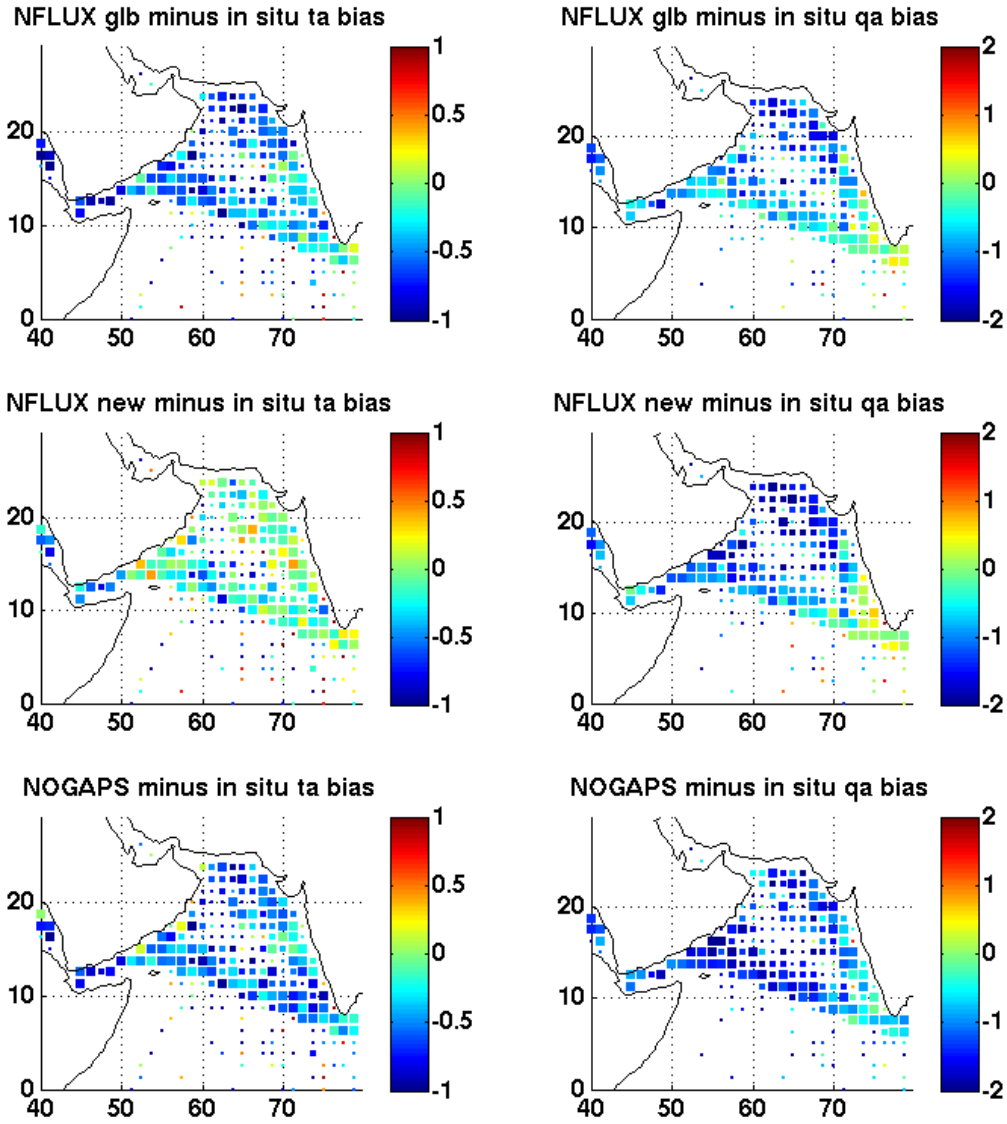

Figure 62: Arabian Sea 2-year average air temperature (°C) and specific humidity (g/kg) bias. The global NFLUX (top), new regional NFLUX (middle), and NOGAPS (bottom) bias compared to unassimilated observations is shown for both air temperature (left) and specific humidity (right). Colored square sizes represent the number of observations in each grid box, ranging from 5 to 50 observations.

Air temperature and specific humidity test statistics over the Arabian Sea are shown in Table 25and Table 26 using assimilated and unassimilated *in situ* matchups. The corresponding open ocean scatterplots using unassimilated matchups are shown in Figure 63.

Table 25: Air temperature errors over the Arabian Sea region. Errors are shown relative to both assimilated (left columns) and unassimilated (right columns) *in situ* observations for all comparisons (regional), near land (coastal), and open ocean (ocean). The best test statistic in each column is highlighted in blue. Means and standard deviations that are not significantly different compared to NFLUX at the 95% confidence interval are denoted with an asterisk (*).

	ME	SD	RMSE	R^2	SS		ME	SD	RMSE	R^2	SS
Regional		N = 13133									
NFLUX global	-0.4646	1.5053	1.5753	0.6840	0.6353	NFLUX 12h persist glb	-0.4873	2.1439	2.1526	0.4503	0.3190
NFLUX new	-0.1589	1.3353	1.3446	0.7403	0.7343	NFLUX 12h persist new	-0.1908	1.9709	1.9800	0.4843	0.4239
NOGAPS Analysis	-0.4509	1.5880	1.6507	0.6540	0.5996	NOGAPS 12h persist	-0.4634	2.1439	2.1933	0.4292	0.2930
NOGAPS 12h fcst	-0.3432	1.6058	1.6420	0.6566	0.6038						
Coastal		N = 4974									
NFLUX global	-0.4624	1.8473	1.9041	0.7390	0.6919	NFLUX 12h persist glb	-0.5083	2.8964	2.9404	0.4445	0.2654
NFLUX new	-0.1947	1.5729	1.5847	0.7966	0.7343	NFLUX 12h persist new	-0.2634	2.6711	2.6838	0.4892	0.3880
NOGAPS Analysis	-0.3284	1.9776	2.0045	0.7119	0.5996	NOGAPS 12h persist	-0.3815	2.9646	2.9887	0.4288	0.2410
NOGAPS 12h fcst	-0.2167	2.0505	2.0617	0.7077	0.6038						
Ocean		N = 8159									
NFLUX global	-0.4660	1.2519	1.3358	0.5865	0.5278	NFLUX 12h persist glb	-0.4745	1.4011	1.4792	0.4911	0.4209
NFLUX new	-0.1370	1.1665	1.1744	0.6411	0.6349	NFLUX 12h persist new	-0.1466	1.3778	1.3855	0.5005	0.4919
NOGAPS Analysis	-0.5256	1.2886	1.3916	0.5609	0.4875	NOGAPS 12h persist	-0.5134	1.4265	1.5159	0.4680	0.3918
NOGAPS 12h fcst	-0.4203	1.2538	1.3223	0.5842	0.5372						

Table 26: Specific humidity errors over the Arabian Sea region. Errors are shown relative to both assimilated (left columns) and unassimilated (right columns) *in situ* observations for all comparisons (regional), near land (coastal), and open ocean (ocean). The best test statistic in each column is highlighted in blue. Means and standard deviations that are not significantly different compared to NFLUX at the 95% confidence interval are denoted with an asterisk (*).

	ME	SD	RMSE	R^2	SS		ME	SD	RMSE	R^2	SS
Regional		N = 10320									
NFLUX global	-1.0040	2.3687	2.5726	0.5809	0.4116	NFLUX 12h persist glb	-1.0523	2.2316	2.7910	0.5206	0.3074
NFLUX new	-1.0655	2.2684	2.5061	0.5809	0.4416	NFLUX 12h persist new	-1.1177	2.4570	2.6992	0.5239	0.3522
NOGAPS Analysis	-1.4002	1.8933	2.3547	0.7179	0.5070	NOGAPS 12h persist	-1.4470	2.2316	2.6595	0.6290	0.3711
NOGAPS 12h fcst	-1.8687	2.2152	2.8981	0.6255	0.2532						
Coastal		N = 4299									
NFLUX global	-1.3607	2.5730	2.9104	0.6224	0.4594	NFLUX 12h persist glb	-1.4723	2.8964	3.2488	0.5394	0.3263
NFLUX new	-1.3718	2.4762	2.8306	0.6275	0.4416	NFLUX 12h persist new	-1.4549	2.6969	3.0640	0.5685	0.4008
NOGAPS Analysis	-1.7430	2.2102	2.8146	0.7322	0.5070	NOGAPS 12h persist	-1.7992	2.5426	3.1146	0.6594	0.3809
NOGAPS 12h fcst	-2.2162	2.6358	3.4435	0.6372	0.2532						
Ocean		N = 6021									
NFLUX global	-0.7494	2.1759	2.3012	0.5352	0.3413	NFLUX 12h persist glb	-0.7524	2.2913	2.4115	0.5039	0.2766
NFLUX new	-0.8468	2.0803	2.2459	0.5263	0.3726	NFLUX 12h persist new	-0.8770	2.2397	2.4051	0.4725	0.2805
NOGAPS Analysis	-1.1554	1.5853	1.9615	0.7071	0.5214	NOGAPS 12h persist	-1.1955	1.9413	2.2797	0.5912	0.3535
NOGAPS 12h fcst	-1.6206	1.8175	2.4350	0.6181	0.2625						

For air temperature, the region-specific NFLUX not only shows improvement in each test statistic over the global NFLUX, but also over NOGAPS. For specific humidity, we see an increase in the ME with the region-specific NFLUX compared to the global NFLUX. The

region-specific NFLUX does show improvement in the remaining test statistics compared to the global NFLUX; however, NOGAPS still outperforms NFLUX.

As shown in the results, the region-specific NFLUX shows a smaller standard deviation compared to the global NFLUX. This can also be seen in the scatterplots shown in Figure 63 (right). As discussed previously, NFLUX applies a correction to high specific humidity values that eliminates the 20 g/kg capping effect seen in NOGAPS. The region-specific NFLUX eliminates much of the noise seen at the high values in the global NFLUX while still maintaining a broad one-to-one relationship. NOGAPS still shows a closer one-to-one fit however.

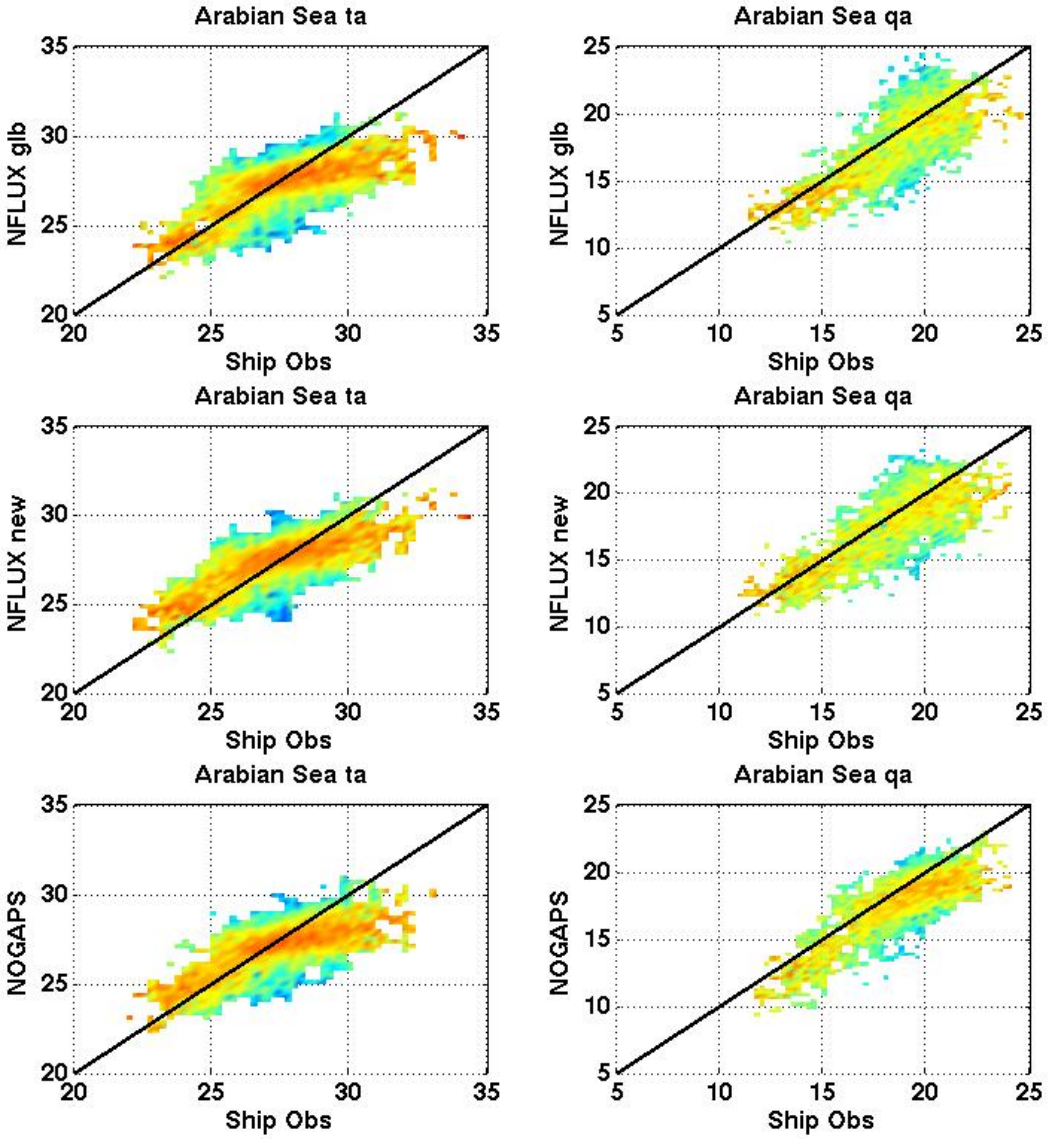

Figure 63: Air temperature and specific humidity over the Arabian Sea open ocean region using unassimilated *in situ* data. Scatterplots of the *in situ* observations versus global NFLUX analysis (top), new regional NFLUX analysis (middle), and NOGAPS analysis (bottom) are shown for both air temperature (left) and specific humidity (right).

6.3 South China Sea

Figure 64 shows mean air temperature (left) and specific humidity (right) error over the South China Sea using unassimilated *in situ* observations and global NFLUX (top), region-specific NFLUX (middle), and NOGAPS (bottom). For the air temperature bias, the global NFLUX shows an overall warm bias, while the region-specific NFLUX and NOGAPS show a near neutral bias. For the specific humidity bias, the global NFLUX shows a strong moist bias. The region-specific NFLUX greatly reduces the global NFLUX bias; however, there is still a moist bias present over most of the region. Unlike NFLUX, NOGAPS shows a strong dry bias throughout the region.

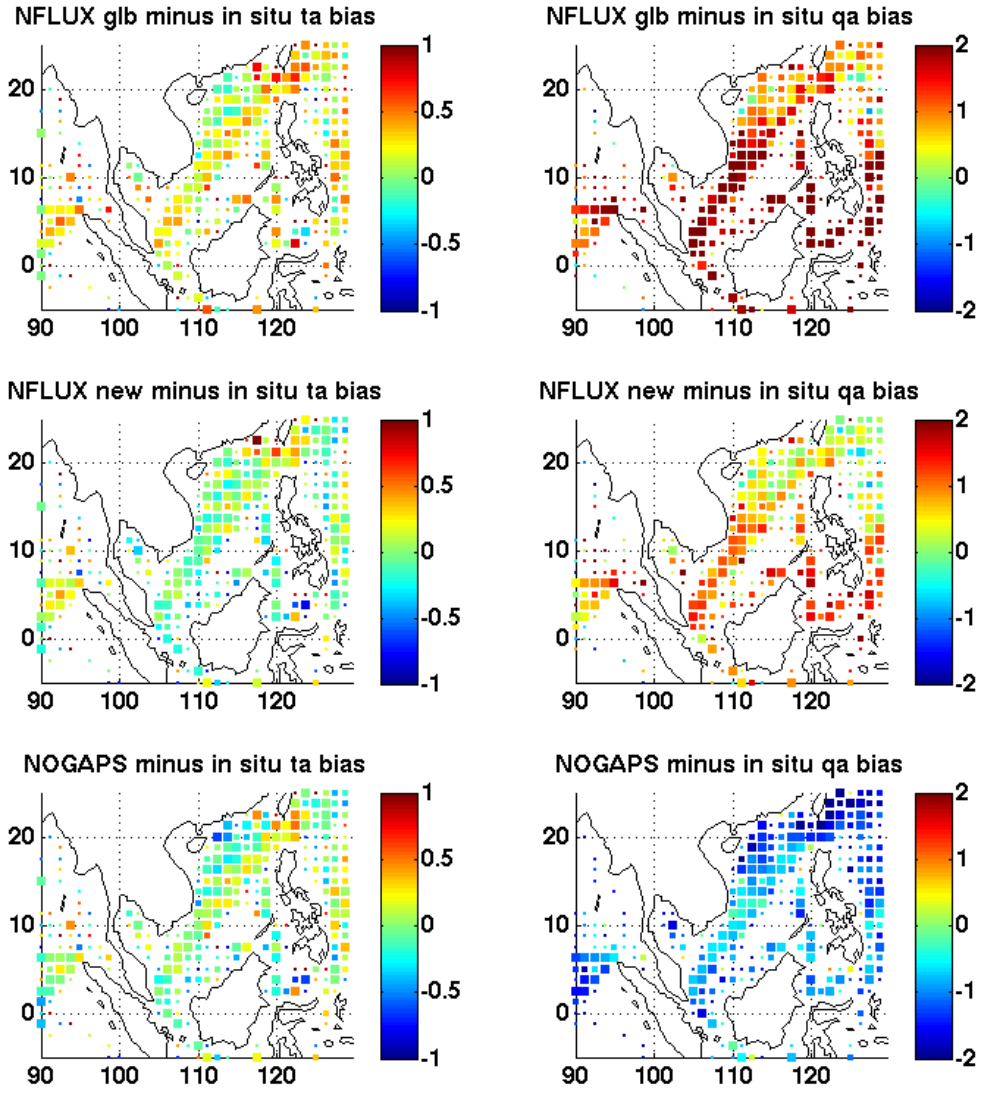

Figure 64: South China Sea 2-year average air temperature (°C) and specific humidity (g/kg) bias. The global NFLUX (top), new regional NFLUX (middle), and NOGAPS (bottom) bias compared to unassimilated observations is shown for both air temperature (left) and specific humidity (right). Colored square sizes represent the number of observations in each grid box, ranging from 5 to 50 observations.

Air temperature and specific humidity test statistics over the South China Sea are shown in Table 27and Table 28 using assimilated and unassimilated *in situ* matchups. The corresponding open ocean scatterplots using unassimilated matchups are shown in Figure 65.

Table 27: Air temperature errors over the South China Sea region. Errors are shown relative to both assimilated (left columns) and unassimilated (right columns) *in situ* observations for all comparisons (regional), near land (coastal), and open ocean (ocean). The best test statistic in each column is highlighted in blue. Means and standard deviations that are not significantly different compared to NFLUX at the 95% confidence interval are denoted with an asterisk (*).

	ME	SD	RMSE	R^2	SS		ME	SD	RMSE	R^2	SS
Regional		N = 18376									
NFLUX global	0.1910	1.1623	1.1779	0.8025	0.7970	NFLUX 12h persist glb	0.2159	1.3457	1.3281	0.7489	0.7419
NFLUX new	-0.0323	1.0697	1.0701	0.8362	0.8324	NFLUX 12h persist new	-0.0071	1.3007	1.3006	0.7527	0.7524
NOGAPS Analysis	-0.0698	1.2295	1.2314	0.7805	0.7781	NOGAPS 12h persist	-0.0431	1.3457	1.3464	0.7392	0.7347
NOGAPS 12h fcst	0.0069	1.2471	1.2471	0.7737	0.7724						
Coastal		N = 6610									
NFLUX global	0.2069	1.3293	1.3452	0.8393	0.8353	NFLUX 12h persist glb	0.2480	1.5823	1.6015	0.7729	0.7666
NFLUX new	-0.0463	1.2136	1.2144	0.8700	0.8658	NFLUX 12h persist new	-0.0103	1.5695	1.5694	0.7763	0.7759
NOGAPS Analysis	-0.1083	1.3790	1.3831	0.8291	0.8259	NOGAPS 12h persist	-0.0622	1.6106	1.6117	0.7695	0.7636
NOGAPS 12h fcst	-0.0051	1.4201	1.4200	0.8188	0.8165						
Ocean		N = 11766									
NFLUX global	0.1821	1.0569	1.0725	0.7491	0.7411	NFLUX 12h persist glb	0.1979	1.1290	1.1462	0.7131	0.7043
NFLUX new	-0.0245	0.9795	0.9798	0.7874	0.7839	NFLUX 12h persist new	-0.0054	1.1218	1.1217	0.7170	0.7168
NOGAPS Analysis	-0.0482	1.1363	1.1373	0.7104	0.7088	NOGAPS 12h persist	-0.0324	1.1708	1.1712	0.6941	0.6912
NOGAPS 12h fcst	0.0137	1.1385	1.1385	0.7087	0.7082						

Table 28: Specific humidity errors over the South China Sea region. Errors are shown relative to both assimilated (left columns) and unassimilated (right columns) *in situ* observations for all comparisons (regional), near land (coastal), and open ocean (ocean). The best test statistic in each column is highlighted in blue. Means and standard deviations that are not significantly different compared to NFLUX at the 95% confidence interval are denoted with an asterisk (*).

	ME	SD	RMSE	R^2	SS		ME	SD	RMSE	R^2	SS
Regional		N = 14585									
NFLUX global	1.5679	2.2822	2.7688	0.5773	0.0876	NFLUX 12h persist glb	1.6474	1.6801	2.9268	0.535	-0.0195
NFLUX new	0.7515	1.8345	1.9824	0.6468	0.5323	NFLUX 12h persist new	0.8222	1.9864	2.1498	0.5954	0.4500
NOGAPS Analysis	-1.1846	1.4576	1.8782	0.7551	0.5802	NOGAPS 12h persist	-1.1402	1.6801	2.0305	0.6833	0.5093
NOGAPS 12h fcst	-1.5874	1.5713	2.2335	0.7147	0.4063						
Coastal		N = 5922									
NFLUX global	1.6429	2.2774	2.8080	0.6269	0.2797	NFLUX 12h persist glb	1.7278	2.4225	2.9754	0.5853	0.1913
NFLUX new	0.8162	1.8901	2.0586	0.6949	0.6128	NFLUX 12h persist new	0.9022	2.0703	2.2582	0.6416	0.5341
NOGAPS Analysis	-1.3709	1.5854	2.0958	0.7732	0.5988	NOGAPS 12h persist	-1.3131	1.8049	2.2319	0.7115	0.5450
NOGAPS 12h fcst	-1.7628	1.6825	2.4367	0.7429	0.4576						
Ocean		N = 8663									
NFLUX global	1.5166	2.2842	2.7417	0.5393	-0.1297	NFLUX 12h persist glb	1.5925	2.4156	2.8931	0.4967	-0.2580
NFLUX new	0.7072	1.7943	1.9285	0.6018	0.4410	NFLUX 12h persist new	0.7676	1.9251	2.0724	0.5524	0.3545
NOGAPS Analysis	-1.0572	1.3487	1.7137	0.7411	0.5587	NOGAPS 12h persist	-1.0221	1.5785	1.8804	0.6573	0.4686
NOGAPS 12h fcst	-1.4675	1.4787	2.0832	0.6914	0.3478						

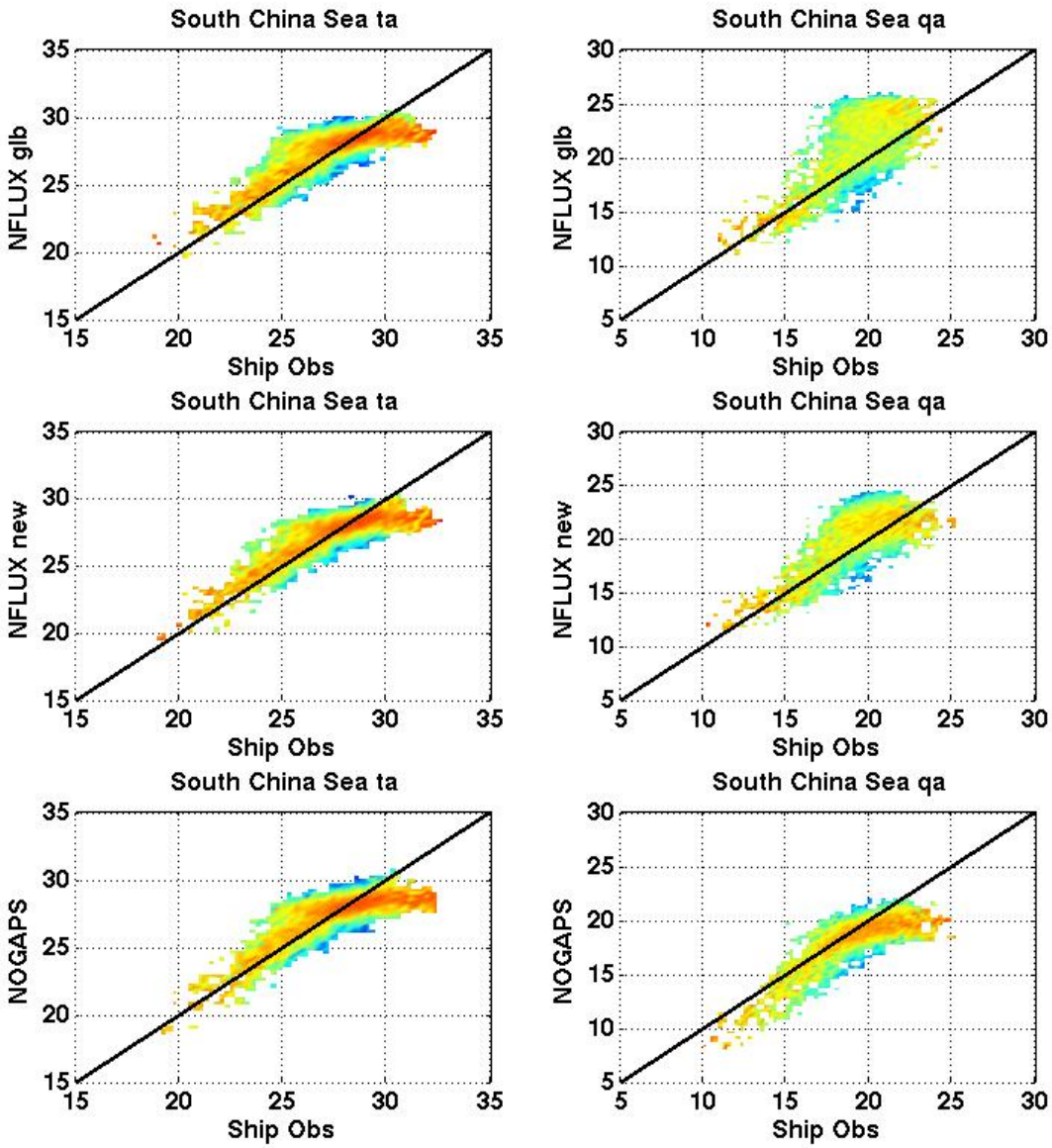

Figure 65: Air temperature and specific humidity over the South China Sea open ocean region using unassimilated *in situ* data. Scatterplots of the *in situ* observations versus global NFLUX analysis (top), new regional NFLUX analysis (middle), and NOGAPS analysis (bottom) are shown for both air temperature (left) and specific humidity (right).

For air temperature, the region-specific NFLUX shows improvement in over both the global NFLUX and NOGAPS for each test statistic with the exception of the ME using assimilated matchups. For specific humidity, the region-specific NFLUX shows a significant improvement over each of the test statistics when compared to the global NFLUX; most notable is the global NFLUX showing a negative SS and the region-specific NFLUX showing positive SS. NOGAPS still shows improvement over the region-specific NFLUX in each test statistic except the ME. By examining the scatterplots in Figure 65, we see a larger scatter at high specific humidity values for the region-specific NFLUX compared to NOGAPS, although the scatter is greatly reduced

from the global NFLUX. This feature has been discussed before as the result of a correction applied to high specific humidity values to eliminate the capping effect seen in NOGAPS around 20 g/kg.

6.4 Okinawa Trough

Figure 66 shows mean air temperature (left) and specific humidity (right) error over the Okinawa Trough using unassimilated *in situ* observations and global NFLUX (top), region-specific NFLUX (middle), and NOGAPS (bottom). The spatial patterns for the air temperature and specific humidity biases are similar for each model: global NFLUX shows an overall warm, moist bias; region-specific NFLUX shows near neutral biases; and NOGAPS shows an overall cold, dry bias.

Air temperature and specific humidity test statistics over the Okinawa Trough are shown in Table 29 and Table 30 using assimilated and unassimilated *in situ* matchups. The corresponding open ocean scatterplots using unassimilated matchups are shown in Figure 67. For air temperature, the region-specific NFLUX shows improvement in over both the global NFLUX and NOGAPS for each test statistic with the exception of the ME. The global NFLUX shows a smaller ME than the region-specific NFLUX; however, the region-specific NFLUX shows a smaller ME than NOGAPS.

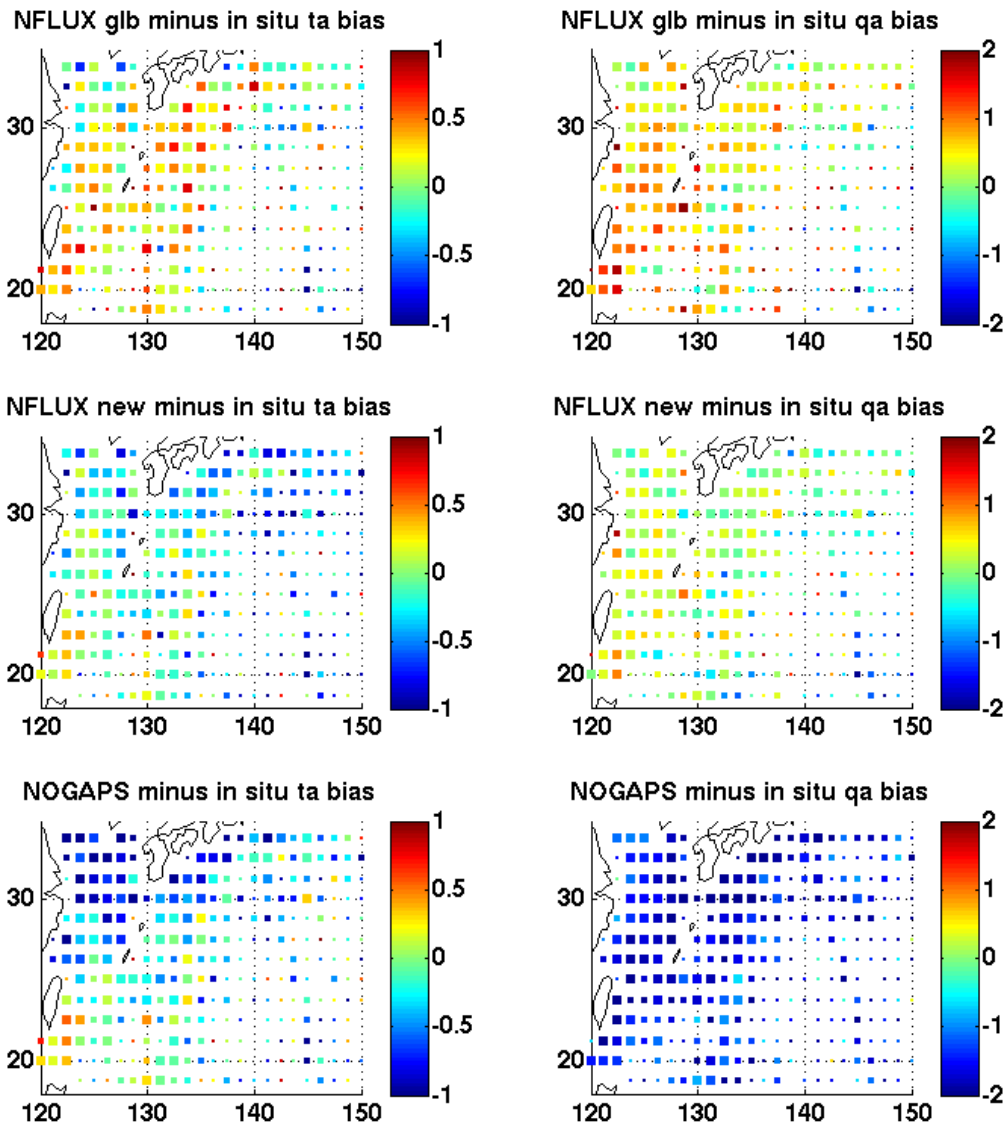

Figure 66: Okinawa Trough 2-year average air temperature (°C) and specific humidity (g/kg) bias. The global NFLUX (top), new regional NFLUX (middle), and NOGAPS (bottom) bias compared to unassimilated observations is shown for both air temperature (left) and specific humidity (right). Colored square sizes represent the number of observations in each grid box, ranging from 5 to 50 observations.

Table 29: Air temperature errors over the Okinawa Trough region. Errors are shown relative to both assimilated (left columns) and unassimilated (right columns) *in situ* observations for all comparisons (regional), near land (coastal), and open ocean (ocean). The best test statistic in each column is highlighted in blue. Means and standard deviations that are not significantly different compared to NFLUX at the 95% confidence interval are denoted with an asterisk (*).

	ME	SD	RMSE	R^2	SS		ME	SD	RMSE	R^2	SS
Regional		N = 16763									
NFLUX global	0.1646	1.4788	1.4879	0.9560	0.9553	NFLUX 12h persist glb	0.1689	1.8464	1.7854	0.9362	0.9356
NFLUX new	-0.1196	1.2961	1.3016	0.9661	0.9658	NFLUX 12h persist new	-0.1368	1.7113	1.7167	0.9412	0.9404
NOGAPS Analysis	-0.4199	1.4710	1.5297	0.9613	0.9527	NOGAPS 12h persist	-0.4242	1.8464	1.8944	0.9383	0.9275
NOGAPS 12h fcst	-0.3942	1.4680	1.5200	0.9605	0.9533						
Coastal		N = 7127									
NFLUX global	0.2789	1.6187	1.6424	0.9538	0.9523	NFLUX 12h persist glb	0.2986	2.0267	2.0485	0.9274	0.9258
NFLUX new	0.0526	1.4396	1.4405	0.9635	0.9633	NFLUX 12h persist new	0.0492	1.9670	1.9675	0.9326	0.9316
NOGAPS Analysis	-0.3969	1.6475	1.6945	0.9577	0.9492	NOGAPS 12h persist	-0.3858	2.1327	2.1672	0.9281	0.9170
NOGAPS 12h fcst	-0.3864	1.6577	1.7021	0.9558	0.9488						
Ocean		N = 9396									
NFLUX global	0.0800	1.3601	1.3624	0.9460	0.9457	NFLUX 12h persist glb	0.0729	1.5610	1.5626	0.9288	0.9286
NFLUX new	-0.2469	1.1625	1.1884	0.9606	0.9587	NFLUX 12h persist new	-0.2744	1.4794	1.5045	0.9369	0.9338
NOGAPS Analysis	-0.4369	1.3252	1.3953	0.9563	0.9431	NOGAPS 12h persist	-0.4526	1.6016	1.6642	0.9354	0.9190
NOGAPS 12h fcst	-0.3999	1.3102	1.3698	0.9561	0.9451						

Table 30: Specific humidity errors over the Okinawa Trough region. Errors are shown relative to both assimilated (left columns) and unassimilated (right columns) *in situ* observations for all comparisons (regional), near land (coastal), and open ocean (ocean). The best test statistic in each column is highlighted in blue. Means and standard deviations that are not significantly different compared to NFLUX at the 95% confidence interval are denoted with an asterisk (*).

	ME	SD	RMSE	R^2	SS		ME	SD	RMSE	R^2	SS
Regional		N = 9543									
NFLUX global	0.5337	1.8787	1.9529	0.8877	0.8644	NFLUX 12h persist glb	0.5866	1.7720	2.2053	0.8583	0.8271
NFLUX new	0.1193	1.6074	1.6118	0.9084	0.9077	NFLUX 12h persist new	0.1446	1.8706	1.8761	0.8770	0.8749
NOGAPS Analysis	-1.6078	1.4586	2.1708	0.9294	0.8325	NOGAPS 12h persist	-1.6260	1.7720	2.4049	0.8963	0.7944
NOGAPS 12h fcst	-1.8846	1.6009	2.4727	0.9164	0.7827						
Coastal		N = 2834									
NFLUX global	0.7249	1.8018	1.9419	0.9031	0.8746	NFLUX 12h persist glb	0.8006	2.0828	2.2310	0.8729	0.8345
NFLUX new	0.3002	1.6203	1.6476	0.9130	0.9097	NFLUX 12h persist new	0.3558	1.8745	1.9077	0.8847	0.8790
NOGAPS Analysis	-1.6412	1.5335	2.2460	0.9242	0.8323	NOGAPS 12h persist	-1.6315	1.8113	2.4375	0.8954	0.8024
NOGAPS 12h fcst	-1.7910	1.6116	2.4092	0.9177	0.8070						
Ocean		N = 6709									
NFLUX global	0.4529	1.9046	1.9576	0.8771	0.8524	NFLUX 12h persist glb	0.4962	2.1377	2.1944	0.8472	0.8145
NFLUX new	0.0429	1.5959	1.5964	0.9023	0.9018	NFLUX 12h persist new	0.0554	1.8619	1.8625	0.8685	0.8663
NOGAPS Analysis	-1.5937	1.4257	2.1383	0.9288	0.8239	NOGAPS 12h persist	-1.6237	1.7552	2.3910	0.8920	0.7798
NOGAPS 12h fcst	-1.9242	1.5948	2.4991	0.9128	0.7594						

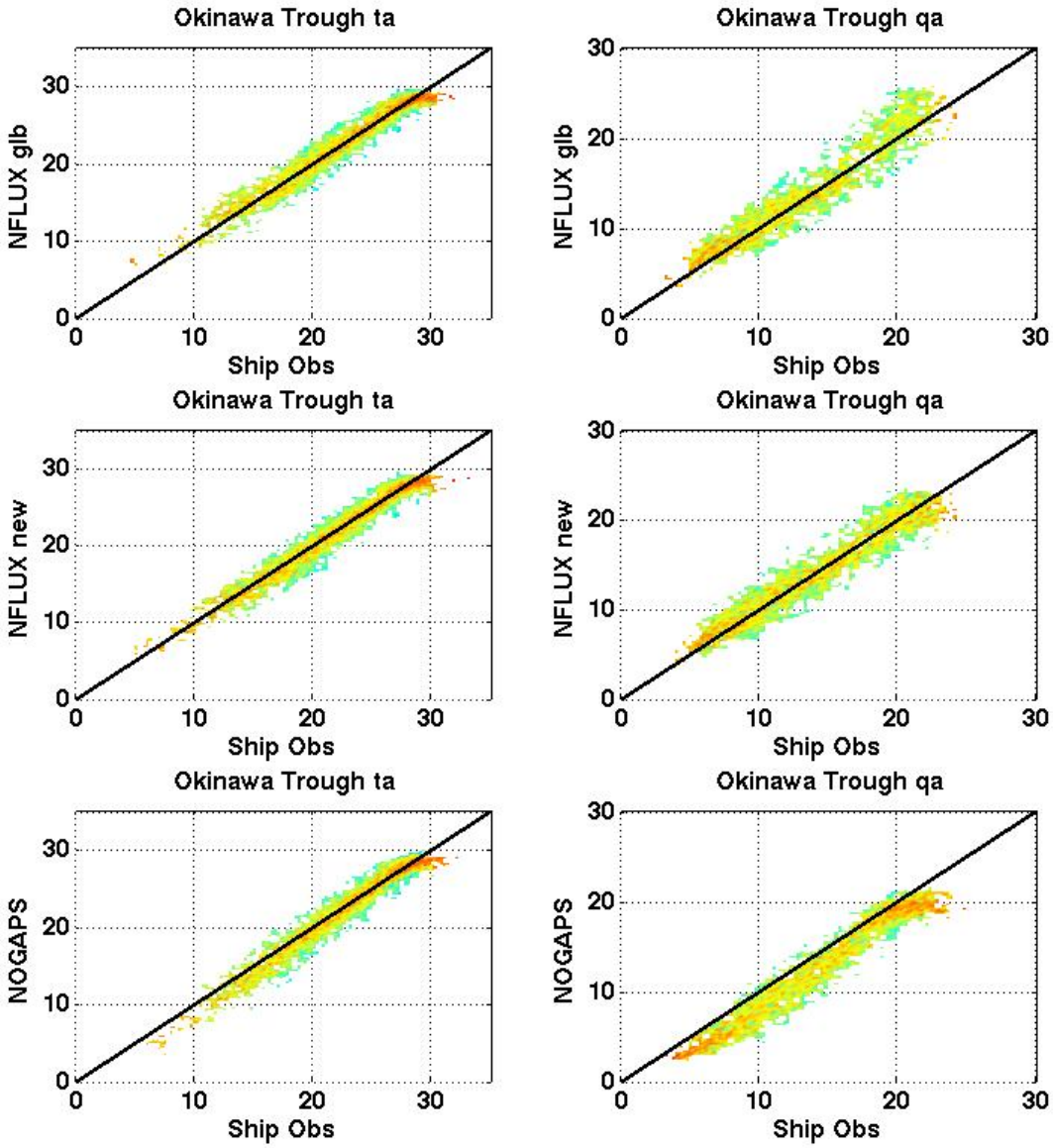

Figure 67: Air temperature and specific humidity over the Okinawa Trough open ocean region using unassimilated *in situ* data. Scatterplots of the *in situ* observations versus global NFLUX analysis (top), new regional NFLUX analysis (middle), and NOGAPS analysis (bottom) are shown for both air temperature (left) and specific humidity (right).

For specific humidity, the region-specific NFLUX shows improvement in the ME and RMSE over both the global NFLUX and NOGAPS. As seen in the scatterplots in Figure 67, the region-specific NFLUX shows a closer one-to-one fit than global NFLUX; however, NOGAPS shows a smaller spread. This results in NOGAPS having a smaller SD and R^2 than the region-specific NFLUX. These combined effects give the region-specific NFLUX a higher SS than NOGAPS.

7.0 CONCLUSION

The validation experiments presented in this report were performed to assess NFLUX in comparison with the current atmospheric models that are used to provide ocean forcing fields. The global test case compared NFLUX to NOGAPS. The western and eastern Pacific regional test cases compared NFLUX to COAMPS as well as NOGAPS. The regional test cases using enhanced region-specific algorithms compared NFLUX to NOGAPS. Each test case was run for two years, from January 1, 2010 through December 31, 2011.

The analysis skill of each of the models was assessed using assimilated as well as unassimilated *in situ* matchup comparisons in terms of the mean error (*ME*), standard deviation (*SD*), root mean square error (RMSE), and correlation coefficient (R^2). The matchups were split into coastal (within 111km of land) and open ocean (greater than 111km of land) data sets, with the focus of this report on the open ocean results. For each of the test cases, the open ocean matchups were examined by season. In addition, the global test case was examined by latitude band.

To summarize the overall performance of NFLUX versus NOGAPS and COAMPS, an overall skill score (SS) was calculated using the unassimilated observation matchups over the open ocean for each of the test cases and each of the surface parameters (Table 31).

Table 31: Skill scores of each of the models using unassimilated *in situ* observations. Skill scores are shown for each of the surface parameters in the global, eastern, and western Pacific test cases for the open ocean.

	TA	QA	WS
Global - NFLUX	0.9759	0.8746	0.2687
Global - NOGAPS	0.9740	0.8874	0.2597
EPAC - NFLUX	0.9194	0.7681	0.1282
EPAC - COAMPS	0.8299	0.7298	-0.0079
EPAC - NOGAPS	0.9144	0.7438	0.0654
WPAC - NFLUX	0.9566	0.8028	0.3233
WPAC - COAMPS	0.9356	0.8477	0.1881
WPAC - NOGAPS	0.9497	0.8528	0.3184

NFLUX shows an improved SS for each test case in air temperature and wind speed. For specific humidity, NFLUX shows an improved skill score only in the eastern Pacific test case. As discussed in each of the test cases for specific humidity, NFLUX generally had a lower mean bias and a larger standard deviation. At high specific humidity values, NOGAPS and COAMPS display a capping effect which does not allow for very high specific humidity values. NFLUX applies a correction in the satellite retrieval process to allow for higher specific humidity values. This creates a closer one-to-one relationship between NFLUX and the *in situ* observations; however, it also creates more spread which means a larger standard deviation and lower correlation.

NFLUX also has the capability to provide region-specific satellite retrievals and assimilation for air temperature and specific humidity. This application was demonstrated for four regions of interest: the California Current System, the Arabian Sea, the South China Sea, and the Okinawa Trough. In the California Current System, the region-specific NFLUX performed similar to or slightly worse than the global NFLUX. One possibility for this may be the limited data set; in general the more observations that are used for the algorithm development, the better the retrievals are. Another possibility is that other atmospheric factors may need to be considered for better retrievals, such as cloud cover. For the other three regions, the region-specific NFLUX showed an improvement over the global NFLUX, with the most noticeable improvement in the specific humidity over the South China Sea.

8.0 REFERENCES

Cravatte, S., T. Delcroix, D. Zhang, M. J. McPhaden, and J. Leloup, 2009: Observed freshening and warming of the western Pacific Warm Pool, *Clim. Dyn*., **33**, 565–589, doi:10.1007/s00382-009-0526-7.

Cummings, J.A., 2005: Operational multivariate ocean data assimilation. *Quart. J. Royal Met. Soc.*, Part C, **131**(613): 3583:3604.

Curry, J. A., and Coauthors, 2004: SEAFLUX. *Bull. Amer. Meteor. Soc.*, **85**, 409–424. doi: http://dx.doi.org/10.1175/BAMS-85-3-409.

Dayem, K. E., D. C. Noone, and P. Molnar, 2007: Tropical western Pacific warm pool and maritime continent precipitation rates and their contrasting relationships with the Walker Circulation, *J. Geophys. Res*., **112**, D06101, doi:10.1029/2006JD007870.

Fairall, C. W., E. F. Bradley, J. E. Hare, A. A. Grachev, and J. B. Edson, 2003: Bulk parameterization of air-sea fluxes: Updates and verification for the COARE algorithm, *J. Climate*, **16**, 571-591.

Graham, N. E. and H. F. Diaz, 2001: Evidence for intensification of North Pacific winter cyclones since 1948. *Bull. Amer. Meteor. Soc*., **82**, 1869–1893.

Hodur, R. M., 1997: The Naval Research Laboratory's Coupled Ocean/Atmosphere Mesoscale Prediction System (COAMPS). *Mon. Wea. Rev.*, **125**, 1414–1430. doi: http://dx.doi.org/10.1175/1520-0493(1997)125<1414:TNRLSC>2.0.CO;2

Hogan, T. F. and T. E. Rosmond, 1991: The description of the navy operational global atmospheric prediction system's spectral forecast model. *Mon. Wea. Rev.*, **119**, 1786–1815.

Kent, E. C., S. D. Woodruff, and D. I. Berry, 2007: Metadata from WMO Publication No. 47 and an Assessment of Voluntary Observing Ship Observation Heights in ICOADS. *J. Atmos. Oceanic Technol.*, **24**, 214–234. doi: http://dx.doi.org/10.1175/JTECH1949.1

Klein, S. A., and D. L. Hartmann, 1993: The seasonal cycle of low stratiform clouds. *J. Climate,* **6,** 1587–1606.

Murphy, A.H., 1988: Skill scores based on the mean square error and their relationships to the correlation coefficient. *Mon. Wea. Rev.*, **116**, 2417-2424.

Murphy, A.H., 1995: The Coefficients of Correlation and Determination as Measures of performance in Forecast Verification. *Wea. Forecasting*, **10**, 681–688.

Rosmond, T. and L. Xu, 2006: Development of NAVDAS-AR: non-linear formulation and outer loop tests. *Tellus*, 58A, 45-58.

WMO, 2006: *Guide to Meteorological Instruments and Methods of Observation*, Preliminary Seventh edition WMO-No. 8, World Meteorological Organization, Geneva, Switzerland.

Xu, H., M. Xu, S.-P. Xie, Y. Wang, 2011: Deep Atmospheric Response to the Spring Kuroshio over the East China Sea*. *J. Climate*, **24**, 4959–4972. doi: http://dx.doi.org/10.1175/JCLI-D-10-05034.1

Xu, L., T. Rosmond and R. Daley, 2005: Development of NAVDAS-AR: formulation and initial tests of the linear problem. *Tellus*, 57A, 546-559.

9.0 ACRONYMS

AMSU	Advanced Microwave Sounding Unit
COAMPS	Coupled Ocean Atmosphere Prediction System
DJF	December-January-February
DoD	Department of Defense
DMSP	DoD Meteorological Satellite Program
EUMETSAT	European Organization for the Exploitation of Meteorological Satellites
JJA	June-July-August
MAM	March-April-May
ME	Mean Error
NCODA	Navy Coastal Ocean Data Assimilation
NFLUX	NRL Ocean Surface Flux
NOAA	National Oceanic and Atmospheric Administration
NOGAPS	Navy Operational Global Atmospheric Prediction System
NRL	Naval Research Laboratory
QC	Quality Control
R^2	Correlation Coefficient
RMSE	Root Mean Square Error
SD	Standard Deviation
SON	September-October-November
SS	Skill Score
SSMIS	Special Sensor Microwave Imager/Sounder
SST	Sea Surface Temperature
VOS	Voluntary Observing Ships